Università degli Studi di Padova

Dipartimento di Biologia

SCUOLA DI DOTTORATO IN BIOCHIMICA E BIOTECNOLOGIE

Indirizzo in Biotecnologie

Ciclo XXI

INSIGHTS ON ALPHA-SYNUCLEIN INTERACTION NETWORK AND AGGREGATION PATTERN

Direttore della Scuola: Ch.mo Prof. Giuseppe Zanotti

Supervisore: Ch.mo Prof. Luigi Bubacco

Dottorando: Laura Tosatto

02 febbraio 2009

Abstract

Parkinson's disease (PD) is the most important neurodegenerative disease which regards movement. The 1% of the population over 65 years old is affected by this disorder. The main symptoms are bradykinesia, resting tremor, postural instability, muscle rigidity and sometimes cognitive and personality problems. The cause of the disease is a selective death of dopaminergic neurons in *substantia nigra pars compacta*. Actually, the best therapy can help to solve only symptoms and it is based on the supply of the precursor of dopamine, which is the neurotransmitter lacking in the disease, or inhibitors of the activity of enzymes involved in the metabolism of dopamine. This therapy does not prevent further neuronal loss. Two are the links that correlate the protein alpha-synuclein (α-syn) to PD: this protein is found as amyloid fibrils in proteinaceous aggregates known as Lewy bodies, which are present in PD patients' brains, and second, single point mutation of α-syn are correlated to early onset of autosomic dominant forms of the disease. In this frame an understanding the molecular cause that lead to neuronal loss and protein aggregation becomes crucial for the development of new therapeutic strategies.

α-Syn is expressed in all the central nervous system and it is localized at the presynaptic terminal but its biological role is still not clear. α-Syn is natively unfolded and it is able to acquire different conformations in different conditions such as the presence of membranes or organic solvents. The central region of the protein is able to fold into β-sheet structure comparable with amyloid fibrils found in Lewy bodies. Point mutants implied in the early onset PD (A30P, E46K and A53T) have a higher propensity for the formation of oligomers. Recently, the hypothesis that the oligomers are the main cause of α-syn toxicity is gaining support. Studying the oligomerization process seem to be now more important for the comprehension of neuronal death. The first steps of self-interaction are extremely rare events

and thus difficult to observe with bulk methods; fibrils are insoluble, so structure can not be solved by NMR, nor by X-ray crystallography.

Moreover, α-syn was found to interact with a wide variety of proteins as detected by co-immunoprecipitation or affinity techniques. The biological relevance and the molecular basis of this processes require further investigation by high resolution methods like NMR (Nuclear Magnetic Resonance) or SPR (Surface Plasmon Resonance). Furthermore, every interacting partners may sequester α-syn from cytosol to decrease the probability of self-interaction that lead to aggregation.

In this PhD thesis investigations were done in order to improve α-syn interaction network knowledge. As any event correlated with an altered balance of α-syn interaction network may favour α-syn self-interaction, the experimental approach was divided into three parts to get information about: protein-protein interaction, membrane binding and aggregation studies.

SPR studies was performed to verify the interaction between α-syn and 14-3-3η. 14-3-3 chaperone family can bind and regulate a wide variety of proteins. Sato et al. (2006) measured 1.1 μM dissociation constant between α-syn and 14-3-3η by SPR. However, these data were not reproduced, and also HSQC spectra of ^{15}N labelled α-syn in the presence of a three molar excess of 14-3-3η did not provide evidences of an interaction between the two molecules.

Interaction between membranes and α-syn was studied by circular dichroism (CD). The first hundred residues of the proteins acquire α-helix structure upon binding with micelles and liposomes. Interesting data come from the interaction between α-syn dimers formed by two mutants produced in our lab (V3C and Syn141C): the dimer formed by disulfide bond between the Cys at the C-terminal end of the protein (C-term dimer) forms a distorted α-helix upon the binding with 50 nm diameter small unilamellar vesicles (SUVs) composed of 50% DMPG 50% DMPC, while the dimer formed by V3C mutants (N-term dimer) acquires an amount of α-helix comparable to the one observed upon binding to SDS micelles. It is possible that SUV dimensions (i.e. curvature) and the covalent constrain in C-term dimer are the cause of helix distortion.

Finally, self-interaction of α-syn was investigated by fibrillogenesis and aggregation assays. Fibrillogenesis was monitored with Thioflavin T (ThT) fluorescence; samples of wild-type α-syn, C-term dimer, pathological mutant A30P, E46K and A53T were incubated at 37°C under shaking; aliquots were collected at fixed time, mixed with ThT solution and fluorescence intensity measured at 485 nm. This assay revealed that E46K, A53T and C-term

dimer form fibrils faster than wild-type α-syn and the A30P mutant presents a longer lag phase. It was not possible to obtain good sigmoidal curves with this method in the case of α-syn, probably because of α-syn fibrils disruption or precipitation and light scattering events. Hence, a protocol applied by Lük et al. (2007) was applied. This method measures fluorescence polarization (FP) of samples of α-syn incubated in a 96 wells plate at 37°C under agitation. α-Syn wild type protein, pathological mutants, C-term and N-term dimer were mixed with Oregon Green 488 maleimide labelled α-syn (1:100=Syn-OregonGreen:α-syn), to then measured FP variations in time. The comparison between the samples shows that wild-type α-syn aggregates faster than pathological mutants and N-term dimer. The C-term dimer shows an increase of FP with the shortest lag phase. The covalent constrain seem to favour intramolecular interaction and then aggregation and fibrillogenesis. NMR spectra was recorded for C-term dimer formed with 1:5 protein mixture of (^{15}N labelled Cys C-term mutant):(^{14}N Cys C-term mutant), but no intramolecular interaction was detected. In addition, α-syn was tested in the presence of three proteins. While DJ1 provides no significance effect on α-syn aggregation, 3T protein seem to have an aspecific influence on oligomers enlargement rate. Moreover, 14-3-3η mixed in three molar ratios to α-syn seems to have a concentration dependent effect on α-syn aggregation, although experimental errors do not allow a conclusive interpretation of this finding. However, 1:1=14-3-3η:α-syn shows significantly slower aggregation rate compared to α-syn incubated alone.

In conclusion, progress on the understanding on the molecular mechanism of α-syn aggregation was reached, specifically for what concern the orientation of intramolecular interaction that lead to the formation of oligomers and fibrils, and proteins able to host α-syn oligomers growth. Moreover, a new method based on fluorescence polarization was used to reveal differences on lag phase and rate of the aggregation process of α-syn and its variants. This technique can be use to test conditions, molecules and proteins able affect the aggregation of α-syn.

Riassunto

Il morbo di Parkinson (PD) è la più importante malattia neurodegenerativa riguardante la funzionalità motoria. L'1% della popolazione sopra i 65 anni è affetto da questa malattia. I sintomi principali sono bradichinesia, tremore a riposo, instabilità posturale, rigidità muscolare e, talvolta, problemi cognitivi e della personalità. La causa della malattia è una morte selettiva dei neuroni dopaminergici nella *substantia nigra pars compacta*. In realtà, la migliore terapia attualmente applicata è puramente sintomatica, e si basa sulla somministrazione del precursore della dopamina, che è il neurotrasmettitore assente nella malattia, o su inibitori delle attività degli enzimi coinvolti nel metabolismo della dopamina. Questa terapia non impedisce un'ulteriore perdita neuronale. Due evidenze correlano la proteina alfa-sinucleina (α-syn) al PD: questa proteina è presente come fibrille amiloidi in aggregati proteici noti come corpi di Lewy, che sono presenti nel cervello dei pazienti, e in secondo luogo, mutazioni di un singolo amminoacido del gene di α-syn sono correlati all'insorgenza di forme precoci della malattia, con trasmissione autosomica dominante. In questo contesto, la comprensione delle cause molecolari che conducono alla perdita di neuroni e all'aggregazione di α-syn diventa fondamentale per lo sviluppo di nuove strategie terapeutiche.

α-Syn è espressa in tutto il sistema nervoso centrale ed è localizzata presso i terminali presinaptici, tuttavia il suo ruolo biologico non è ancora chiaro. α-Syn è una *natively unfolded protein*, ma è in grado di acquisire conformazioni diverse in diverse condizioni, quali la presenza di membrane o solventi organici. La regione centrale della proteina è in grado di acquisire strutture a foglietto β nelle fibrille amiloidi che vengono riscontrate nei corpi di Lewy. I mutanti patologici (A30P, E46K e A53T) hanno una maggiore propensione per la formazione di oligomeri. Recentemente, si sta rafforzando l'ipotesi che gli oligomeri siano la principale causa della tossicità causata da α-syn. Studiare il processo di oligomerizzazione è

quindi di enorme importanza per la comprensione dei processi che portano alla morte neuronale. I primi passaggi nella creazione di piccoli aggregati sono eventi estremamente rari, e quindi difficili da osservare con maggior parte dei metodi; in più, essendo le fibrille insolubili, la loro struttura non può essere risolta da NMR, né dalla cristallografia a Raggi-X.

Diversi studi riportano l'interazione di α-syn con una grande varietà di proteine, come rilevato da esperimenti di co-immunoprecipitazione o cromatografia di affinità. La rilevanza biologica e la base molecolare di questo processo necessitano di un'ulteriore indagine con metodi ad alta risoluzione come NMR (Risonanza Magnetica Nucleare) o SPR (Surface Plasmon Resonance). Inoltre, tutte le macromolecole in grado di interagire con α-syn ne provocano il sequestro dal citosol, diminuendo le probabilità di auto-interazione che portano alla sua aggregazione.

In questa tesi di dottorato sono stati realizzati studi al fine di ampliare la conoscenza sulla rete di interazione di α-syn. Dal momento che ogni evento correlato ad un alterato l'equilibrio nel network di interazioni di α-syn può favorire la fibrillogenesi, l'approccio sperimentale è stato diviso in tre parti: interazioni proteina-proteina, legame alle membrane e studi di aggregazione.

Esperimenti mediante SPR sono stati effettuati per verificare l'interazione tra α-syn e 14-3-3η. La famiglia di chaperone 14-3-3 può interagire e regolare una grande varietà di proteine. Sato et al. (2006) hanno misurato con tecniche SPR la costante di dissociazione tra α e syn-14-3-3η, riportando un valore di (1,1 μM). Negli esperimenti effettuati questo dato non è stato riprodotto, e anche lo spettro HSQC di α-syn marcata con ^{15}N in presenza di tre volte eccesso molare di 14-3-3η non ha fornito prove di un'interazione tra le due molecole.

Il legame alle membrane di α-syn è stato studiato mediante dicroismo circolare (CD). I primi 100 residui della proteina sono in grado di acquisire struttura α-elicoidale in presenza di micelle e liposomi carichi negativamente. Dati interessanti provengono dallo studio di dimeri di α-syn costituiti da due mutanti prodotti nel nostro laboratorio (V3C e Syn141C): l'omodimero formato da un ponte disolfuro tra la cisteina posizionata al C-terminale della proteina (dimero C-term) forma un'α-elica distorta in presenza di liposomi di 50 nm di diametro, composti di 50% DMPG 50% DMPC. Il dimero formato dal mutante V3C (dimero N-term) acquisisce struttura α-elicoidale paragonabile a quella osservata per il legame con micelle di SDS. È possibile che la dimensione (cioè la curvatura) dei liposomi e il legame covalente vincolante la coda C-terminale nel dimero C-term siano la causa dell'alterazione della struttura dell'α-elica.

Infine, la self-interazione di α-syn è stata oggetto di indagine con saggi di fibrillogenesi e di aggregazione. La formazione di fibrille è stata rilevata sulla base della variazione di intensità della fluorescenza della molecola Tioflavina T (ThT); campioni di wild-type α-syn, dimero C-term e mutanti patologici A30P, E46K e A53T sono stati incubati a 37 °C sotto agitazione; aliquote sono state raccolte a tempi fissi, miscelate con una soluzione di ThT e l'intensità di fluorescenza misurata a 485 nm. Il test ha rivelato che E46K, A53T e il dimero C-term formano fibrille più velocemente rispetto a wild-type α-syn, il mutante A30P presenta invece un ritardo nella lag-phase. Non è stato possibile ottenere una buona interpolazione dei dati con questo metodo, probabilmente a causa della precipitazione o della rottura delle fibrille di α-syn, o di eventi di light scattering in cuvetta dovuti alle fibrille. Pertanto, un protocollo pubblicato da Luk et al. (2007) è stato applicato. Questo metodo misura l'aumento della polarizzazione di fluorescenza (FP) di campioni di α-syn incubati a 37 °C sotto agitazione in una piastra a 96 pozzetti. α-Syn wild-type, mutanti patologici, dimeri C-term ed N-term sono stati mescolati con α-syn marcata con Oregon Green 488 (1:100 = Syn-OregonGreen: syn-α), e le variazioni nel tempo di FP sono state registrate. Il confronto tra i campioni dimostra che α-syn wild-type aggrega più veloce rispetto ai mutanti patologici e al dimero N-term, mentre il dimero C-term presenta il più veloce aumento di FP, con la minor lag-phase.. Il legame covalente al C-terminale sembra favorire l'interazione intramolecolare e quindi l'aggregazione e la fibrillogenesi. Lo spettro NMR è stato registrato per il dimero C-term formato per il 20% da molecole di α-syn marcate con ^{15}N, ma non è stata rilevata interazione intramolecolare. Inoltre, l'aggregazione di α-syn è stata testata in presenza di tre proteine. Mentre la presenza di DJ1 non comporta effetti statisticamente significatici sull'aggregazione di α-syn, la proteina chimerica 3T influenza la velocità di ingrandimento degli oligomeri di α-syn. Inoltre, il chaperone 14-3-3η mescolato in tre rapporti molari con α-syn sembra avere un effetto concentrazione dipendente sull'aggregazione di α-syn, anche se gli errori sperimentali non consentono una interpretazione conclusiva di questa osservazione. Tuttavia, α-syn in presenza di 14-3-3η equimolare mostra una velocità di aggregazione significativamente più lenta rispetto ai campioni di α-syn incubati in assenza di 14-3-3η.

In conclusione, sono stati raggiunti dei progressi sulla comprensione sul meccanismo molecolare di aggregazione α-syn, in particolare per ciò che riguarda l'orientamento dell'interazione intramolecolare che porta alla formazione di oligomeri e fibrille, e le proteine in grado di ostacolare la crescita di oligomeri di α-syn. Inoltre, un nuovo metodo basato sulla polarizzazione di fluorescenza è stata utilizzato per rilevare differenze in velocità di aggregazione e lag phase tra α-syn e sue varianti. Questa tecnica può essere utilizzata per

testare diverse condizioni, molecole e proteine in grado di influenzare l'aggregazione in vitro di α-syn.

Table of contents

Abbreviations

α-syn	α-synuclein
α-synHT	Histidine-Tagged α-syn
AD	Alzheimer's disease
AFM	Atomic Force Microscopy
β-syn	β-synuclein
CNS	Central Nervous System
DA	dopamine
DAQ	dopamino-quinone
DTT	ditiothreitol
EtOH	ethanol
FP	fluorescence polarization
FRET	Forster Resonance Energy Transfer
γ-syn	γ-synuclein
HFIP	hexafluoroisopropanol
HSQC	Heteronuclear Single Quantum Coherence
IE	Ion Exchange
K_d	Dissociation constant
LB	Lewy Bodies
LMW	Low Molecular Weight
MBT	2-(4-Maleimidophenyl)-6-methylbenzothiazole
NMR	Nuclear Magnetic Resonance
OG	Oregon Green 488
PA	phosphatidyc acid
PC	phosphatidylcholine

PD	Parkinson's Disease
PE	phosphatidylethanolamine
PG	phosphatidylglycerol
PS	phosphatidylserine
ROS	reactive oxygen species
rpm	revolutions per minute
RT	retention time
SDS	sodium dodecyl sulphate
SMFM	Single Molecule Force Microscopy
SN	*substantia nigra*
SNpc	*substantia nigra pars compacta*
SNpr	*substantia nigra pars reticulata*
SUV	small unilamellar vesicle
SynOG	Oregon Green labeled α-syn
synr	synoretin
TCEP	tris-carboxy-ethyl-phosphine
TEM	Transmission Electron Microscopy
TFE	trifluoroethanol
ThT	Thioflavin T
wt	wild type

Amino acids

Alanine	Ala	A
Arginine	Arg	R
Aspartic acid	Asp	D
Asparagine	Asn	N
Cisteine	Cys	C
Glutammic acid	Glu	E
Glutammine	Gln	Q
Glycine	Gly	G
Histidine	His	H
Isoleucine	Ile	I
Leucine	Leu	L
Lysine	Lys	K
Methionine	Met	M
Phenylalanine	Phe	F
Proline	Pro	P
Serine	Ser	S
Threonine	Thr	T
Tryptophan	Trp	W
Tyrosine	Tyr	Y
Valine	Val	V

Chapter 1: Introduction

1.1 Parkinson's Disease

1.1.1 The disease

Parkinson's disease (PD) was first described by James Parkinson in 1871 (Parkinson, 1871). PD is one of more important movement neurodegenerative disease of the present age; about 1-2% of people over 65 is affected. It becomes evident in the second half of life, with rising incidence with age. It causes a progressive loss of the ability to start movements and it is clinically characterized by bradikinesia, resting tremor, muscle rigidity. Moreover, patients can show non-motoric symptoms like autonomic, cognitive and psychiatric problems. To date, there is no remedy for PD and it ends with the premature death of the patient.

In 1912 Friederich Lewy described the inclusions characteristic of PD (Lewy, 1912). The microscopic analysis of Lewy bodies (LB) was done in 1960 (Duffy & Tennyson, 1965); this paper reported the accumulation of abnormal filaments in such inclusions. In 1919 Tretiakoff reported LB are particularly abundant in the *substania nigra* (SN) (Tretiakoff, 1919). He also observed neuronal degeneration in SN and supposed a correlation between neuronal loss and PD symptoms. This correlation was confirmed by Hassler in 1938 (Hassler, 1938). Later, LB were found also in post-mortem brains of patients of other disease like frontemporal dementia and multiple system atrophy (Lippa et al., 1998; Tu et al., 1998; Spillantini et al., 1998; Lippa et al., 1999; Duda et al., 2000).

Neurologically, PD symptoms are caused by a progressive loss of dopaminergic neurons of *substantia nigra pars compacta* (SNpc), which is the area of the brain involved in the project and the activation of the movement. The disease becomes evident after the death of about 70% of the dopaminergic neurons (Bernheimer et al., 1973). Dopaminergic neuron are less than 1% of the total number of brain neurons, but they are necessary for tasks specific

to the brain regions that they innervate, including motor behaviour, motivation and working memory (Chinta & Andersen, 2005). Moreover, SNpc is a "harsh" region of the brain, which is DA rich and contains both redox available neuromelanin and a high ion content (Chinta & Andersen, 2005).

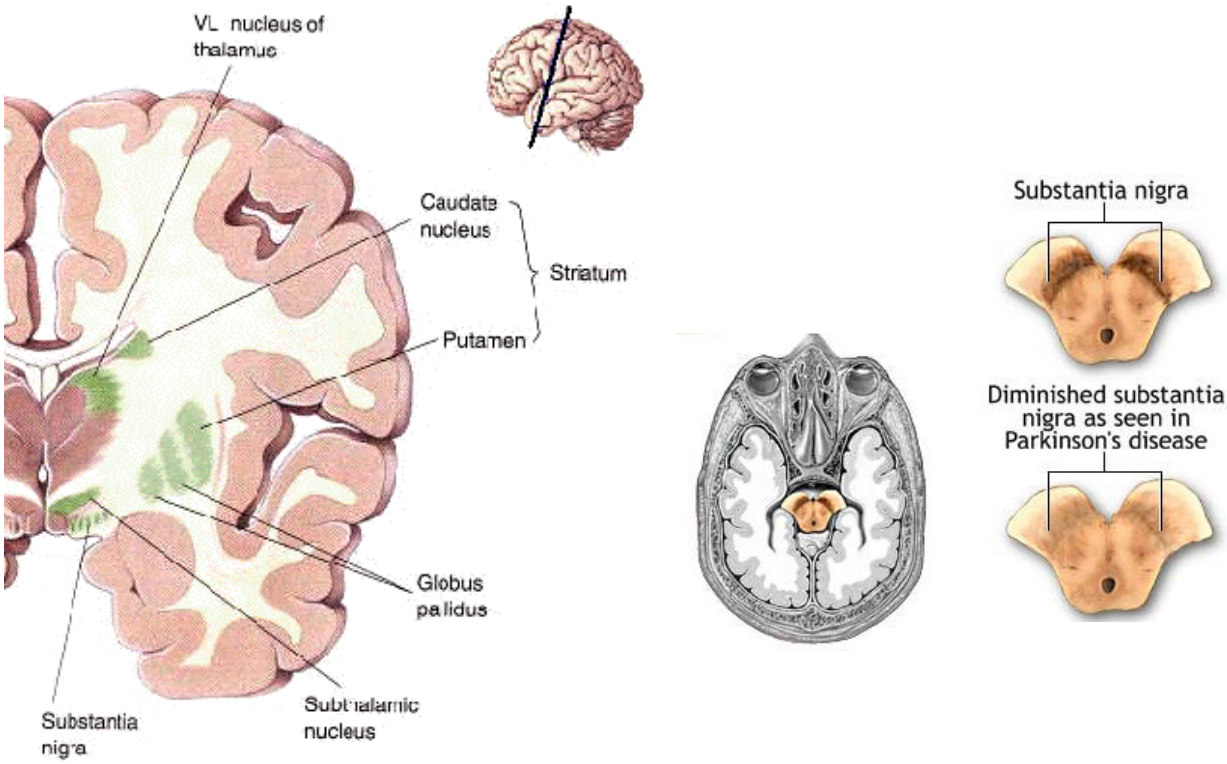

Figure 1.1.1: Localization of basal ganglia and substantia nigra in human brain (left). The loss of dopaminergic neurons in substantia nigra pars compacta can be seen as a depigmentation of the area in post-mortem brains of PD patients (right).

The pharmaceutical therapy consists of the chronic administration to patients of Levodopa (L-DOPA), a precursor of dopamine (DA) that can pass the blood brain barrier and it is internalized by neurons where it enters in the metabolic pathway of the synthesis of cathecolamines. Other treatments are based on inhibitors of enzymes involved in the metabolism or recaptation of DA, like monoamino oxidase B and DA decarboxylase inhibitors. However, these therapies are only symptomatic, as they do not solve neuronal loss nor they hamper further neuronal loss. Morevover, L-DOPA falls in efficacy because the numbers of neurons decreases with the development of the illness. The patient show some transitory improvements for the first years of the treatment, but with time a warning off mechanism leads to a decrease of effectiveness for this therapy. Furthermore, L-DOPA

therapy is merely symptomatic and do not avoid further neuronal death. A severe side effect of this drug, is schizophrenic-like syndromes or involuntary movements.

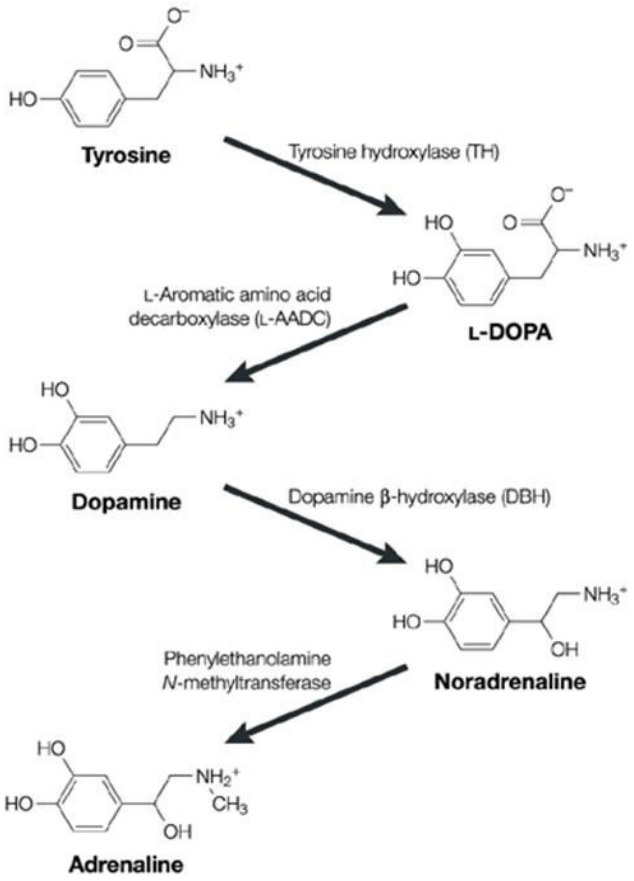

Figure 1.1.2: Dopamine, levodopa, and the metabolic pathway of catecholamines synthesis.

From the observation of post-mortem brains of PD patients show the presence of proteinaceous and lipidic aggregates in *substantia nigra pars compacta*, called Lewy bodies (LB) (Figure 1.1.3), and neuritis as inflammatory response signal. The analysis of LB reveals the presence of amyloid fibrils composed of alpha-synuclein (α-syn) (Spillantini et al., 1997; Spillantini et al. 1998), a protein that is normally and abundantly expressed at pre-synaptic level in all the central nervous system (CNS). A fragment of the same protein is present in amyloid plaques found in Alzheimer's disease (AD) patients. α-Syn LB are also found in dementia with LB. Nowadays, it is still unknown whether this kind of aggregates is responsible of neuronal death, or whether oligomeric annular species (Lashuel et al., 2002) can pierce cell membrane and zeroing transmembrane potential. LB can otherwise act as scavenger of excess α-syn that was not degraded by proteasome.

PD seems to be the result of several factors which affects specifically dopaminergic neurons. Several causes have been proposed but we are still far from a comprehension of the ethiopatogenesis of this disease.

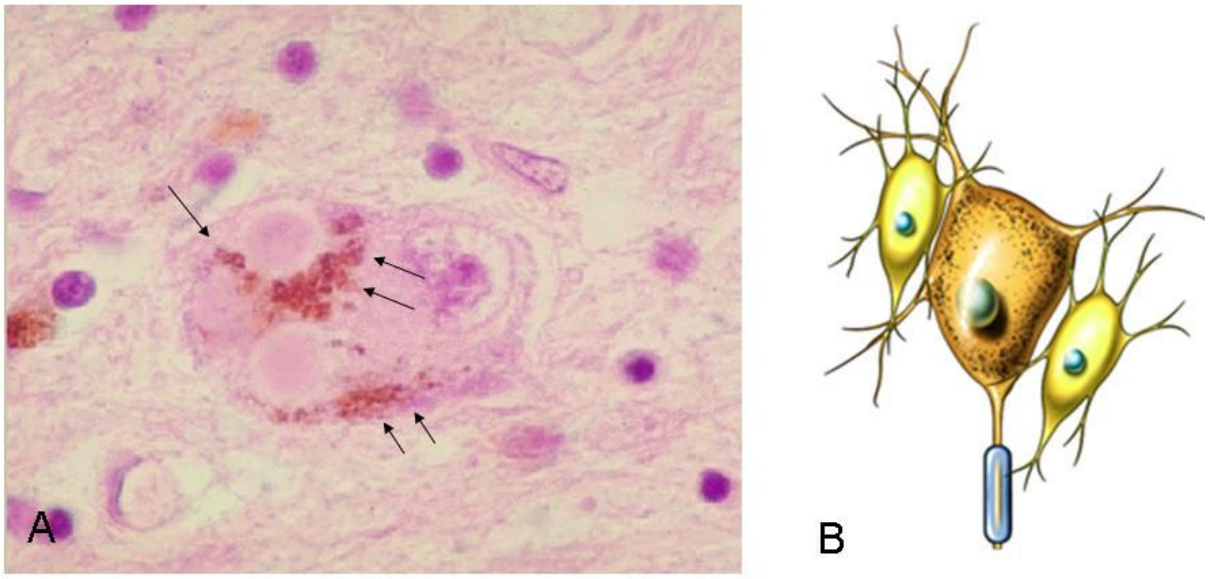

Figure 1.1.3: Lewy bodies (black arrows) found in dopaminergic neurons in SN of post-mortem brains of PD patients. Immunohistological pigmentation is positive for α-syn (A). Picture indicating the location of LB in neuron cell body (B)(© 2009 Nucleus Medical Art).

1.1.2 Genetics of PD

Ninety per cent of PD cases are sporadic. The remaining minority fraction of PD patients carries genetic form of the disease. Genetic linked PD can be autosomic dominant or autosomic recessive. A distinction has to be done between two terminologies. Parkinsonism defines the syndromic features of PD patients movement disorders. It is consistent with the loss of dopaminergic neurons in SNpc and consequent nigral degeneration. The second term is synucleinopathy, that identifies all the pathologies linked to α-syn accumulation in LB. This definition includes PD, dementia with Lewy bodies and multiple system atrophy.

All PD patients shows parkinsonism , but not all present α-syn accumulation. Generally, these latter cases are directly correlated with autosomic recessive PD. While autosomic dominant PD is linked to point mutant of α-syn A53T (Polymeropoulos et al., 1997), A30P (Krüger et al., 1998) and E46K (Zarranz et al., 2004) (§ 1.4.3), some recessive genes are associated with mitochondria and oxidative-stress related survival pathways, other with ubiquitin proteasomal system. Table 1.1 summarizes genes associated to PD known so far:

Table 1.1 Genes involved in PD (Wood-Kaczmar et al., 2006).

Locus	MOI	Gene (protein)	Protein function	Clinical presentation	Neuropathology	Age at onset
PARK1 (*PARK4*)	AD	*SNCA* (α-synuclein)	Unknown synaptic function	Duplications: Idiopathic PD; some postural tremor; slow progression	LBs	Mid 30–mid 60
				Triplications: PD; PD with dementia; diffuse LBs disease; aggressive course	LBs and LNs; ± glial inclusions; hippocampal CA2 and CA3 loss	Mid 20–30
				Mutations A53T, A30P, E46K: Idiopathic PD; parkinsonism and diffuse LBs	LBs and LNs; ± tau inclusions; amyloid plaques	30–60
PARK2	AR	Parkin	E3 ubiquitin ligase	Parkinsonism; slow progression	Variable presence of LBs	Juvenile to 40
PARK5	AD	*UCHL1*	Ubiquitin hydrolase and ligase	PD	Unknown	30–50
PARK6	AR	*PINK1*	Mitochondrial Ser–Thr kinase	Parkinsonism	Unknown	30–50
PARK7	AR	*DJ-1*	Oxidative stress response?	Parkinsonism	Unknown	20–40
PARK8	AD	*LRRK2* (dardarin)	Unknown protein kinase	PD	Diffuse LBs; LNs;± tau inclusions; ± amyloid plaques	40–60

Abbreviations: AD, autosomal dominant; AR, autosomal recessive; LBs, Lewy bodies; LNs, Lewy neurites; MOI, mode of inheritance; OE, overexpressed; PD, Parkinson's disease.

Mammalian parkin is primarily localized in the cytoplasm but a fraction appears to associate with the outer mitochondrial membrane (Darios et al., 2003). Parkin is an E3 ubiquitin protein ligase by targeting misfolded proteins to the ubiquitin proteasome pathway for degradation (Zhang et al., 2000). Mutations in the parkin gene are linked to autosomal recessive early-onset PD (Kitada et al., 1998; Zhang et al., 2000; Shimura et al., 2000). Mutated parkin seems unable to tag proteins that have to be removed, which accumulate in neurons.

Loss-of-function mutations in the DJ-1 locus are associated with rare forms of autosomal recessive early-onset parkinsonism (Bonifati et al., 2003). DJ-1 is a homodimeric, highly conserved protein of 19 kDa expressed in several tissues including brain (Bandopadhyay et al., 2007). Oxidative stress leads to an acidic shift of DJ-1's isoelectric point by oxidation of its Cys106 residue (Canet-Aviles et al., 2004). Also, since it undergoes autooxidation to remove H_2O_2, it may function as a scavenger of reactive oxygen species (ROS) (Canet-Aviles et al., 2004; Taira et al., 2004). Recently, some research groups suggested that oxidized DJ-1 acts as a chaperone that prevents early steps in the formation of α-syn aggregates (Shendelman et al., 2004) or α-syn fibrillogenesis (Zhu et al., 2006).

Some rare forms of familial PD are correlated to mutated PINK1, a mitochondrial serine/threonine kinase. Silvestri et al. (2005) demonstrated that PINK1 protein accumulates within the intermembrane space of mitochondria. Over expression of wild type PINK1 in some cell lines prevents mitochondrial cytochrome c release and subsequent apoptosis; this function is abolished in familial PD-linked PINK1 mutants (Petit et al., 2005).

Mutations in the leucin-rich repeat kinase 2 (LRRK2) cause autosomal dominant PD (Paison-Ruiz et al., 2004; Zimprich et al., 2004). Point mutations have been associated with 1-2% of apparently "sporadic" PD cases (Di Fonzo et al., 2005; Gilks et al., 2005; Nichols et al., 2005). The cellular and molecular mechanisms of LRRK2 toxicity remain to described, however a role for LRRK2 as a modulator in a mitochondrial dependent cell death pathway has been suggested (Paisan-Ruiz et al., 2004; Greggio et al., 2007; Lewis et al., 2007).

The ethiopathogenesis of PD is not completely understood. However, in the cases of sporadic PD patients, cells undergo a series of toxic insults that lead to proteasomal impairments and increase of oxidative stress damage. Several genes and cellular pathways are implicated (Figure 1.1.4), and single characters of neuronal death are becoming evident step-by-step. Neuronal death can not be prevented yet. Until the causes that triggers PD will not be understood, the development of drugs able to block nigral impairment and possibly restore motor functionality in patients will be very hard.

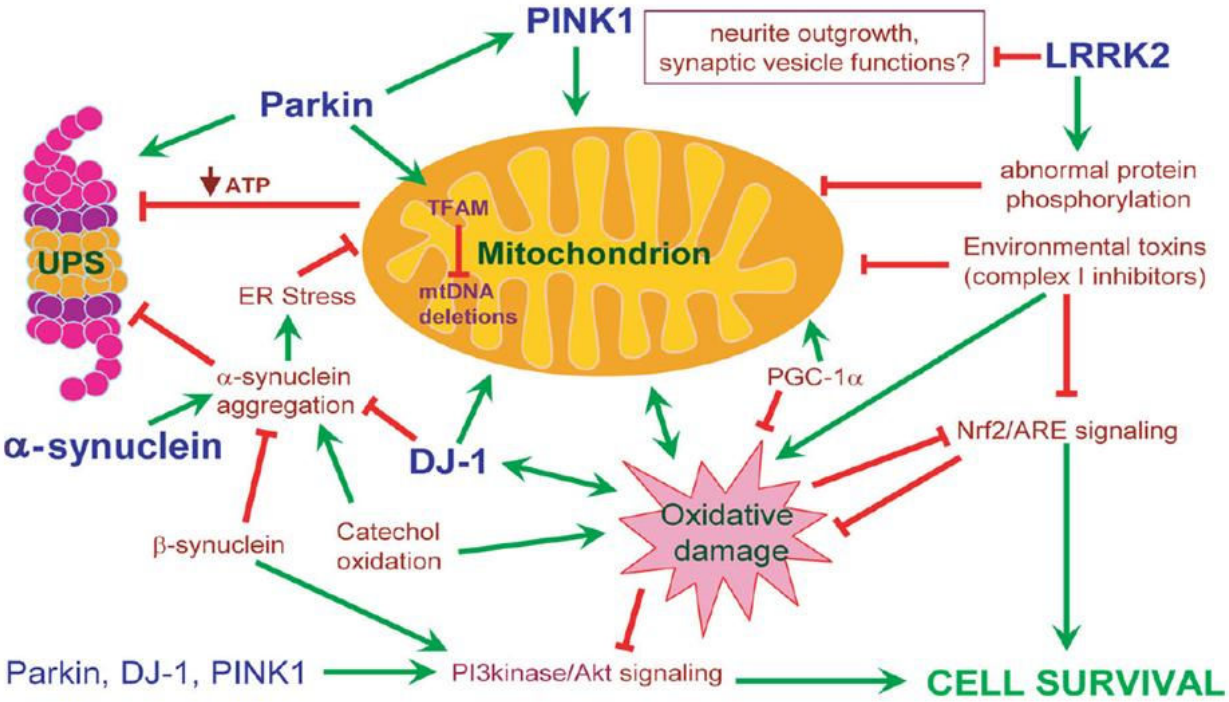

Figure 1.1.4.: Schematic representation of the cellular pathways mainly involved in damage that leads to PD (Thomas et al., 2007).

1.2 Alpha-synuclein

1.2.1 Location and putative biological role

α-Syn is a natively unfolded protein composed of 140 amino acids and its molecular weight is 14460 Da. It is expressed in all the Central Nervous System (CNS) at the pre-synaptic level (Kahle et al., 2004), and locally it is estimated to reach the concentration of 70-140 μM (van Raaij et al., 2008). Although it seems to be associated with synaptic vesicles (Clayton & George, 1999), it does not copurify with them (Takamori et al., 2006). α-Syn family is composed of four proteins: α-synuclein, β-synuclein, μ-synuclein and synoretin (Fig. 1.1).

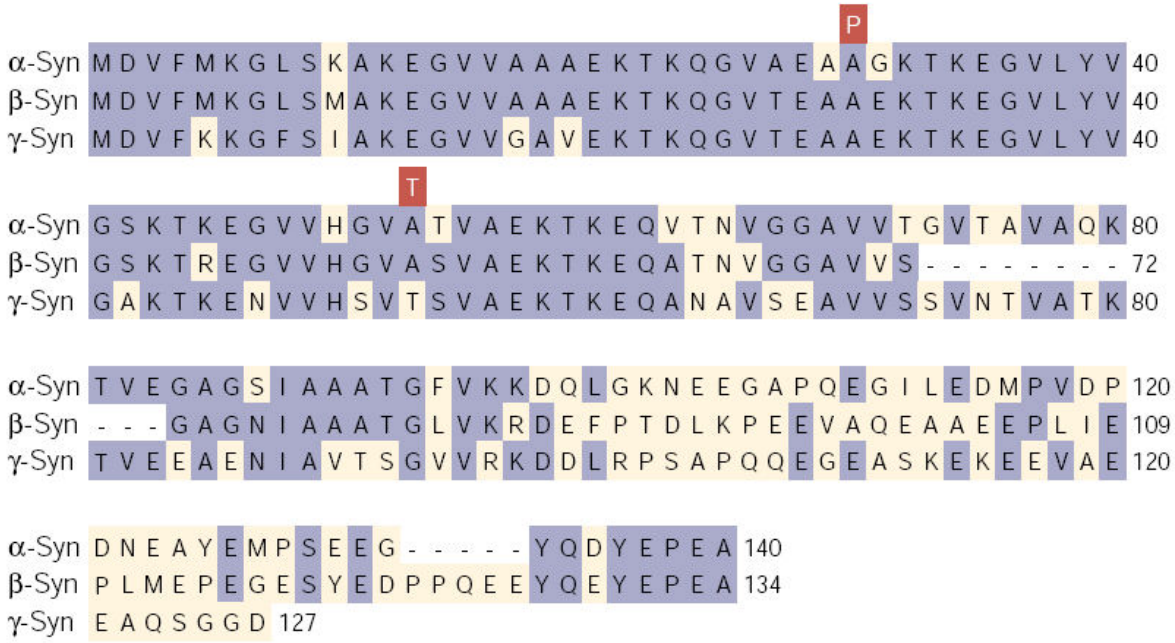

Fig. 1.2.1 Primary structure of synuclein family components (Goedert, 2001). Position of residues involved in early onset PD are coloured in brown.

α-syn and β-syn have similar level of cellular expression and distribution, while μ-syn and synr are prevalently expressed in peripheral terminals. The proteins in the family show a high degree of homology, however only α-syn is found in LB. In fact, β-syn is not included in amyloidogenic fibrils because it does not contain aa 71-82 of α-syn, believed to drive fibrillogenesis (Giasson et al., 2001).

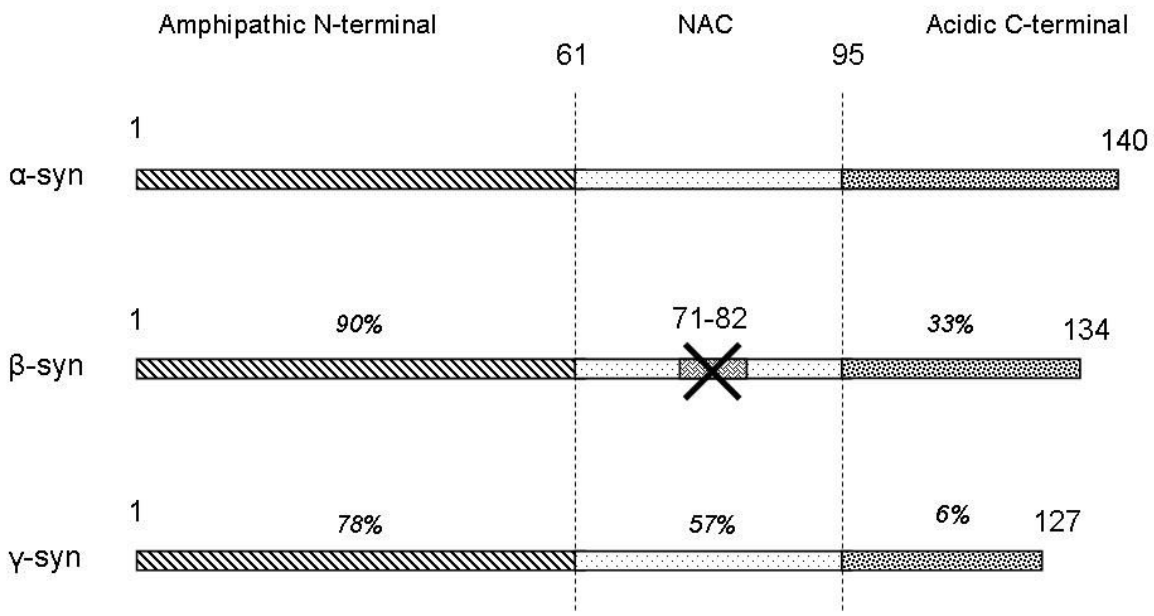

Figure 1.2.2: Sequence homology comparison between α-, β- and γ-syn. % of homology between distinct parts of the molecule are indicated in italics (Uversky & Fink, 2002).

The function of these proteins is still unknown. They are proposed to regulate dopamine neurotransmission by modulation of vesicular dopamine storage (Lotharius and Brundin, 2002). In addition, they seem to be involved in synaptic plasticity and learning (Clayton & George, 1998), but knockout mice present only minor deficits in nigrostriatal dopamine system (Abeliovich et al., 2000) as regards wild type ones. Nevertheless, α-syn overexpression rescues lethality associated with the lack of CSPα, a co-chaperone (HSP40 kind) associated with synaptic vesicles and implicated in folding of SNARE proteins, suggesting that α-syn may act as an auxiliary chaperone preserving the function and integrity of the synapse (Chandra et al., 2005).

1.2.2 Primary structure

The amino acid sequence of α-syn can be divided into three parts:

- N-terminal part, comprehending the first sixty residues, This region contains six imperfect repeats of the motif KTKEGV that is involved in the binding of detergents micelles and liposomes. In fact, this part of the molecule and the NAC one can form an amphipathic alpha-helix when it is in contact with such interactors, that it is compared to A2 helix type of apolipoproteins (§ 1.2.3). At the interface between the hydrophobic half and the hydrophilic one lysine residues are present to mediate the interaction, as the amine is positively charged and the

aliphatic chain can interact with lipids. This is why α-syn prefers negatively charged vesicle to interact with.

```
1        10          20          30          40          50
MDVFMKGLSK AKEGVVAAAE KTKQGVAEAA GKTKEGVLYV GSKTKEGVVH

51       60          70          80          90         100
GVATVAEKTK EQVTNVGGAV VTGVTAVAQK TVEGAGSIAA ATGFVKKDQL

101    110         120         130         140
GKNEEGAPQE GILEDMPVDP DNEAYEMPSE EGYQDYEPEA
```

Figure 1.2.3 : Primary structure of α-syn. Basic amino acid are coloured in blue, while acidic ones are red. The motive KTKEGV is underlined.

- NAC region, which corresponds to aa 61-95. The name is the acronym of Non β-Amyloid Component, as this part of the molecule is also found in amyloid plaques of Alzheimer's disease patients brains. This region is highly hydrophobic, and it can acquire β-sheet structure as it is the leader of amyloid fibril formation. In particular, aa 71-82 was described to be the responsible (Giasson et al., 2001) of α-syn aggregation, as deletion mutants do not form β-sheet structured fibrils, neither do β-syn, which lacks this region.
- The C-terminal tail of α-syn contains a large number of acidic amino acids and several prolines, so this region does not acquire structure in any condition. A regular repetition of the acidic residues can be observed:

```
109                 124
    QEGILEDMPVDPDNEA
    YEMPSEEGYQDYEPEA
125                 140
```

Figure 1.2.4: The last 30 aa in α-syn C-terminal tail. Acidic residues are coloured in red.

The region has a mM affinity for the binding of metals like Ca^{2+}, $Fe^{2+/3+}$, Al^{3+}, Co^{2+} and Mn^{2+} (Uversky et al., 2001). Divalent metal binding has been shown to increase fibril

formation rate. Ser129 is site of phosphorylation (Takahashi et al., 2003) and phosphorylated α-syn forms fibrils slower than wild type protein (Paleologou et al., 2008); phosphorylated α-syn is also found in PD patients LB (Takahashi et al., 2003). Also C-terminal tail seems to be involved in intermolecular interaction with the N-terminal part of the region, just for electrostatic interactions (§ 1.2.3).

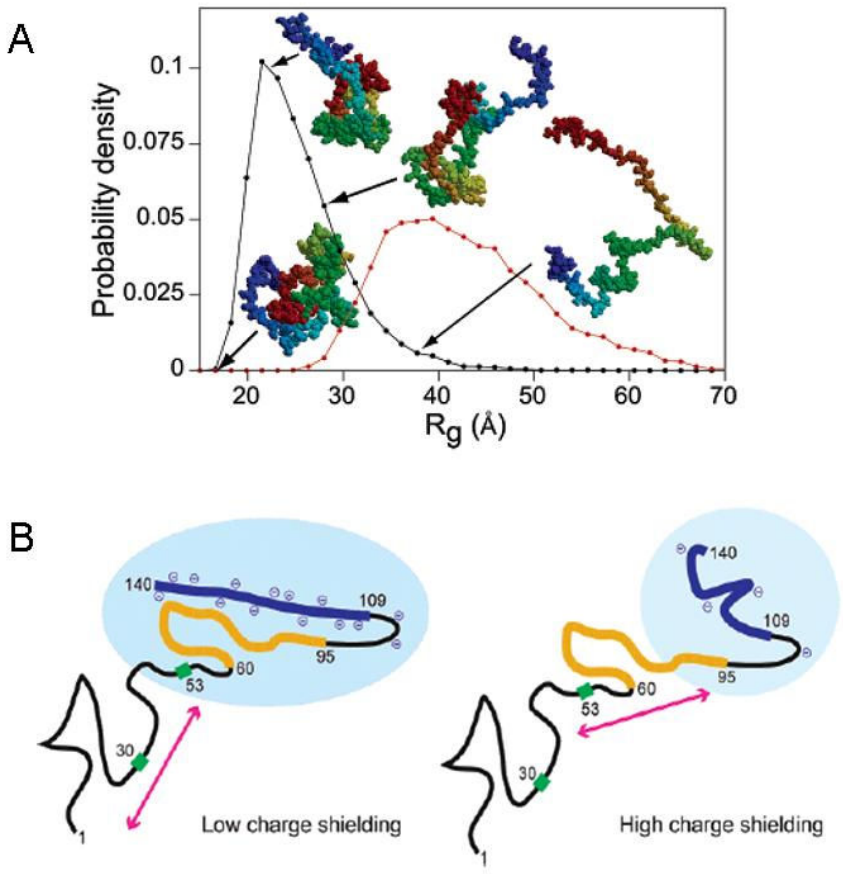

Figure 1.2.5: (A) Radius of gyration (Rg) probability distributions calculated for native (black) and random coil (red) models of α-syn. Representative structures are shown with arrows pointing to their corresponding Rg values. The structures are color-coded according to sequence, ranging from dark blue to red at the N- and C-termini, respectively (Dedmon et al., 2005). (B) Tertiary interaction formed by different regions in α-syn (Hoyer et al., 2004); intramolecular interactions are disrupted in high salt concentration conditions.

1.2.3 Structural flexibility

α-Syn can assume a wide range of conformations in different conditions, thus it is also named chameleon (Uversky, 2003). It is a natively unfolded protein, but paramagnetic relaxation enhancements (PRE) methods (Dedmon et al., 2005; Bertoncini et al., 2005) and

fluorescence based studies (Lee et al., 2004; 2005) demonstrated that the protein is no simply an unrolled polypeptide chain but there are some kind of intramolecular interactions that give the protein some kind of tertiary structure. Contacts between residues ~120–140 and ~30–100 were detected (Dedmon et al., 2005). This phenomenon implies that α-syn is not a simple polypeptide chain floating in solution with the gyration radius of a complete unfolded protein of 140 aa, but gyration radius value is intermediate between complete unfolded state and the value for a globular protein of the same MW (Dedmon et al., 2005). The forces involved singnificantly decrease in high salt concentration (Hoyer et al., 2004), as shown in Figure 1.2.5B.

This kind of interaction are important for the shielding of NAC region, which has been proposed to lead protein aggregation. So, all the conditions that favour the shielding action of the C-terminal tail result in a faster protein aggregation; these conditions include metal ions binding, high ionic strength or the proteolytic cleavage of the C-terminal region itself.

Some authors report the capacity of α-syn to transiently assume α-helical or β-sheet conformations. Eliezer et al. (2001) documented the tendency of the first 100 residues of α-syn towards α-helical torsion angles, and the following paper of the same group quantified this trend to exists for the about the 10% of the time (Bussell & Eliezer, 2001). Kim et al. (2007) found that region comprehending aa 39–98 of α-syn polypeptide chain is able to populate β-sheet conformations in solution at supercooling temperatures. This finding is relevant for the understanding of the first steps leading to amyloid fibril formation by α-syn. Also other works confirmed that α-syn is present in solution as an ensemble of conformers able to interchange each other in the microsecond timescale (Maiti et al., 2004; Lee et al., 2004; 2005).

A recent application in Atomic Force Microscopy (AFM) introduce the possibility to study unfolding resistance on single molecules (Kellermayer et al., 1997; Forman & Clarke, 2007). This method was applied to α-syn chimera proteins and it yielded relative distribution between α-syn conformers (Sandal et al., 2008; Brucale et al., 2009). Three distinct classes of structures were described: random coil, β-like structures and conformations stabilized by short- and long-distances weak interactions. Authors reported that α-syn was present is solution for 38.2% as random coil, 7.3% as β-like structured and 54.5% characterized by intramolecular interactions.

Hence, α-syn appears to be a very dynamic molecule. Conditions that alter the relative conformers distribution favouring one secondary structure tendency or another can influence fibril formation capacity of α-syn.

As α-syn contains apolipoprotein repeats motive in its first 100 residues,, it can assume α-helical structure as the protein binds to detergent micelles or liposomes. There are several papers that analyze such kind of interaction to describe the nature of α-syn helix. All the papers published agree that the C-terminal tail remains unfolded, and that α-syn prefers acidic detergents like sodium dodecyl sulphate, and phospholipids, like phosphatidylserine (PS), phosphatidylglycerol (PG) and phosphatidyc acid (PA) composed vesicles, or mixture with neutral phospholipids (phosphatidylcholine (PC) and phosphatilylethanolamine (PE)). (Davidson et al., 1998; Zhu & Fink, 2003; Zhu et al., 2003; Rhoades et al., 2006).

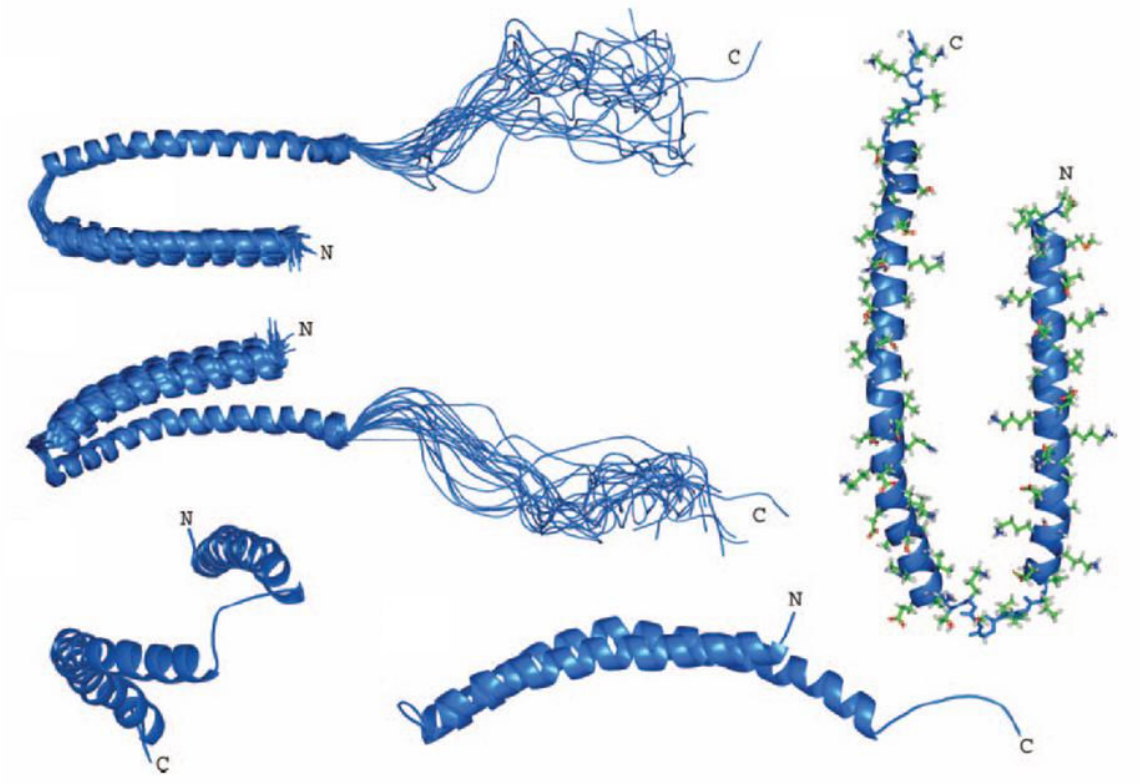

Figure 1.2.6: Model of α-syn bounded to membranes (adapted from Ulmer et al., 2003).

Circular dichroism (CD) suggested a cooperative adhesion to vesicles by α-syn motive repeats (Bisaglia et al., 2006), but fine structure calculation of α-syn membrane-bounded state is not possible, due to NMR signals broadening. Then all the investigations about the structure of α-syn bound to membranes were done in the presence of SDS micelles. Ulmer et al. (2003)

first describes SDS bound α-syn as two α-helix composed by aa 3-92, interrupted by a break at the level of residues 37-45 (Figure 1.2.6). Other two studies confirmed the formation of two α-helix interrupted by break (Chandra et al., 2004; Bisaglia et al., 2005). Other models suggest the formation of a non-canonical α-helix characterized by a periodicity of 11/3 (Figure 1.2.7), to better arrange to membrane curvature and place lysine residues on the interface between solvent and SUV surface (Bussell & Eliezer, 2003; Bussell et al., 2005; Jao et al., 2004; 2008). In this way, ε-amino group of lysine is responsible of the electrostatic interaction with negative charged headgroups of phospholipids, while the acylic chain suits well in the hydrophobic environment due to lipids tails. Other papers, by the same group, reported instead the absence of such break in an EPR studies of α-syn in association with liposomes (Jao et al., 2004; 2008). This suggests that helix breakage found in SDS bound α-syn can be an artefact due to micelle curvature. A recent paper based on EPR experiments reported the presence of both extended and interrupted α-helix (Drescher et al., 2008), in dependence of liposome dimensions. Finally, Georgieva et al (2008) described the presence of an extended helix, but introduced the possibility that α-syn can assume both conformations when bound to membranes.

Three main factors regulate α-syn interaction with lipids:

- the interaction with lipids is dependent on ionic strength of the solution and hydrophobic interaction stabilize the binding (Davidson et al., 1998; Jo et al., 2000; Zhu et al., 2003);
- vesicle size seems to influence α-syn affinity for membrane; in particular, α-syn has higher affinity for small unilamellar vesicles (∅ 25nm) compared to larger ones (∅ 125 nm) (Davidson et al., 1998). Another work does not report such a preference (Rhoades et al., 2006)
- binding is function of the mass ratio of α-syn to lipids (Zhu & Fink, 2003). The higher the ratio, the higher the tendency to assemble on lipid surface and starts protein aggregation. A low ratio α-syn assume α-helical conformation and does not proceed in fibril generation.

As α-syn was found to be associated to synaptic vesicles (Clayton & George, 1999), the investigation about α-syn binding equilibria, preferences and structure seems to be important for the comprehension of PD ethiopathogenesis, since vesicle bounded α-syn does not attend to fibril formation events.

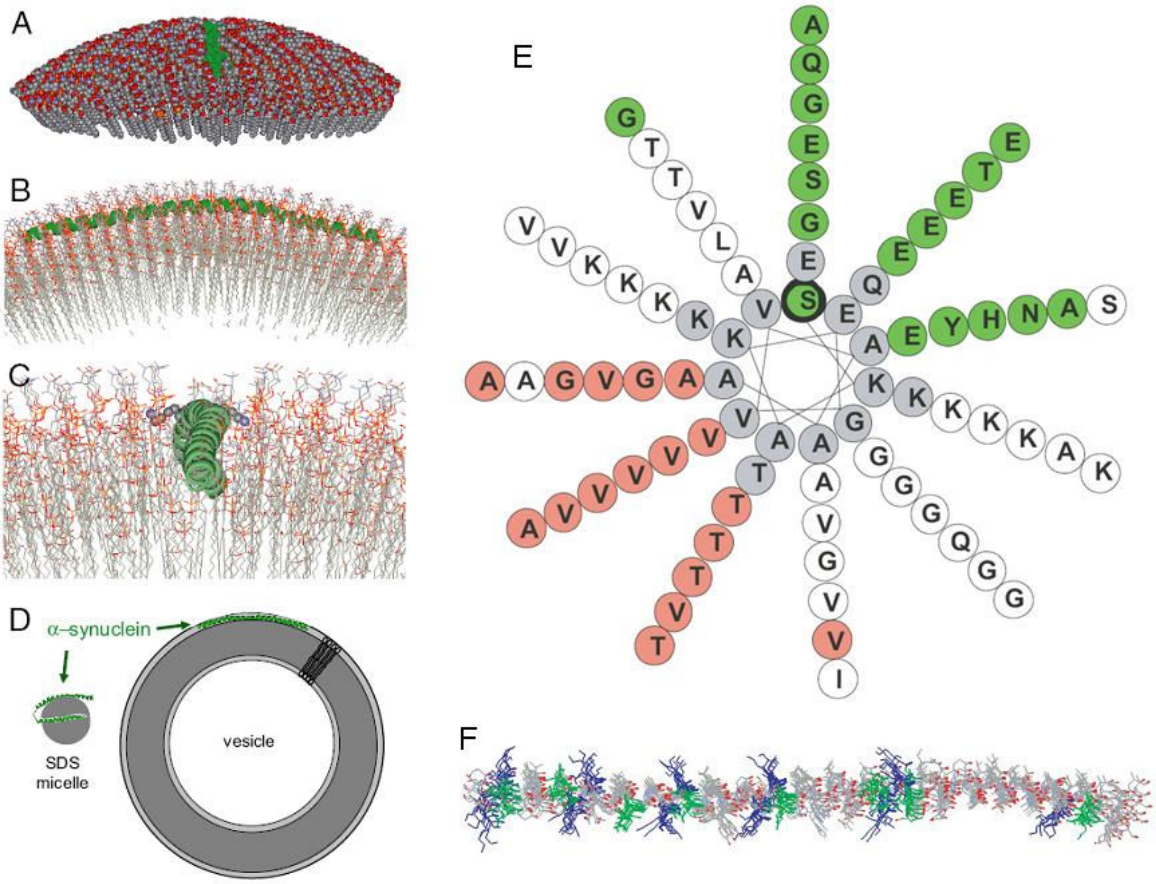

Figura 1.2.7: Model of vesicle bounded α-syn proposed by Jao et al. (2008). (A) and (B) are representations of the interaction of α-syn with a curved lipid surface. (C) A more detailed image of the protein–lipid interaction, viewed from the same angle as the image in A. The N terminus of the α-helix is in the foreground. Lysine residues 58 and 60 are shown in space-filling format. (D) Cartoon representations of the structures of α-syn on micelles and SUVs. The small and highly curved micelles cannot accommodate the extended helical structure present on the membrane. (E) The repeat region residues are plotted onto a helical wheel in which 11 aa make up three turns. Lipidexposed sites (red) fall onto one side, while solvent-exposed sites (green) lie on the opposite side. (F) View of the overlaid structures from above the lipid surface. The 11 lysine residues (blue) are oriented approximately perpendicular to the helical axis.

α-Syn secondary structure can also be induced by the presence of organic solvents. Munishkina et al. (2003) investigated on the effect of simple and fluorinate alcohols. In particular, hexafluoroisopropanol (HFIP) can induce alpha-helix starting from 2.5% v/v; the transition is complete at 30% HFIP in water. Ethanol (EtOH) is able to induce β-sheet conformation, the transition is complete at 60% v/v. Trifluoroethanol (TFE) is able to induce a more complex transition pathway, because the protein assume β-sheet conformation at 16%

v/v TFE than it evolves to alpha-helix at 40% TFE. Moreover, the protein becomes in about 15% TFE, than it comes back to monomer at 40% TFE.

Also acidic pH is able to induce some kind of conformation in α-syn. pH 3.0 is indicated as tertiary structure inducer. It is also demonstrated that acidic pH promotes α-syn aggregation perhaps favouring partial structure intermediates that led to a faster fibrils formation (Uversky et al., 2001b).

Finally, as α-syn is found in amyloid fibrils taken from post-mortem brains of Parkinson's disease patients (Pappolla, 1986). Amyloid fibrils are large ordered self-assembled structures formed by in register flanked β-sheet strands (Figure 1.2.8), firstly described from Amyloid β peptides involved in Alzheimer's disease pathogenesis, and then found to be formed also by other proteins. Those macromolecular structures accumulates in a lot of neurodegenerative disorders, like lateral amyotrophic slerosis, dementia with LB, mutiple system atrophy and systemic amyloidosis.

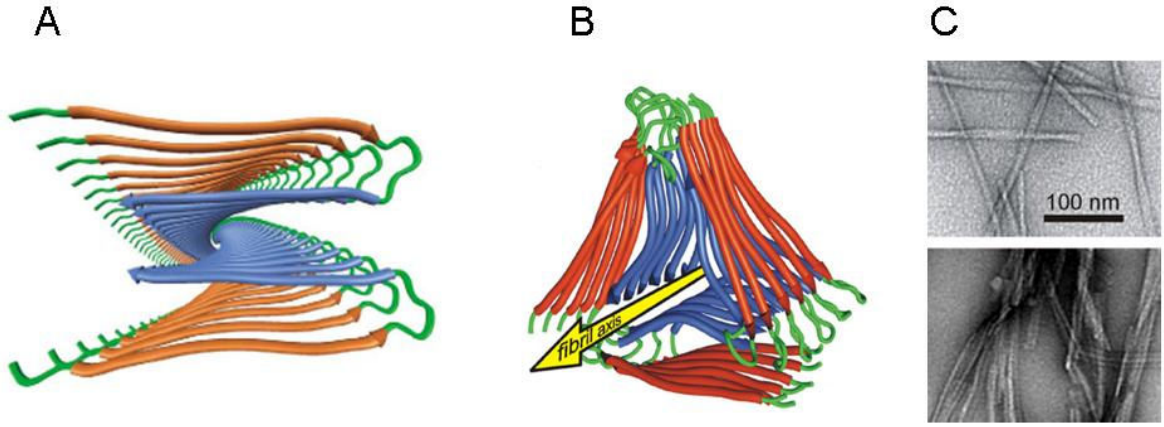

Figure 1.2.8: Models supposed for Amyloid β peptide fibrils (A and B). TEM images of Aβ fibrils formed in vitro (C).Adapted from Tycko (2004) and Parvastu et al. (2008).

As soon as α-syn fibrils was reproduced in vitro, they started to be studied to identify 3D structure. As they are not soluble, the determination of structure details is quite difficult. X-ray diffraction succeeded in describing dimensions of α-syn fibrils: a cross β-pattern constituted by a 0.47 nm spacing between main chains α-strands and 1.0 to 1.1 spacing between the β-sheet making the polymer (Serpell et al., 2000). This finding confirm that α-syn fibrils structure is analogous to amyloid fibrils. Several solid state NMR based studies reported region comprehending aa 38-98 as core of α-syn fibrils (Heise et al., 2005; Chen et al., 2007; Vilar et al., 2008). Findings about structure details of α-syn fibrils are reviewed by Bisaglia et al. (2009) and summarized in Figure 1.2.9.

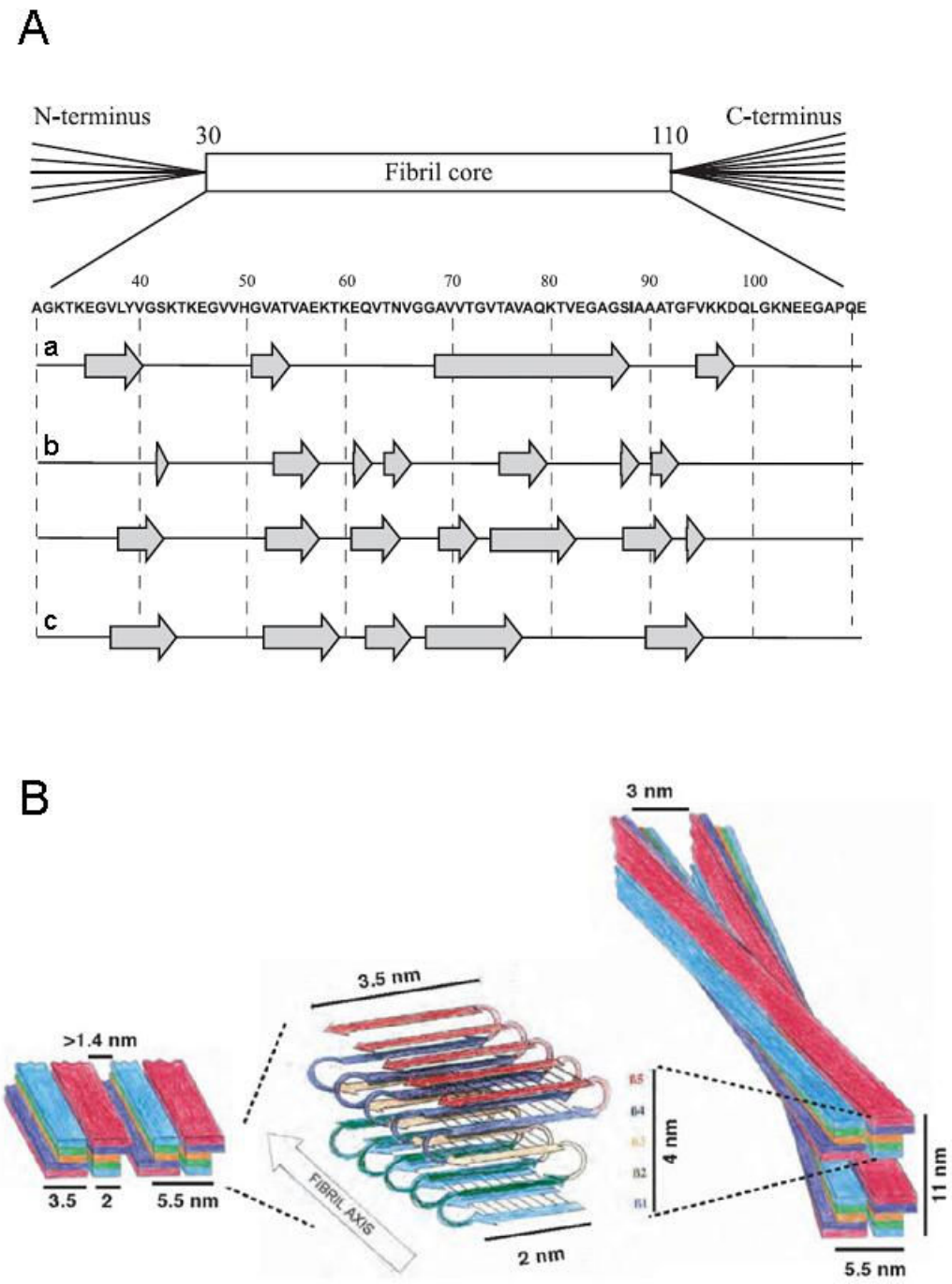

Figure 1.2.8: (A) Scheme of α-syn polypeptide residues supposed of chain involved in fibrils structure (Bisaglia et al., 2009). Models proposed respectively by Chen et al., (2007) (a), Heise et al. (2005) (b) and Vilar et al., (2008) (c). (B) Hypothetical model of α-syn fibril structure (Vilar et al., 2008).

While the central region of the protein is involved in fibril formation, the C-terminus is disordered and mobile and the N-terminal is unstructured till residue 2, from which the polypeptide chain shows some degree of rigidity (Vilar et al., 2008). The same work reports

also the presence of two kinds of structures, twisted or straight fibrils: straight fibrils are formed by two aligned protofilaments that can align again themselves. Twisted protofibrils are composed by two protofilaments twisted around each other, and then twisted again with other two twisted filaments. Hence authors proposed the possibility of various packaging types.

No details on aa implied in β-sheet formation is available to date.

1.3 The protein aggregation process

1.3.1 Protein folding and misfolding

Native states of the proteins almost always correspond to the structure that are most thermodinamically stables under physiological conditions. The folding of the proteins into their native 3D structure is the most important and elegant example of self assembly (Dobson, 2003). The mechanism by which a polypeptide chain assumes its unique native three dimensional structure is known as protein folding. Information for the 3D structure acquisition of a protein is encoded in its aa sequence (Anfinsen, 1973), and generally protein folding occurs soon after mRNA translation by ribosomes. Only correctly folded proteins have long-term stability in crowded biological environment and are able to selectively interact with their natural partners. The failure of proteins to fold correctly, or to remain correctly folded, is the origin of a wide variety of pathological conditions.

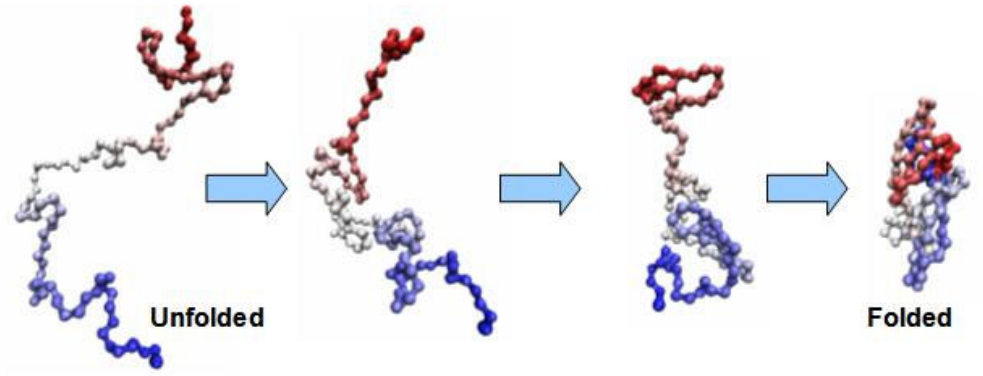

Figure 1.3.1: Protein folding requires the establishment of first intramolecular contacts that lead to the formation of secondary structures, then proceeds with the acquisition of complete native structure.

The total number of possible conformations of a polypeptide chain is so large that a systematic search for this particular structure would take an astronomical length of time. The inherent fluctuations in the conformation of an unfolded or incompletely folded polypeptide chain enable even residues that are highly separated in the amino-acid sequence to come into contact with one other.

The concept of folding funnel (Figure 1.3.2) describes the most probable pathways leading to the adoption of the unique native structure of a protein (Wolynes et al., 1995). In a folding funnel the unfolded state possesses the highest free energy and comprises an ensemble of multiple conformations constituting the starting point of the folding pathway. Unfolded protein starts to interact with other parts of the polypeptide chain and native-like contacts involving key residues are energetically favoured. This causes a fast collapse of the polypeptide chain, often driven by the formation of hydrophobic clusters decreasing the free energy of the system.

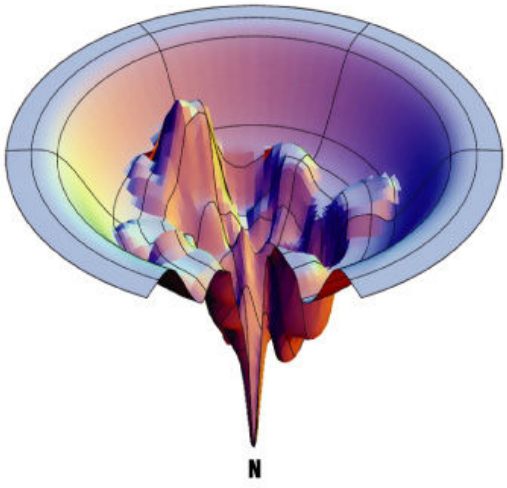

Figure 1.3.2: Protein folding funnel (Petsko & Ringe, 2004).

In some cases, protein folding requires the presence of other proteins known as chaperones, whose function is to assist proper folding especially big proteins. Some chaperones interact with the nascent chains as they emerge from the ribosome, whereas others are involved in guiding later stages of the folding process (Hardesty & Kramer, 2001; Bukau &Horwich, 1998). Importantly, processes like translocation across membranes, trafficking, secretion, the immune response and regulation of the cell cycle are directly dependent on folding and unfolding events (Radford & Dobson, 1998). Failure to fold correctly, or to remain correctly folded, will therefore give rise to the malfunctioning of living systems and hence to disease (Thomas et al., 1995; Dobson, 2001; Horwich, 2002). Whether impairments of the cell machinery devolved in misfolded protein elimination occur, the increase of

proteins that expose hydorphobic patches can lead to amyloid fibril formation. Some pathologies, including AD, PD, Prion diseases and late-onset diabetes are associated with the deposition of these structurally defined protein aggregates (Koo et al., 1999; Serpell, 2000).

Amyloid is defined in terms of empirical observations from X-ray fiber diffraction, electron microscopy, FTIR and specific chemical staining with dyes such as Congo Red and Thioflavine T. Deposits should be straight, unbranched, of about 10 nm in diameter, reach a μm in length, present a cross-β diffraction with two sharp reflections at 4.7 Å and 10 Å, and display green birefringence after staining with Congo Red.

Each amyloid disease involves predominantly the aggregation of a specific protein, although a range of other components including additional proteins and carbohydrates are incorporated into the deposits when they form in vivo. In neurodegenerative diseases, the quantities of aggregates involved can sometimes be so small as to be almost undetectable, whereas in some systemic diseases literally kilograms of protein can be found in one or more organs (Tan & Pepys, 1994). The ability of polypeptide chains to form amyloid structures is not restricted to the relatively small number of proteins associated with recognized clinical disorders, and it now seems to be a generic feature of polypeptide chains (Dobson, 1999; Dobson, 2001). The most compelling evidence for the latter statement is that fibrils can be formed in vitro by many other peptides and proteins, including myoglobin (Dobson, 2001). Even though the ability to form amyloid fibrils seems to be generic, the propensity to do so under given circumstances can vary markedly between different sequences. The relative aggregation rates for a wide range of peptides and proteins correlates with the physicochemical features of the molecules such as charge, secondary-structure propensities and hydrophobicity (Chiti et al., 2003).

1.3.2 Fibrillogenesis

In order to deposit in the form of ordered filamentous protein-rich aggregates, a dramatic change in the structure of a protein has to occur. A conformational change triggered on the polypeptide chain cause a transition from its natural soluble conformation towards a more insoluble state. In a globular protein the polypeptide main chain and the hydrophobic side chains are largerly buried within the folded structure. Only when they are exposed the conversion into amyloid fibril is possible. Independently of the originating protein, they all form a common cross-β structure in which continuous β-sheets are formed with β-strands running perpendicular to the fibril axis (Makin and Serpell, 2005). Many of the pathogenic

mutations that are associated with familial deposition diseases increase the population of partially unfolded states by decreasing the stability of the native state or reducing its global cooperativity. The aggregation process proceeds after the partially unfolded states are reached, then the number of β-sheet secondary structure enriched conformers increases. The probability of interaction of two of these species is low, but it may occur the case in which stable hydrogen bonds formation is established. Later, dimers can form stable contacts with other units, and oligomers start to grow. Soluble oligomers convert to fibrillation intermediates, designated protofibrils (Harper et al., 1997). Early formed metastable protofibrils typically comprise 10 to 50 monomers, depending on the protein involved, and appear to be spherical in nature. These spheres may anneal to form chainlike protofibrils, which can further form annular pore-like species or proceed to amyloid fibrils (Ding et al., 2002; Lashuel et al., 2002; Nichols et al., 2002).

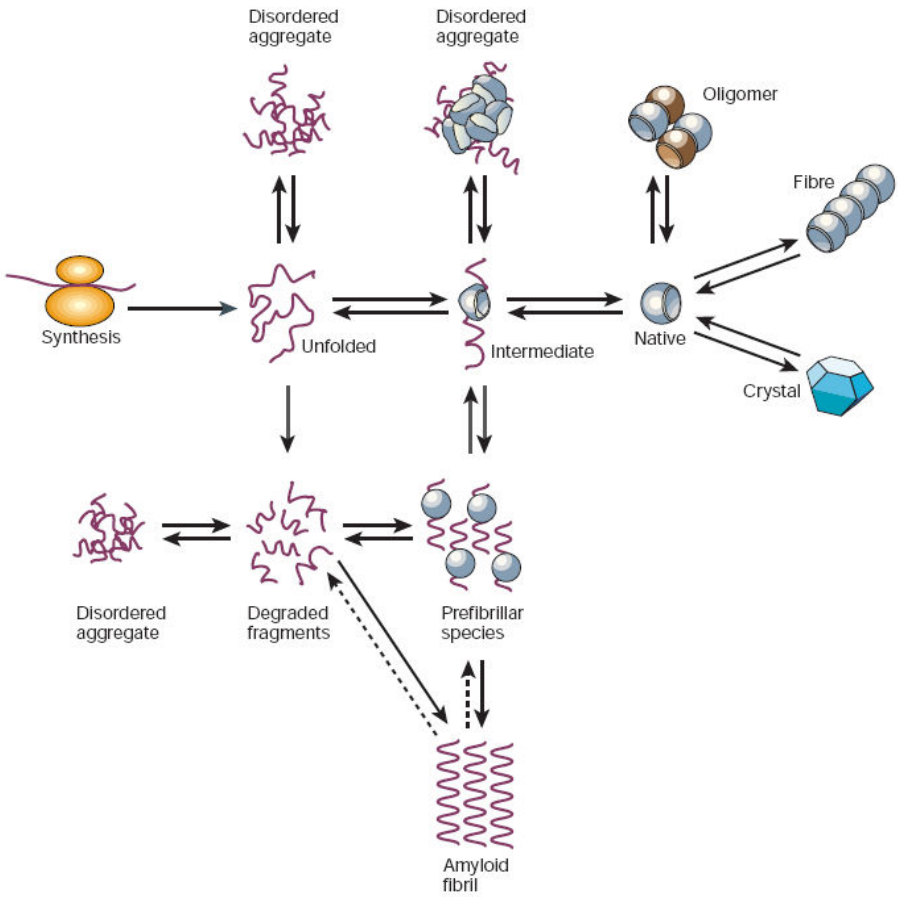

Figure 1.3.3: Conformational states of a protein in a cell and subsequent destinies (Dobson, 2003). The unfolded polypeptide chain can assume 3D structure after ribosome translation or can be degraded or form amorphous aggregates. Intermediates can assemble into prefibrillar species that lead to amyloid fibril formation.

Some evidences demonstrated that the pathogenic species on this kind of disorders relies on ordered oligomeric intermediate and not the fibrilar end-product of the protein aggregation pathway (Conway et al., 2000; Caughey and Lansbury, 2003). In particular, annular intermediates of α-syn fibril formation was observed (Lashuel et al., 2002), and it was demonstrated their ability to disrupt membranes (Zhu et al., 2003). Transmembrane channel-like currents were also recorded (Quist et al 2005; Zakharov et al., 2007) when α-syn oligomers were mixed with membranes. Also, protofibrils seem to affect cell viability, while amyloid fibrils were non-toxic (Bucciantini et al., 2002).

1.4 Alpha-synuclein aggregation

1.4.1. Molecular mechanism of fibrillogenesis

α-Syn ability to form fibrils and oligomeric species is abundantly documented in literature. Nowadays, the molecular details of the aggregation process leading to LB deposit is still unknown. As oligomers species are retained the more toxic (Conway et al., 2000; Lashuel et al., 2002), the transition rate between α-syn monomer to oligomers and oligomers to fibril elongation in one of the most compelling topic in the comprehension of the aggregation process of α-syn. α-Syn fibril formation is a nucleation dependent process, id est, the rate limiting step is the formation of a nucleus composed of a critical numbers of monomers (Wood et al., 1999; Murphy, 2007). The constitution of the nucleus is hosted, as monomers has to be in those rare and limited conformations prone to a stable interaction ones contact has occurred each other. However, ones this passage has been achieved, elongation or enlargement is a thermodynamically favoured process.

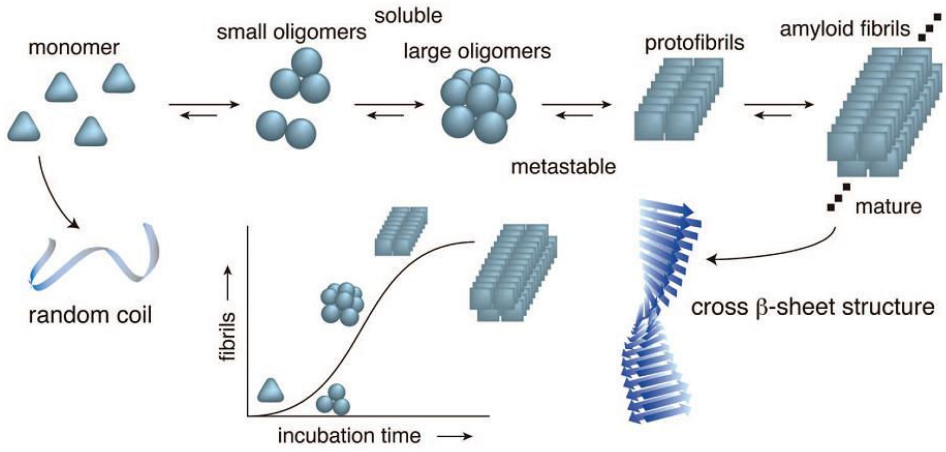

Figure 1.3.4: Intermediates involved in fibril formation (Takahashi & Mihara, 2008).

Table 1.2: List of some α-syn modification that enhance its fibrillogenesis. "+" indicates an enhancement of aggregation, while "–" an inhibition.

Factor	Aggregation	References
Ser129 phosphorylation	+	Muntané et al., 2008.
PD linked mutations	+	Conway et al., 1998; Greenbaum et al., 2005.
↑ Concentration	+	Wood et al., 1999.
↓ pH	+	Uversky et al., 2001b.
↑ Temperature	+	Uversky et al., 2001b.
↑ Ionic strenght	+	Hoyer et al., 2004.
C-terminal truncation	+	Crowther et al., 1998; Hoyer et al., 2004.
Oxidative modification	-	Glaser et al., 2005.
Metals	+/-	Paik et al., 1999; Uversky et al., 2001.
Human β- and γ-syn	-	Uversky et al., 2002.
Lipids	+/-	Perrin et al., 2001; Sharon et al., 2003.
Tau	+	Norris & Giasson, 2005.

1.4.2 Factors that influence alpha-synuclein aggregation process

Even if the comprehension of the aggregation and fibril formation processes is incomplete, several factors was found to inhibit or increase α-syn fibrillogenesis. Table 1.2 lists some documented factors that modifies aggregation rate of α-syn.

Some post-trasductional modifications seem to enhance α-syn fibril formation propensity. α-Syn is predominantly present as non-phosphorylated in normal in vivo conditions. However, Ser129 phoshorylation forms occur in α-syn inclusions in post-mortem patients brains (Fujiwara et al., 2002). Ser129 α-syn accumulation was also demonstrated in *Drosophila melanogaster* models of PD and transgenic mouse (Takahashi et al., 2003; Kahle et al., 2001).In vitro, Ser129 phoshorylation was found to increase the formation of α-syn mature fibrils. The role of α-syn phosphorylation remains to be clarified, oxidative stress increase α-syn phosphorylation by casein kinase 2 (Takahashi et al., 2007).

As α-syn aggregation is a nucleation dependent mechanism, every factor that increase the probability of the formation of the critical nucleus enhance fibrillogenesis. Thus, the increase in temperature is directly correlated with kinetic energy of molecules, then to enhanced reactivity of species. However, it must be noted that high temperatures can also change the relative conformers distribution. In addition, the higher the protein concentration, conformers able to form the critical nucleus are more concentrated and then the probability of

oligomer formation is higher. A familiar form of PD presents the triplication of α-syn, leading to autosomal dominant PD (Singleton et al., 2004).

Proteolytic cleavage of α-syn seems to occur naturally in neuronal cell (Li et al., 2005), and in vitro studies (Crowther et al., 1998; Hoyer et al., 2004) demonstrated that C-terminal truncation is able to increase fibrillogesis of α-syn by exposition of hydrophobic NAC region. Also high ionic strength conditions, masking C-terminal negative charges and then disrupting tertiary contacts between N-terminal and the C-terminal of the protein, enhance fibrillogesis due to high exposition of hydrophobic patches (Hoyer et al., 2004). The same mechanism seem to regard divalent and trivalent metals, as they interact electrostatically with α-syn C-terminal tail (Uversky et al., 2003). A distinction has to be done for Cu^{2+}, as it binds specifically to α-syn making contacts between N-terminal acidic residues and Histine 50 of α-syn, with a dissociation constant of 0.1 μM (Binolfi et al., 2006). The presence of Cu^{2+} in solution enhance aggregation properties of α-syn.

A destabilization of tertiary structure is caused by acidic pH. As the isoelectric point of α-syn is 4.6, lowering pH in solution involves the decrease of net charge of the molecule, and the disruption of tertiary contacts established between acidic C-terminal tail and positive charges N-terminal region. The consequence is the modification of conformers ensemble and a higher tendency to fibril formation (Uversky et al., 2001b).

While the interaction with membranes implies an α-helix acquisition of α-syn, submicellar lipids and detergents enhance aggregation propensity of α-syn, expecially in the case of polyunsaturated fatty acids like arachidonic acid and docosohexaenoic acid (Perrin et al., 2001). Also high protein:lipid molar ratios increase fibril formation probabilities (Zhu et al., 2003). The mechanism of this latter finding can be a recruitment of non α-helical characterized conformers of α-syn that may start protein-protein interaction.

While incubating α-syn with non amyloidogenic members of its family implies the inhibition of fibrils formation in vitro (Uversky et al., 2002), other proteins produce opposite effects. Some proteins have been identified to stimulate α-syn in vitro aggregation at substoichometric concentrations, like tau (Norris & Giasson, 2005), histones (Goers et al., 2003), brain specific protein p25α (Lindersson et al., 2005) and tubulin (Alim et al., 2002). Size-exclusion chromatography and native gel experiments performed by Zhou et al. (2006) showed no interaction between α-syn and DJ-1 (§ 1.1.2), although the same authors reported an inhibition of α-syn fibril formation by the oxidized form of the protein, whereas reduced DJ-1 does not provide the same effect.

The demonstration of oxidatively nitrated α-syn in the α-synucleinopathic inclusions suggests that oxidative insults may be relevant to the pathogenesis (Duda et al., 2000b; Giasson et al., 2000). Exposing recombinant α-syn to nitrating agents induces formation of stable nitrated α-syn oligomers (Yamin et al., 2003). Modifying α-syn by oxidative attachment of a dopamine adduct results in a stabilization and subsequent accumulation of α-syn oligomers (Conway et al., 2001). Iron and cytochrome c catalysed oxidation by H_2O_2 also stimulate α-syn aggregation (Hashimoto et al., 1999; 1999b; Ostrerova-Golts et al., 2000). An opposite effect of oxidizing α-syn has been demonstrated as methionine-oxidized α-syn is non-fibrillogenic and inhibits aggregation of unmodified α-syn (Uversky et al., 2002b).

1.4.3. Early onset pathological mutants. Structural features and fibrillogesis

Autosomal dominant early-onset PD has been linked to three point mutations (A30P, A53T, and E46K) in the gene encoding α-syn (Polymeropoulos et al., 1997; Krüger et al., 1998; Zarranz et al., 2004). In vitro studies have indicated that the mutations influence the kinetics of α-syn fibrillation: the rate is increased for the A53T and the E46K substitutions (Conway et al., 1998; Greenbaum et al., 2005), while it is decreased in the case of A30P (Conway et al., 2000). Moreover, in comparison with the wt protein, both the A53T and the A30P mutations promote accumulation of prefibrillar oligomeric species (Conway et al., 2000), while the E46K protein reduces the formation of such aggregates (Fredenburg et al., 2007). As A53T and A30P mutants are able to form prefibrillar intermediates with pore-like activity, a model of cytotoxicity has been proposed in which the toxic species were the oligomeric species (Conway et al., 2001; Volles & Lansbury, 2002). The same tendency to form pore-like soluble aggregates similar to annular species was observed also for E46K, displaying permeabilizing activity (Fredenburg et al., 2007).

The structural studies on the point-mutated α-syn variants were performed mainly on the first mutants discovered. NMR analyses indicated that A30P and A53T mutations have no global effects on the structural properties of the protein or on the dynamic behaviour of the α-syn backbone (Bussell & Eliezer, 2001). Nevertheless, the secondary structure propensity for the free disordered state of the wt protein was different the two PD-linked variants. Specifically, the analysis of the Cα secondary shifts revealed that the A30P mutation decrease the helical propensity found in the N-terminal region of wt α-syn, whereas the A53T mutation induce a more subtle and local preference for extended β-sheet like conformations around the site of mutation (Bussell & Eliezer, 2001). More recently, an additional NMR study indicated that the E46K mutation results in only very minor conformational changes in the free state of

α-syn (Fredenburg et al., 2007). Bertoncini et al. (2005b) analyzed the perturbation induced by A30P and A53T mutantion in α-syn conformers ensemble. The two variants show increased backbone flexibility and the absence of the long-range interactions that were previously observed in the wt protein. In these mutants the number of conformation available are larger and possibly there is a reduced shielding of hydrophobic NAC. The possibility to an easier overcome of the energetic barrier for self-association has been suggested by the authors as the cause for the increased propensity of these proteins to aggregate. A modified distribution of conformers, compared to the wt protein, was also observed for A30P in a single-molecule AFM study (Sandal et al., 2008).

The effect of the PD-linked mutations on the interactions of α-syn with membranes has been widely investigated. While the A53T mutation seems to have little effect on membrane binding (Perrin et al., 2000; Bussell & Eliezer, 2004), several reports indicate that the A30P mutation decreases the extent of lipid interactions in vitro (Perrin et al., 2000; Jo et al., 2002) and in vivo (Jensen et al., 1998). In contrast, E46K mutation increases the ability of the protein to bind to negatively charged liposomes (Choi et al., 2004). Structural analyses on α-syn mutants were performed only in the presence of SDS micelles. In the first study, the Cα chemical shift deviations of A30P and A53T α-syn variants were compared with those found for wt α-syn (Bussell & Eliezer, 2004). A53T data provide no structural difference in the binding to SDS micelles relative to wt α-syn. On the contrary, A30P mutation appears to destabilize the helical structure of the protein around the site of the mutation (Figure 1.4.1). A similar NMR analysis of the E46K variant in its helical state indicated structural modifications that are not large enough to suggest a disruption of the secondary structure of the protein. Rather, they seem to suggest some rearrangement of the helical structure with respect to its surrounding environment (Fredenburg et al., 2007).

No difference in structure and dynamics were observed comparing A53T mutant and wt α-syn. In the case of the A30P mutation, the introduction of a Pro residue causes the interruption of N-terminal helix at the level of A27 instead of A37, but the two helices of A30P are found in an antiparallel orientation (Ulmer & Bax, 2005), in analogy for what found for α-syn (§ 1.2.3). Structural studies on familial PD-linked mutations in a more physiologically relevant membrane-mimetic system are still lacking. In a recent study, wt α-syn, E46K and A53T mutants were found able to form helix-based ion channels with well-defined conductance states in membranes on application of a trans-negative potential (Zakharov et al., 2007). The basic character of KXKE repeats are suggested to allow voltage sensing, serving as energy-transducer elements to drive the helices into a trans-membrane

orientation. The observation that the A30P mutant did not form ion channels was rationalized by assuming that the helix break due to the mutation close to the apex of the helix hairpin would increase the energy cost of this hairpin movement across the hydrophobic core of the membrane.

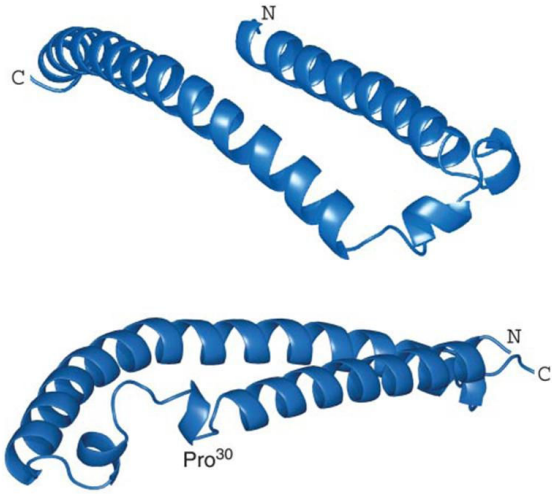

Figure 1.4.1: Average secondary structure of micelle bound A30P (Ulmer & Bax, 2005).

1.5 Interaction with proteins

Co-immunoprecipitation and affinity experiments allowed the identification of a wide variety of proteins that can interact with α-syn. All the interactions found are matter of debate into the scientific community because not all the cases reported were confirmed. In some cases, opposite assertions were done. Then, the investigation of α-syn interaction is still an actual topic as it can also help in the comprehension of the biological role of α-syn.

Experimental evidences found that Synphilin-1 is able to interact in vivo with α-syn (Engelender et al., 1999). Synphilin-1 is a protein of 919 amino acids, which contains different domains, such as ankyrin-like repeats, a coiled-coil domain and a putative ATP,GTP-binding domain (Engelender et al., 1999); its biological role is still unknown. It localizes to the presynapse where it binds to synaptic vesicles (Ribeiro et al., 2002) and may affect dopamine release (Nagano et al., 2003). Various synphilin-1 regions were found to contribute to the interaction with α-syn, with both the N-terminus and the central region involved in the interaction (Kawamata et al., 2001; Ribeiro et al., 2002; Neystat et al., 2002). Thus, synphilin-1 may also play a central role in PD. In fact, co-expression of synphilin-1 and

α-syn in cells in culture leads to the formation of Lewy body-like inclusions (Engelender et al., 1999). Besides interacting with α-syn, synphilin-1 interacts with other proteins involved in the pathogenesis of PD: parkin (Chung et al., 2001) and LRRK2 (Smith et al., 2006), a protein kinase involved in both autosomal dominant and sporadic PD (Zimprich et al., 2004). The interaction of synphilin-1 with different proteins involved in PD suggests that it may assemble these proteins into a multi-protein complex. Synphilin-1 was found to be present in the core of Lewy bodies from PD brains (Wakabayashi et al., 2000). The observation that synphilin-1 is an integral component of Lewy bodies implies that it may play a role in their formation (Szargel et al., 2008).

Sidhu et al. (2004) reported the modulation of α-syn on DA transporter (DAT), and that the disruption of this modulatory process permits increased re-uptake of high levels of intracellular dopamine by DAT, causing profound neurotoxicity. In addition, Perez et al. (2002) observed a modulation of tyrosine hydroxylase in vivo, favouring the hypothesis of a direct role of α-syn in DA homeostatis.

A recent study on PLD2 inhibition by α-syn was published (Rappley et al., 2009), although Payton et al. (2004) reported details on α-syn modulation on PLD2. Hence, this argument remains controversial. The regulation of the activity of PLD2 by α-syn would lead to relevant implication in membrane interaction of α-syn, as PLD2 hydrolizes phospholipids producing phosphatidic acid. This influences membranes curvature, which was reported to be important in α-syn interaction with membranes.

Several publications reported the interaction of α-syn with protein involved in signal transduction. Two of them documented α-syn binding to calmodulin (CaM), reporting respectively a ~ 0.3 μM and a 20 nM dissociation constant (Lee et al., 2002; Martinez et al., 2003). These findings would have a relevant biological implication whenever it was found a calcium dependence of this interaction. However, Bertini et al. (2007) measured with paramagnetic-based NMR a dissociation constant in the μM range, levelling the physiological importance of this event.

14-3-3 proteins are a family of highly conserved acidic proteins, expressed in all eukaryotic cells (Gardino et al., 2006). They are expressed in almost all tissue, and they represent the 1% of total brain proteins (Berg et al., 2003). The diverse biological function ascribed to 14-3-3 proteins depend on their ability to bind and regulate a wide variety of proteins. At the moment approximately 200 different cellular proteins, involved in almost every cellular process, such as cell cycle progression, the DNA damage response, apoptosis, protein trafficking, signal transduction, cytoskeletal rearrangements, metabolism,

transcriptional regulation of gene expression, development and stress response, and cell adhesion, are described as binding partners for the 14-3-3 proteins (Aitken, 2006). By the binding and activity modulation of such a wide variety of proteins, 14-3-3 bind have a fundamental role in the coordination of key points in the biological functions network. Several line of evidence, supported by proteomic (Zhou et al., 2004), immunological (Ostrerova et al., 1999) and biophysical (Sato et al., 2006) studies, suggest that α-syn and 14-3-3 proteins can interact both in vivo and in vitro. Ostrerova et al. (1999) demonstrated that the first 60 residues of α-syn and the fragment spanning from 40 to 100 residues of 14-3-3 proteins share over 40% homology. Moreover, the complex of the two proteins (specifically ε and β isoforms were detected) can be isolated from both brain homogenate and neuronal cell culture using specific antibodies. The interaction was further confirmed by Zhou et al. (2004) that identify the ensemble of proteins, from a brain homogenate, trapped by synuclein immobilized in a chromatographic matrix. By quantitative proteomics approach they detect both 14-3-3 ζ, θ, τ and ε isoforms and TH as α-syn binding partners. The strongest data supporting an interaction between 14-3-3 proteins and a-synuclein derives from Surface Plasmon Resonance analysis (Sato et al., 2006). These experiment provided a K_d value of 1.1 μM for the complex formation in solution between recombinant α-syn and 14-3-3η isoform.

1.6 Aim of this thesis

α-Syn is one of the most challenging protein to study. In fact, it is evidently implied in PD and in other neudegenerative disease, its function is still unknown and the molecular mechanism that lead to its oligomerization and fibril formation are poorly clarified. More importantly, the causes of protein accumulation and neuronal death in PD are not clarified, thus hosting the possibility to design pharmaceutical strategies that prevent the progression of this disease.

α-Syn is a natively unfolded protein, but its conformational plasticity makes it able to interact with a wide variety of biological partners. The binding to membranes entails the acquisition of α-helical structure, while self-interaction implies the conversion into β-sheet characterized amyloid fibrils. Moreover, α-syn is not a simply unrolled polypeptide chain in solution, but it exists as an ensemble of conformers constituted by distinct partially folded states or intramolecular tertiary contacts characterized molecules. Each single conformer can interact with biological partners such as protein, ions and small molecules, membranes and

itself. It is possible that early onset PD linked single point mutations can alter the conformation ensemble of α-syn, leading to a higher propensity in self-assembly and fibrillogenesis. Protein modification like oxidation and the interaction with ions also alter the possibility of conformation rearrangement. It was demonstrated that protein oxidation favours the formation of α-syn oligomers, while it hampers the consequent fibril formation. Divalent metals instead involve the exposition of hydrophibic NAC region, by the interaction with the acidic C-terminal end of α-syn. Protein-protein interaction and membrane binding confiscate α-syn molecules from the equilibrium that lead to some of them to protein aggregation. Hence, understanding the equilibria that govern these events is important both for the comprehension of the biological role of α-syn and the identification of molecular mechanisms that trigger fibrillogenesis. Moreover, alterations in such equilibria can shift the preferred conformers in solution, thus favouring those implied in molecular aggregation.

In the Figure 1.5.1 reported below, there is a scheme of α-syn interaction network. The aim of this PhD thesis is the improvement of this scheme with the analysis of some aspects of protein-protein interaction and membrane-α-syn association. Particular emphasis will be given to α-syn aggregation. Early stages of α-syn oligomeration are poor characterized. Another aim of this thesis is the validation of a method recently applied to α-syn aggregation based on fluorescence polarization. The setting up of a high throughput method able to test several conditions and interacting protein will provide a useful tool for the advance in the knowledge in α-syn aggregation process.

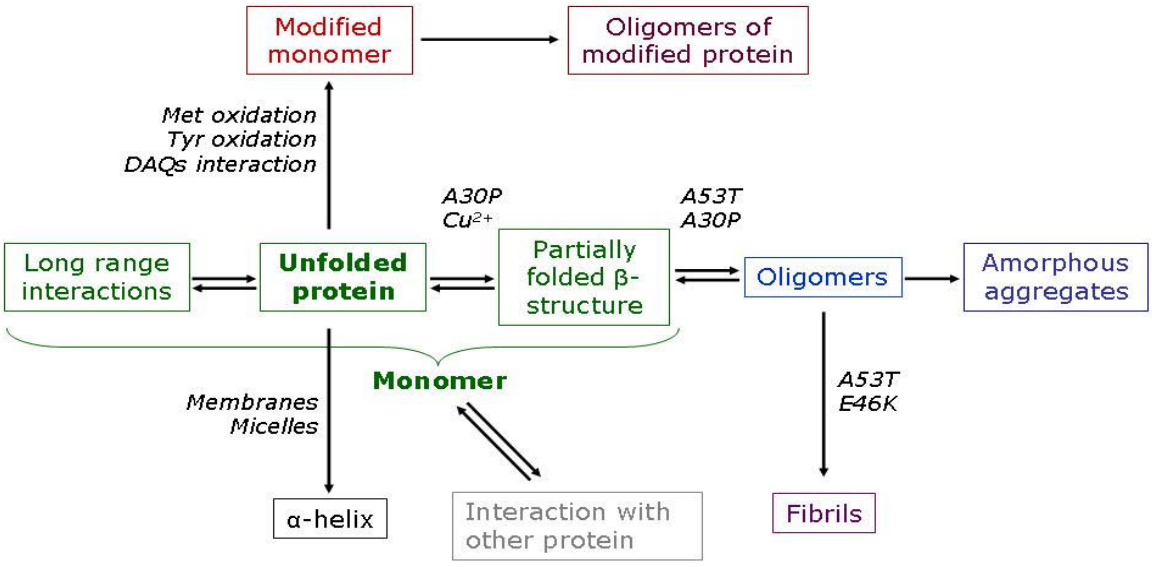

Figure 1.5.1: The interaction network of α-syn.

Chapter 2: Materials & Methods

2.1 Principles of Fluorescence Polarization and Surface Plasmon Resonance

2.1.1 Fluorescence Polarization

When a sample containing a fluorophore is subjected to a polarized incident radiation, only molecules which dipole moment is oriented parallel to the excitation plane can absorb a photon and then emit light. Fluorescence polarization (FP) and anisotropy (r) can be expressed with these formulae:

$$FP = \frac{I_{\parallel} - I_{\perp}}{I_{\parallel} + I_{\perp}} \qquad r = \frac{I_{\parallel} - 2I_{\perp}}{I_{\parallel} + 2I_{\perp}}$$

where FP is fluorescence polarization; r is fluorescence anisotropy; $I_{||}$ is fluorescence emission intensity parallel to the excitation plane; $I_{\perp}$ is fluorescence emission intensity perpendicular to the excitation plane.

As exciting molecules in only one direction implies a photoselection of fluorophores, and as fluorescence decays only after a small interval of time, which mean value can be represented by fluoscence lifetime, r and FP are dependent on the dimensions of the fluorescent object in solution because a just excited molecule reorient before emitting light as rapidly as its dimension allows. There is a direct correlation of r with Stoke's diffusion law:

$$r(t) = e^{-6Dt} \qquad D = \frac{kT}{8\pi\eta r^2}$$

This relationship implies that the bigger the molecule, the more r or FP is maintained. Also viscosity and fluorescence lifetime has an influence on r and FP, in particular too short fluorescence lifetimes do not allow the molecule to rotate enough to give changes in r that it has already emitted light. High viscose buffers slow down molecular diffusion and rotation, so the higher the viscosity of the medium, the more r and FP are maintained.

Luk and coworkers (2007) set up an aggregation experiment on FP principle. Authors used a 96 well plate fluorescence reader equipped with excitation and emission polarizers, and incubated α-syn in mixture with Oregon Green 488 (OG) labeled α-syn, conjugated with succimidyl-ester chemistry to amine groups of the polypeptide chain. An aggregation kinetic was prepared incubating α-syn at 37°C under 1000 rpm agitation speed in 50 mM Tris, 100 mM NaCl, pH 7.0. Also ThT and K114 fluorescence assay was set up to compare kinetics obtained. ThT and K114 are two dyes that modify fluorescence properties with the binding to amyloid fibrils; the method was performed in continuous using 96 well plates to reduce inconvenient due to aliquot sampling, like low reproducibility of discontinuous fluorescence measurements. FP based technique lies on changes of molecular mass proper to a growing oligomer, so the method is able to detect large aggregates and not only mature amyloid fibrils. The comparison between kinetic obtained with ThT, K114 and FP method is here reported:

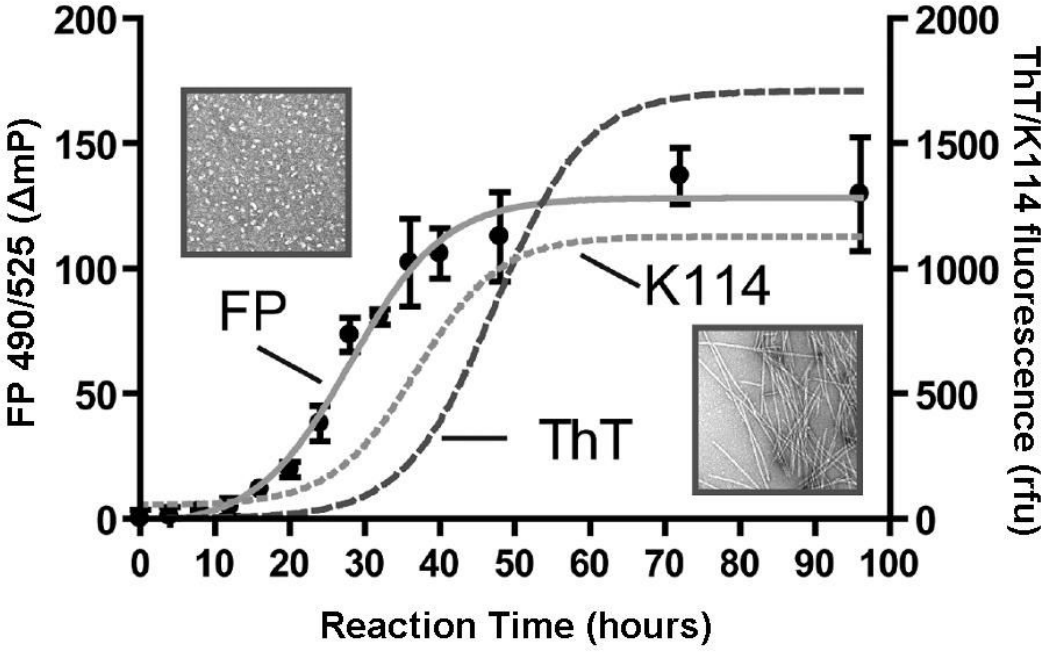

Figure 2.1.1: Comparison between aggregation kinetic obtained with OG FP increase and ThT or K114 fluorescence assay. Inserts are micrographies of 30 and 72 hours of incubation of 1 mg/ml α-syn. Adapted from Luk et al. (2007).

Figure 2.1.1 shows that increase in FP starts earlier than for ThT and K114 dyes assay. TEM images also show the presence of oligomers at 30 hours of incubation, detected only by FP signal and not by fibril sensibles fluorophores.

2.1.2 Surface Plasmon Resonce

The excitation of surface plasmons by light is denoted as a surface plasmon resonance (SPR) for planar surfaces. This phenomenon is the basis of many standard tools for measuring adsorption of material onto planar metal (typically gold and silver) surfaces or onto the surface of metal nanoparticles.

Surface plasmons, also known as surface plasmon polaritons, are surface electromagnetic waves that propagate in a direction parallel to the metal/dielectric (or metal/vacuum) interface. Since the wave is on the boundary of the metal and the external medium (air or water for example), these oscillations are very sensitive to any change of this boundary, such as the adsorption of molecules to the metal surface.

Biacore system exploits the phenomen of SPR to monitor the interaction between molecules in real time. The technology involves attaching one interacting patners to the surface of a sensor chip, and then passing sample containing other interaction partners over the surface. Binding of molecules to the sensor surface generates a response which is proportional to the bound mass, and changes in amount bound can be detected down to few picograms or less per square millimeter on the sensor surface, corresponding to concentrations in the pM to nM range in the bulk sample solution. Binding events are followed in real time and a range of interaction characteristics can be determined. Among the questions that can be addressed with Biacore are:

- the specificity of biomolecules interactions, investigated by testing the extent of binding between different pairs of molecules.
- the kinetics and affinity of an interaction, investigated by analyzing the time curve and level of binding in terms of molecular interaction models.
- the concentration of specific molecules present in the sample, investigated by measuring the level of response obtained from the sample.

As “ligand” is defined the molecule attached to the surface, while the “analyte” is the interaction partner that is passed in solution over the immobilized ligand. Samples are carried out in a continuous flow of buffer, termed “running buffer”. The removal of bound analyte from the surface is called “regeneration”; the ideal regeneration step removes all the residual

analyte from the chip surface mantaining unaltered the attached ligang, thus allowing the performance of other analysis. Response is measured in resonance units (or response units), RU, and a "sensorgram" is a plot of the response agaist time. The interactions being studied takes place on the gold-covered side of the "sensor chip", opposite to the side where the light is reflected. Samples containing analyte is supplied in a controlled fashion to the sensor surface through a microfluidic system. The sensor surface itself forms one wall of a flow cell which is an integral part of the microfluidic system. The delivery of the sample and buffer to the flow cell is precisely controlled by the pump system and the valves. The cell where the ligand has been attached is defined as analysis cell; an empty one is used as reference (reference cell).

In a typical interaction experiment performed by SPR, the binding is monitored injecting analyte into analysis and reference cells, and the signal subtracted to remove eventual aspefic interactions of the analyte on the Sensor Chip surface. Figure 2.1.2 reports an example of molecular binding detected by SPR. An increase of response units can be observed whether the analyte interacts with ligand bound to the surface, as the analyte is injected into analysis cell. The increase of the signal is proportional to the amount of the analyte that accumulate on the surface. As analyte injection stops, SPR signal starts to decrease monitoring the dissociation between the analyte and the ligand. Finally, regeneration is needed to remove all the remaining molecules of analyte from the Sensor Chip. Generally, regeneration is done with solutions that do not alter or remove the ligand attached to the surface; 1M NaCl or mild acidic or basic solutions are used.

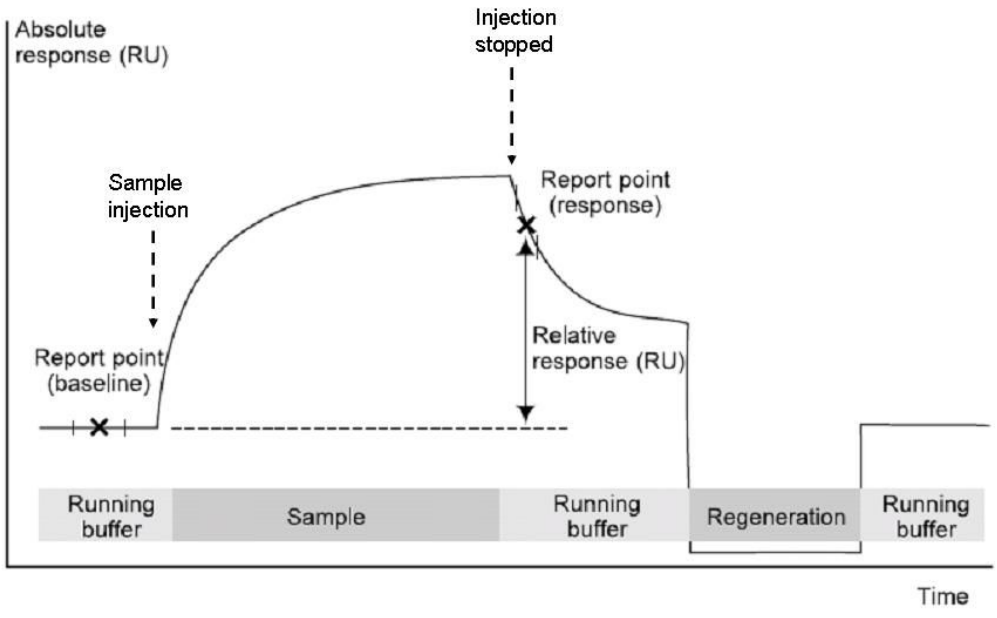

Figure 2.1.2: SPR signal detecting the interaction between ligand and analyte.

The Sensor Chip surface is constituted by a thin gold foil, covered with a carboxy-methyl-dextran matrix. Ligand conjugation to the Sensor chip can be done with covalent chemistry or capturing methods. Covalent chemistry is based on protein amine or sulfhydryl groups reactivity; whether capturing methods imply the used of a molecule atteched to Sensor Chips that binds to ligand in a non covalent way, such as Ni^{2+} complex with Nitrilo Acetic Acid (Ni-NTA) and Histidine Tagged proteins, or streptavidine/biotinylated peptides. In this PhD thesis, Ni-NTA approach was used, injecting Histidine-Tagged peptides or proteins to a Ni-NTA Sensor Chip. In this case, regeneration was done with a 350 mM EDTA solution, stripping both analyte and ligand. Hence, with this experimental approach, for every analysis fresh ligand has to be conjugated on the Ni^{2+} charged NTA Sensor Chip.

Analysis are performed injecting increasing amounts of analyte on the ligand functionalized Sensor Chip, thus obtaining dose-response curves. These are processed with the software supplied with the instrument, that fit curves to 1:1 Langmiur binding models or more complex derived models.

2.2 Materials

2.2.1 Chemicals

All chemicals were purchased by Sigma-Aldrich; otherwise, it will be specifically indicated.

2.2.2 Plasmids

All α-syn variants was cloned in our laboratory into a pET-28 plasmid (Novagen).

Plasmid pET-28 has the gene for resistance to kanamycin, the origin of replication of pBR322 (thus it is a low copy vector), the origin of replication f1 for obtaining a single DNA strand, a sequence coding for the His-tag upstream and downstream of Multiple Cloning Site (MCS), allowing to choose whether to insert the tag at the N- or C-terminus of the protein, a site of recognition for Thrombin proteolytic enzyme immediately downstream of the first His-tag for it (if necessary) removal. Additionally, the control of expression in the plasmid by the phagic promoter of T7 (found also in several other expression vectors) is made even stronger by the presence of a T7lac promoter: thanks to the presence of the lac operator and the coding sequence for the repressor lacI, the system is further regulated and the basal expression of recombinant protein is essentially abolished (For more details see "pET System Manual" -

Novagen). This is very useful especially for the expression of proteins potentially toxic to the host cell.

Referring to table 3.1 in § 3.1.1, α-syn and 57-102 peptide was cloned mantaining His-Tag before the protein sequence. α-Syn, A30P, E46K, A53T, E35C, V3C, Syn141C were cloned into pET28 without the sequence codifying Histidine Tag.

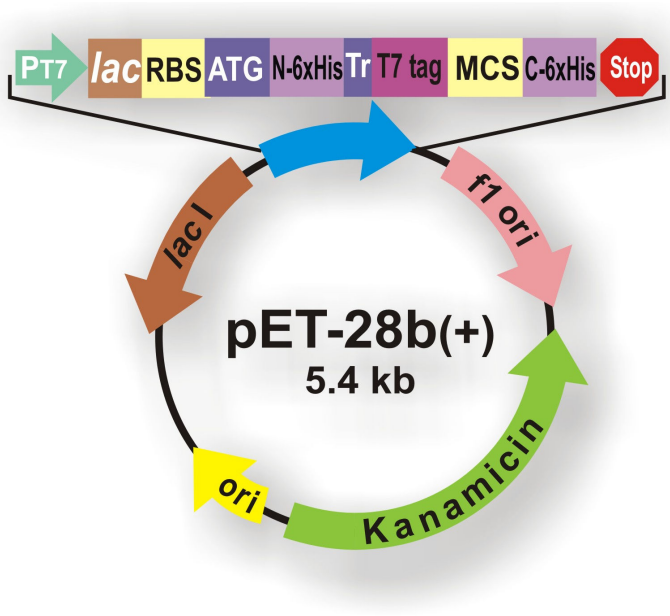

Figure 2.2.1: pET28b(+) plasmid (Novagen).

2.2.3 Proteins

All proteins listed in Table 3.1 (§ 3.1.1) were recombinant, produced and purified in our laboratory.

For the expression of α-syn, A30P, E46K, A53T, E35C, V3C and Syn141C mutants, an overnight culture of BL21(DE3) cell transformed with the relative pET-28b(+) plasmid containg the correct gene sequence, was diluted to a final OD600nm of 0.15 in 1 liter of LB fresh medium (Per litre: 10 g triptone, 5 g yeast extract, 5 g sodium chloride) supplemented with 25 μg/ml kanamicin. The culture was growth in agitation at 37°C and induced at an OD600 of 0.4 for 5 h with 0.1 mM IPTG. Then cell was harvested by centrifugation at 6000 rpm for 10 minutes at 20°C and resuspended in 100 ml Osmotic Shock Buffer (30 mM Tris, 2 mM EDTA, 40% v/v sucrose, pH 7.2), according to Huang et al. (2005). The suspension was incubated at room temperature for 10 min, then it was centrifugated at 12000 rpm for 10 min. Pellet was rapidly resuspended in 90 ml cold deionized water with the addition of 37.5 μl of $MgCl_2$ saturated solution. Protein release from periplasmatic space occurs in this passage. The suspension was kept on ice for 3 min, then bacterial centrifugated at 12000 rpm for 20 min.

The supernatant was boiled for 10 min, then centrifugated at 12000 rpm for 30 min. 8 ml of 1M Tris pH 8 was added to the supernatant, and the solution diluted to a final volume of 100%. Then, two steps of ammonium sulphate fractionation was performed: 30 min centrifugation was carried out on 35% saturation of ammonium sulphate protein solution, then ammonium sulphate was added to the supernatant until 55% solution saturation. The precipitate was recovered with 30 min centrifugation at 12000 rpm, and resuspended in 6-10 ml of 20 mM Tris buffer, pH 8, in a FPLC system. The preparation was dyalized overnight against water, then it was loaded into a 6 ml Resource Q FPLC column (GE Healthcare), preequilibrated with 20 mM Tris, pH 8. The elution was performed with a 40 min linear gradient from 0 to 100% 20 mM Tris, 500 mM NaCl, pH 8. Peaks corresponding to α-syn was collected and dyalized against deionized water overnight, then lyophilized.

The purity was checked by SDS-PAGE and by HPLC, performed with a Jupiter analytical C4 column (Phoenomenex), preequilibrated with 5% solvent A (0.1% trifluoroacetic acid (TFA) in milliQ water) and eluted with a linear gradient from 39 to 46% solvent B (0.085% TFA in acetonitrile) in 14 min, with 0.6 ml/min costant flow.

Whether further purification was needed, this was done in with preparative HPLC, using a preparative C18 HPLC column (Zorbax 300SB-C18 PrepHT, Agilent Technologies), preequilibrated with 5% solvent A (0.1% trifluoroacetic acid (TFA) in milliQ water) and eluted with a linear gradient from 44 to 50% solvent B (0.085% TFA in acetonitrile) in 20 min, with 3 ml/min costant flow.

For expression of peptide 57-102, an overnight culture of C41(DE3) cells trasformed with a pET-28b(+) plasmid, was diluted to a final OD600nm of 0.15 in 1 liter of LB fresh medium supplemented with 25 μg/ml kanamicin. The culture was growth in agitation at 37°C and induced at an OD600 of 0.6 for 5 h with 1 mM IPTG. Then cell was harvested by centrifugation at 6000 rpm for 10 min at 4°C; the pellet was washed with PBS (10 mM Na_2HPO_4, 2 mM KH_2PO_4, 137 mM NaCl, 2.7 mM KCl, pH 7.4) and re-collected by centrifugation at 9000 rpm for 10 min at 4°C. Harvested cells, at this point, can be stored at -20°C or -80°C (for long term storage). If cells have been frozen, pellet was thawed on ice, then it was resuspended on Lysis Buffer (20 mM sodium phosphate pH 7.4, 300 mM NaCl, 10% glycerol) −30 ml for pellet from 1 l of initial culture − and sonicated on ice at a frequence of 0.8 Hz, 6 times for 30 s. Insoluble fraction was separated by centrifugation fo 40 min-1 h at 12000 rpm at 4°C. The sample was supplemented with 100 mM phenyl-methane-

sulphonyl-fluoride (PMSF) and Bacterial proteases inhibitors cocktail (Sigma-Aldrich), according to manufacturing instruction.

Since purification 57-102 was carried out with a batch cromatography with Co^{2+}-NTA resin (His-Select Cobalt Affinity Gel, Sigma-Aldrich), in the meanwhile resin was equilibrated with Washing Buffer (20 mM sodium phosphate pH 7.4, 300 mM NaCl, 20 mM imidazole). Briefly, an appropriate amount of resin was resuspended in 10 volumes Washing Buffer, incubate in agitation for 10 min at 4°C, then centifuged at 2000 rpm at 4°C for 2 min. After centrifugation, the supernatant obtained from cell lysis was applied to equilibrated resin and incubated in agitation at 4°C for 1 h. Then the suspension was centrifuged as described above and supernatant discarded. Resin was washed as before 2 times, finally resuspend in a 1-2 volumes of Washing Buffer and applied to a disposable column. After all Buffer has eluted, proteins of interested was eluted with 5 ml Elution Buffer (20 mM sodium phosphate pH 7.4, 300 mM NaCl, 150 mM imidazole) and collected in 1 ml fractions. Fractions were analysed for protein content, then collected and dialysed overnight against PBS. Eventual His-tag removal was performed by enzymatic cleavege with Thrombin protease (GE Healthcare) in a ratio of 5u/mg of protein, for 5 hours at 20-22°C. Finally, proteins was purified by RP-HPLC with a Jupiter analytical C4 column (Phoenomenex), preequilibrated with 5% solvent A (0.1% trifluoroacetic acid (TFA) in milliQ water) and eluted with a linear gradient from 5 to 60% solvent B (0.085% TFA in acetonitrile) in 30 min, with 0.6 ml/min costant flow. After acetonitrile and TFA clearance, the samples were lyophilized.

Overexpression of proteins for NMR studies (^{15}N-labeled proteins) was achieved by growing cells in M9 minimal medium (Per litre: 200 ml M9* salts solution, 2 ml 1 M $MgSO_4$, 0.1 ml 1 M $CaCl_2$, 200 ml 20% glucose; *M9 salts solution, per litre: 64 g Na_2HPO_4, 15 g KH_2PO_4, 2.5 g NaCl, 5.0 g NH_4Cl) supplemented with 1 g/L [^{15}N]ammonium chloride.

14-3-3η , DJ1 e 3T protein was a kind gift of respectively Dr. Francesca Munari, Dr. Marco Bisaglia and Dr. Isabella Tessari of our research group.

2.2.4 Peptides

ASI1 and ASI4 peptides was synthetized by automated chemistry in the laboratory of Dr. Barbara Biondi (Dipartimento di Scienze Chimiche, Università degli Studi di Padova). Row material was purified by HPLC semipreparative Grace Vydac C18 column (The Separation Group, Hesperia, CA, USA), preequilibrated with 4% solvent A (0.1%

trifluoroacetic acid (TFA) in milliQ water) and eluted with a linear gradient from 4 to 40% solvent B (0.085% TFA in acetonitrile) in 20 min, with 1.8 ml/min costant flow. Peak corresponding to peptides was collected and dried in a Speed-Vac device.

2.2.5 Labelled proteins

70μM E35C or Syn141C was mixed with 2 or 5 molar excess tris-carboxy-ethyl-phosphine (TCEP) in 20 mM Tris buffer, pH 7.0. After 30 min, 10 fold molar excess 2-(4-Maleimidophenyl)-6-methylbenzothiazole (MBT, MW=320.37) previously solubilized in dimethylsulphoxide (DMSO), was added to E35C or Syn141C solution. The reaction was held 2 hour at 25°C, 37°C or 45°C. Then, reaction mixture was separated by HPLC injection into a Jupiter analytical C4 column (Phoenomenex), preequilibrated with 5% solvent A (0.1% trifluoroacetic acid (TFA) in milliQ water) and eluted with a linear gradient from 39 to 46% solvent B (0.085% TFA in acetonitrile) in 14 min, with 0.6 ml/min costant flow. Fractions corresponding to labelled protein was collected and dried with a Speed-Vac device.

70μM Syn141C was mixed with 5 molar excess triscarboxyethylphosphine (TCEP) in 20 mM Tris buffer, pH 7.0. After 30 min, 5 fold molar excess Oregon Green 488 maleimide (Molecular Probes, Invitrogen) (OG, MW=463.35) previously solubilized in 20 mM Tris pH 7.0, was added to Syn141C solution. The reaction was held 4 hour at 45°C. Then, reaction mixture was separated by HPLC injection into a Jupiter analytical C4 column (Phoenomenex), preequilibrated with 5% solvent A (0.1% trifluoroacetic acid (TFA) in milliQ water) and eluted with a linear gradient from 39 to 46% solvent B (0.085% TFA in acetonitrile) in 14 min, with 0.6 ml/min costant flow. Fractions corresponding to labelled protein was collected and dried with a Speed-Vac device.

2.2.6 Liposomes

About 8 mg of a mixture of 50% dimyristoyl phosphatidyl choline and 50% dimyristoyl phosphatidyl glycerol (Avanti Polar Lipids) were used for the preparation of SUV. The lipids were dissolved in 1 ml chloroform/methanol 4:1 and the solutions were evaporated under nitrogen stream in a glass test tube. The dry lipid film was suspended in 100 mM phosphate buffer (pH 7.4) to give a stock solution with a final concentration of 45 mM and mixed for 1 hour above the melting temperature. The product of hydration was filtered through a large pore size (0.45 μm) filter and, subsequently, extruded at least 11 times through a 50 nm pore filter, following the manufacturer's protocol.

2.3 Analytical Techniques

2.3.1 SDS-PAGE

SDS-PAGE was done according to Laemmli (1970). 13% running gel was prepared mixing 3.25 ml 40%acrylamide solution (29:1=acrylamide:bisacrylamide), 2.5 ml 1.5 M Tris, pH 8.9, 100 µl 10% SDS solution, 100 µl 10% ammonium persulphate (APS), 4 µl N,N,N′,N′-Tetramethyl-ethylene-diamine (TEMED), diluting to a final volume of 10 ml with deionized water. 5% stacking gel was prepared mixing 0.62 ml 40%acrylamide solution (29:1=acrylamide:bisacrylamide), 2 ml 0.3 M Tris, pH 6.7, 50 µl 10% SDS solution, 50 µl 10% APS, 5 µl TEMED, diluting to a final volume of 5 ml with deionized water.

The method requires protein denaturation: samples were mixed with 4X loading buffer (0.225 M Tris, pH 6.8, 50% glycerol, 5% SDS, 0.05% bromophenol blue, 0.25 M dithiothreitol (DTT)) and boiled at 100 °C for 5 min before loading. Electrophoretic run was carried out at room temperature applying 100-150 V. Loading of low molecular weight-SDS markers provides the references. Following electrophoresis, gels were stained with Coomassie Stainin Solutiong (0.15 % w/v Coomassie Brilliant Blue R-250, 40% v/v ethanol, 10% v/v acetic acid) and finally washed in Destain solution (10% isopropanol, 10% acetic acid).

2.3.2 Chromatography

FPLC analyses were performed on an AKTA-FPLC System (GE Healthcare) equipped with a 280 nm UV lamp detector.

HPLC analyses were performed on a 1100 Series HPLC system (Agilent Technologies) equipped with a diode array absorbance detector.

2.3.3 Mass spectrometry

Molecules molecular weight measurements were carried out by Dr. Patrizia Polverino de Laureto (CRIBI, Università degli Studi di Padova). ESI-MS spectra was performed on a ESI-Q-TOF Micro spectrometer (Micromass).

2.3.4 Absorbance

UV-visible spectra was recorded on a Agilent 8453 UV-Vis Spectroscopy system (Agilent Technologies). Absorbance was measured with Suprasil 50 µl quarz cells (Hellma),

with 1 cm optical path-length. The software provided with the instrument automatically subtract baseline contribution to absorbance signals. Extinction coefficient applied for all α-syn samples was of 5960 $M^{-1} \cdot cm^{-1}$; ASI1 and ASI4 quantification was performed measuring peptide bonds absorbtion at 205 nm ($\varepsilon = 31\ M^{-1}cm^{-1}$).

2.3.5 Circular dichroism

CD measurements were carried out on a JASCO J-715. The CD spectra were acquired and processed using the J-700 program for Windows. All experiments were carried out at room temperature using HELLMA quartz cells with Suprasil windows and optical path-length of 0.2 cm. All spectra were recorded in the 190-260 nm wavelength range, using a bandwidth of 2 nm and a time constant of 2 s at a scan speed of 50 nm/min. The signal-to-noise ratio was improved by accumulating at least four scans. All spectra are reported in terms of mean residue molar ellipticity $[\Theta]_R$ (deg cm^2 $dmol^{-1}$).

2.3.6 Fluorescence

Fluorescence emission spectra were recorded on a Perkin-Elmer LS 50 spectrofluorimeter equipped with a thermostated cell compartment and interfaced with a personal computer using the FL-WinLab program for Windows. Sample measurements were carried out using a HELLMA ultra-micro cell with Suprasil windows and an optical path length of 10 x 2 mm and volume of 50 µl. Fluorescence spectra were obtained at 25 °C. For Trp emission recording, measures were performed using excitation at 295 nm, with excitation and emission slit of 6 nm for 7.5 µM solutions of 3T protein. SynMBT spectra was recorded with an excitation wavelenght of 334 nm, with 6 nm slit both for excitation and emission of 7.5 µM protein. Scan rate of 120 nm/min was applied for all measurements. The signal-to-noise ratio was improved by accumulating at least four scans.

Thioflavin T fluorescence assay was performed on Suprasil® micro cuvettes with optical path length of 10 x 2 mm, 500 µl volume. Aliquots from protein fibrillogenesis experiments was taken and mixed to ThT solution (25 µM ThT in 25 mM sodium phosphate, pH 6.0) just before the measurement. Final protein concentration for the analysis after the dilution with ThT solution is 30 µg/ml, for a final volume in the cuvette of 500 µl. Signals was recorded with an excitation wavelength of 440 nm, emission of 485 nm, slit 5 nm and 10 nm respectively.

MBT lifetime was measured with a GREG200 (ISS Instruments) with phase-delay method, by Dr. Giancarlo Agostini (Dipartimento di Scienze Chimiche, Università degli Studi di Padova). Excitation and emission wavelength used was respectively of 320 nm and 390 nm, using methyl-POPOV as reference for lifetime.

Fluorescence Polarization measurements were performed fluorescence plate reader DTX 880 Multimode Detector Beckman Coulter, equipped with excitation filter at 485 nm and two emission filters at 535 nm. Excitation and emission filters was equipped with polarizers. Measurements were carried out at 37°C.

2.3.7 Nuclear Magnetic Resonance

HSQC spectra was recorded by Dr. Francesca Munari and Dr. Marco Bisaglia of our research group. All NMR experiments were performed on a Bruker Avance DMX600 spectrometer equipped with a gradient triple-resonance probe. The spectra were processed using GIFA and analyzed using XEASY on a Silicon Graphics workstation. α-Syn and spectra were collected at 283 K, using 256 x 512 complex incremental data points in the F1 (^{15}N) and the F2 (^{1}H) dimensions, with 32 scans per increment and a 1 s relaxation delay. Spectral widths of 26 ppm (centred at 115.7 ppm) and 3 ppm (centred at 7.5 ppm) were used for the ^{15}N and the ^{1}H dimension, respectively. 0.12 mM ^{15}N α-syn samples were prepared in 20 mM sodium phosphate (pH 7.4), with 10% D_2O (v/v) and 0.02% NaN3 (w/v). In the case of α-syn C-terminal dimer, dimer was prepared mixing 20% ^{15}N α-syn and 80% α-syn in the presence of DTT, then dimerization occured dyalizing agaist deionized water. Dimer purification was performed in FPLC as reported in § 2.1.3. HSQC spectrum of α-syn C-terminal cysteine monomer was performed adding 2 molar excess DTT to the dimer sample tested.

2.3.8 Transmission Electron Microscopy

TEM images was performed by Dr. Giorgia De Franceschi of Dr. Patrizia Polverino de Laureto research group. Samples relative to aggregation of α-syn were diluted 3 times with PBS. A drop of the samples solution was placed on a Butvar-coated copper grid (400-square mesh) (TAAB-Laboratories Equipment Ltd, Berks, UK), dried and negatively stained with a drop of uranyl acetate solution (1%, w/v). TEM pictures were taken on a Tecnai G2 12 Twin instrument (FEI Company, Hillsboro, OR, USA), operating at an excitation voltage of 100 kV.

2.3.9 Surface Plasmon Resonance

Surface Plasmon Resonance (SPR) analyses were carried out in a Biacore X instrument (GE Healthcare), with the technical assistence of Dr. Stefania Sarno and Dr. Maria Ruzzene (Dipartimento di Chimica Biologica, Università degli Studi di Padova). Chip for Surface Plasmon Resonance was purchased by GE Healthcare.

The Running Buffer used for experiments on nitriloacetic acid (NTA) Sensor Chip was composed of 10 mM HEPES, 150 mM NaCl, 50 μM EDTA, pH 7.4. Chip functionalization was made firstly injecting Ni^{2+} solution (10 mM HEPES, 150 mM NaCl, 50 μM EDTA, 500 μM $NiCl_2$, pH 7.4) to create Ni^{2+}-NTA complex selectively in analysis cell (§ 2.4.2 for technical details), then 2 μg/ml Histidine-Tagged 57-102 or 2.4 μg/ml Histidine-Tagged α-syn, solubilized in Running Buffer. For binding analysis, increasing amount of analyte was injected as required for the calculation of dissociation constant, spanning from 1/10 to 10 times the molar concentration of ligand bounded to analysis cell. Regeneration was performed with Regeneration Buffer (10 ml HEPES, 150 mM NaCl, 350 mM EDTA, pH 8.3).

2.4 Experimental conditions

2.4.1 Fibrillogenesis experiments

Fibrillogenesis experiments were performed in PBS solubilized 1.8 mg/ml wild-type α-syn and mutants, in the presence and in the absence of five molar excess ASI1 or ASI4 peptides. Every sample contained 0.05% sodium azide to prevent microbial degradation of proteins. Eppendorf 1.5 ml tubes was positioned into a Thermo-mixer apparatus (Eppendorf), set at 37°C and 300 or 500 rpm shaking. Aliquots were taken at different times and submitted to ThT fluorescence assay or gel filtration analysis.

Gel filtration analysis was performed with a Superdex 200 HR chromatographic column pre-equilibrated with PBS. 100 μl of 1.8 mg/ml α-syn samples were injected and chromatographic profile recorded at a constant flow rate of 0.5 ml/min. Eluted peaks was injected into a Jupiter analytical C4 column (Phoenomenex), preequilibrated with 5% solvent A (0.1% trifluoroacetic acid (TFA) in milliQ water) and eluted with a linear gradient from 39 to 46% solvent B (0.085% TFA in acetonitrile) in 14 min, with 0.6 ml/min costant flow.

2.4.2 Aggregation experiments

1mg/ml α-syn, α-syn dimers or pathological mutants A30P, E46K and A53T was solubilized in PBS, 0.05% sodium azide, and mixed with 1/250, 1/100, 1/50 molar ratios α-syn labelled with Oregon Green 488, in the presence or in the absence of putative inteacting proteins or glass beads. Each sample filled 3 or 4 wells of a 96 well plate that was covered with a adhesive film to prevent evaporation. Even more, in each plate outer wells was filled with PBS and not submitted to analysis. Plates was placed in a incubator at 37°C, with 1000 rpm shaking. Every 6 or 12 hours, FP measurements were performed.

No increase of synOG FP values was observed in controls done for all the samples tested, when synOG was incubated alone or in the presence of putative interacting proteins.

Chapter 3: Results

3.1 Cloning, expression, purification and characterization of alpha-synuclein, mutants and fragments

3.1.1 Alpha-synuclein

The protocol for the purification of recombinant α-syn was previously developed in our laboratory (Bisaglia et al., 2005). In the attempt to improve efficiency a new protocol of purification, that implies a controlled osmotic shock that disrupts only the outer membrane, was tested (Huang et al., 2005). The outcome of this comparison allowed to define a protocol that has been used for all purifications described in this thesis, that for the wt protein resulted in a yield of 30 mg per litre of colture. BL21(DE3) bacteria strain was transformed and the purification was realized according to the protocol described in Materials and Methods section. The purification of the protein, that implies an ammonium sulphate precipitation and an anionic exchange chromatographic step, did not resulted in protein samples of the desired purity. To further improve the quality of the sample a reverse phase chromatographic step (C18 column) was added to the procedure. In Figure 3.1.1.A the chromatographic profile is shown with a single peak at an elution time of about 20 minutes. The peak corresponding to α-syn was analyzed by mass spectrometry (Dr. Patrizia Polverino de Laureto, CRIBI, Università degli Studi di Padova) and the deconvoluted spectra is shown in Figure 3.1.1.B. The mass spectrum reveal the presence of three species: the more intense signal corresponding to a MW of 14460 Da, which matches with the expected value for wild type α-syn a second specie with a MW of 14514 Da that correspond to α-syn with oxidized methionines. The third signal, with a signal intensity that correspond to about 20% of intensity of major peak, is assigned to a specie with a MW of 14400 Da. The latter species has a difference of 60 Da less than α-syn wild type; this difference can be explained only with the

mutation of an amino acid residue, because no residues modification or loss can be linked to this value.

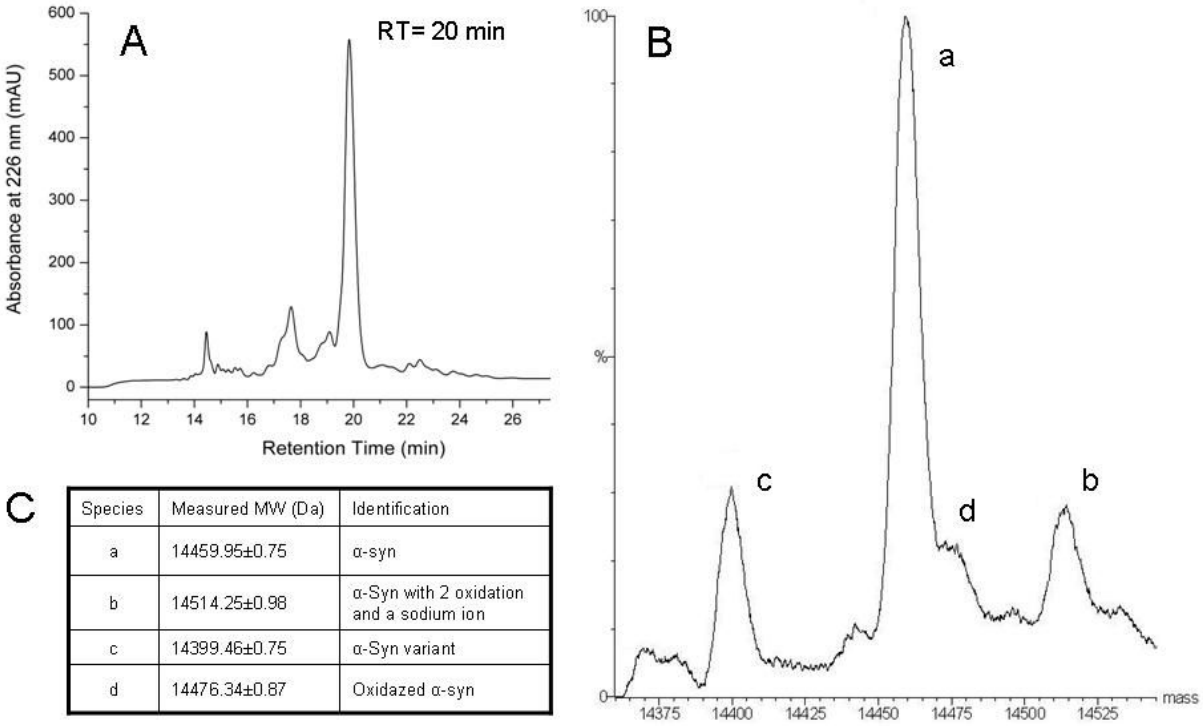

Species	Measured MW (Da)	Identification
a	14459.95±0.75	α-syn
b	14514.25±0.98	α-Syn with 2 oxidation and a sodium ion
c	14399.46±0.75	α-Syn variant
d	14476.34±0.87	Oxidazed α-syn

Figure 3.1.1:A) elution profile obtained by reverse-phase chromatograpy; the main peak is analyzed by ESI-MS. B) Deconvoluted ESI-MS spectrum of the first α-syn batch obtained in E. coli. Species a corresponds to wild type α-syn, while species c presents a difference of 60 Da. C) Table with detected α-syn species that co-elute in peak at RT 20 min in the HPLC chromatogram reported.

While performing these experiments a paper was published by Masuda et al. (2006) that reported the misincorporation of a Cysteine residue at position 136, in place of the originally codified Tyrosine in *E. coli* strains. The particular case of this amino acid position in due to a mistake made by bacteria which codify the codon TAC of mRNA molecule as Cysteine instead of Tyrosine. As shown in Figure 3.1.1.A, the Y136C variant copurify with the wild type protein. The correction of ambiguity in the nucleotide sequence became fundamental as cysteine is a reactive residue leading to the formation of dimers. Moreover, one of the aims of the project was the conjugation of α-syn to fluorophore molecules by maleimide reaction, which is highly specific for cysteine. The laboratory had already several plasmid containing this codon ambiguity, therefore it become necessary to correct all plasmid

containing the original cDNA codifing for human wild type α-syn. The correction was performed substituting the codon TAC codifying for Tyr 136 with codon TAT, which is not ambiguously translated by E. coli strains (Figure 3.1.2). This operation was indeed performed on all plasmid containing α-syn cDNA sequence.

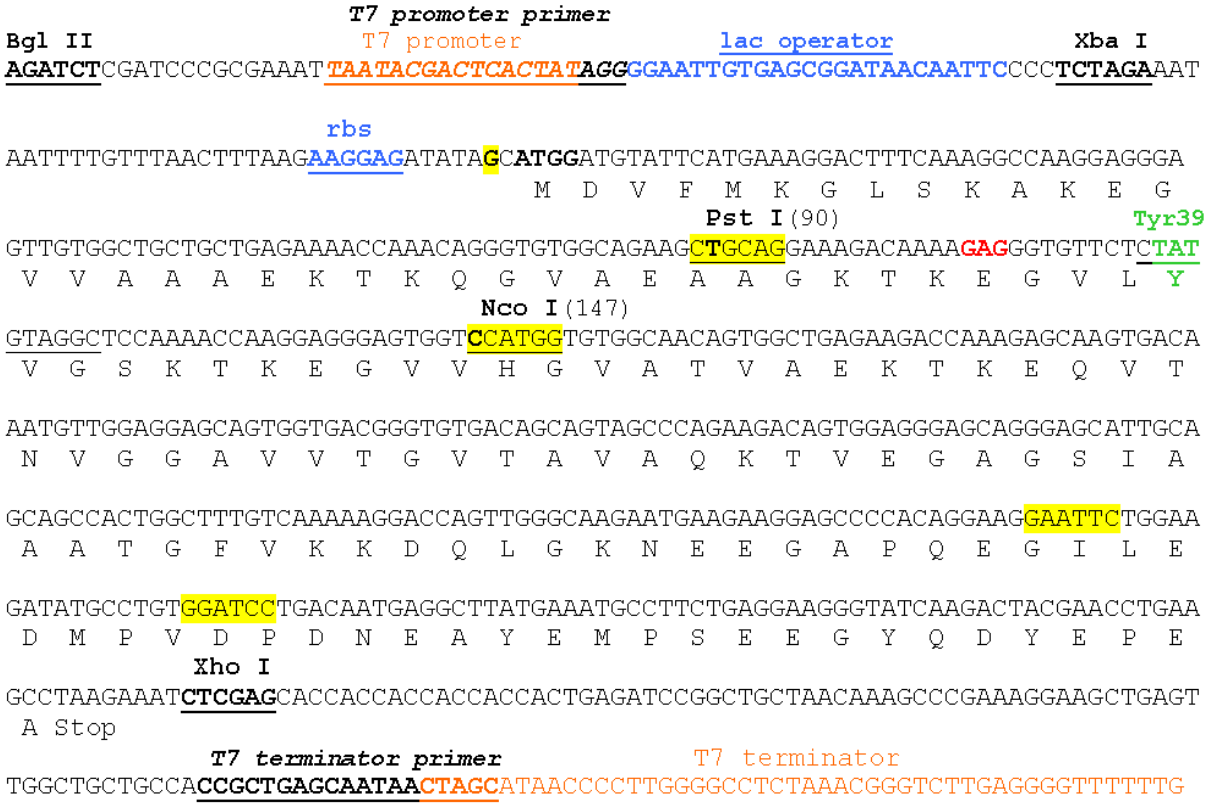

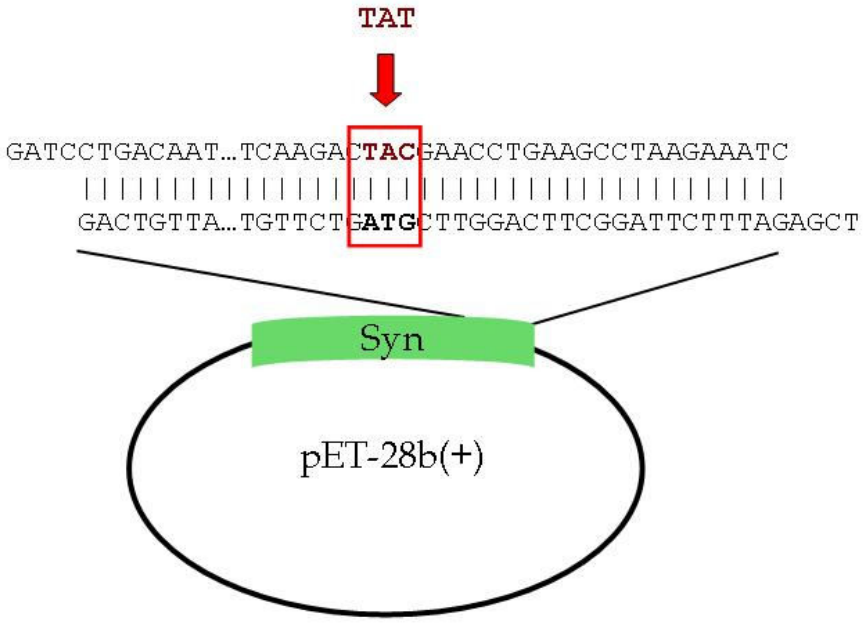

Figure 3.1.2: DNA sequence of α-syn in pET28 and the approach used to correct the plasmid.

Table 3.1: List of available α-syn mutants.

Protein	*Estimated MW*	*Description*
wild type α-syn	14460 Da	*Wild type α-syn*
aa 57-102 (NAC)	4545 Da	*The most hydrophobic part of the molecule.*
Histidine Tagged α-syn (synHT)	16623 Da	
Histidine Tagged 57-102	6840 Da	
A30P	14486 Da	*Early onset mutant (Kruger et al., 1998))*
E46K	14459 Da	*Early onset mutant (Zarranz et al., 2004)*
A53T	14490 Da	*Early onset mutant (Polymeropoulos et al., 1997)*
E35C	14434 Da	
C-terminal Cys (CtM)	14563 Da	*(Syn141C)*
N-terminal Cys (NtM)	14464 Da	*(V3C)*

BL21(DE3) *E. coli* strain was used for the transformation and for the expression of the edited sequence. The protocol used for protein expression and purification was again the adaptation of the one proposed by Huang and coworkers. The protein still produced in large amounts with a yield of about 25-30 mg of protein per litre of culture.

The "Huang" protocol is based on the observation that α-syn is traslocated on the periplasmic compartment ones the protein is translated. This property is not observed for N-terminal fragments of α-syn, suggesting that the recognition motif that allow such traslocation is contained in the C-terminal part of α-syn (Ren et al., 2007). In this work, the author found that α-syn is conveyed to the periplasm by a mechanism involving signal recognition particle (SRP) pathway. The mechanism is not completely understood. Single point mutations of the protein do not affect this transfer to the periplasm, on the other hand the purification protocol originally designed (i.e. without the osmotic shock step) had to be used for the deletion mutants missing the C terminal. Huang protocol employs a specific osmotic shock for the selective lysis of outer membrane; as a consequence, only periplasmic proteins, and then α-syn, are released. This fact allows DNA and citoplasmic proteins to be retained into the inner membrane and simpler purification of α-syn among periplasmic proteins. In fact, after the suspension of pelletted bacteria in 30mM Tris-HCl buffer at pH 7.2 and containing 40% sucrose, bacteria are centrifuged and resuspended in cold deionized water. The protocol yield was improved by the introduction at this point of two steps of ammonium sulphate fractionation. The latters remove the nucleotide pools that was released in combination with α-syn.

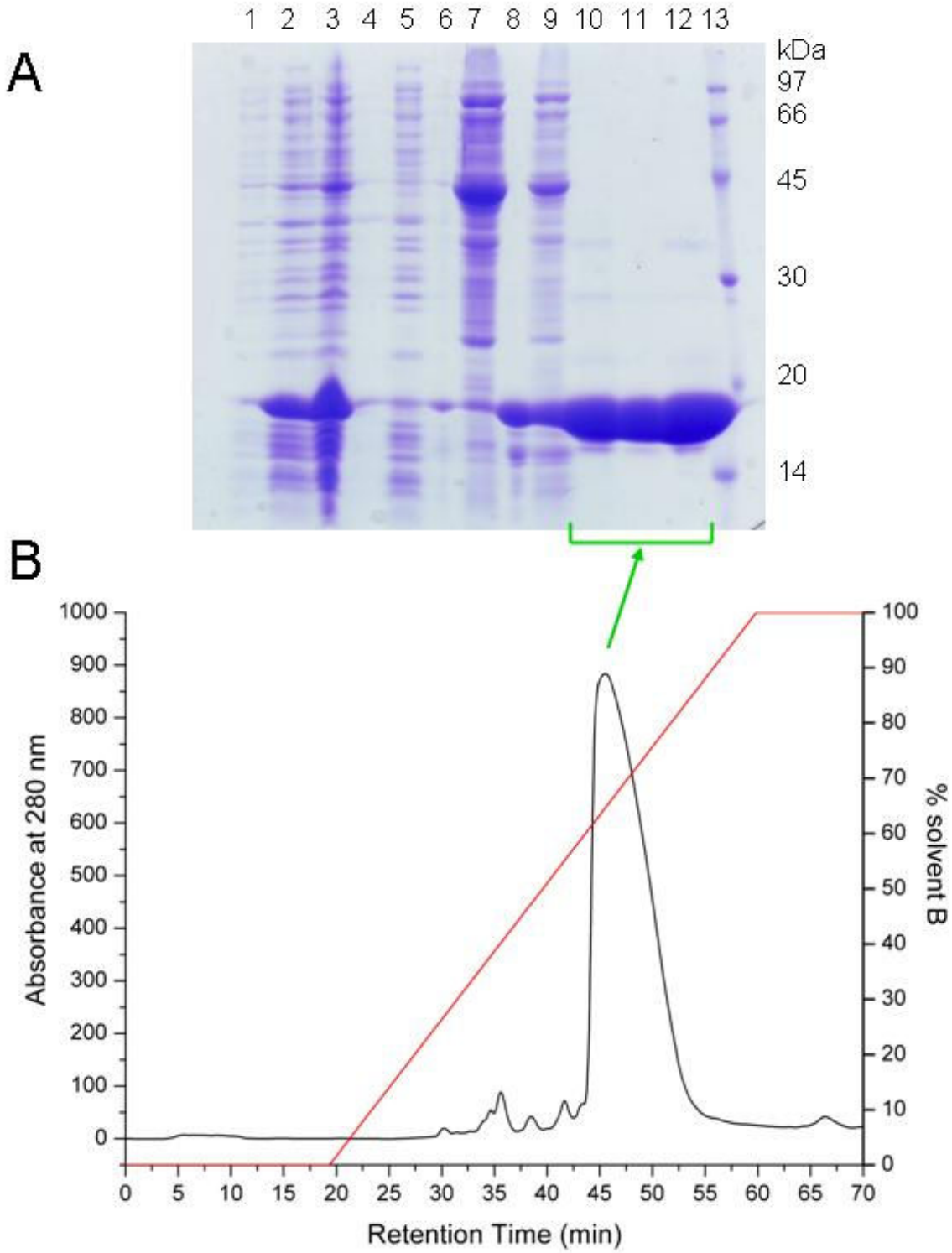

Figure 3.1.3: SDS-PAGE of α-syn expression and purification (A): not induced (1), induced (2), pellet of centrifugation after the osmotic shock step (3), surnatant of centrifugation after osmotic shock step (4), pellet after cells resuspension in water (5), pellet of centrifugation after the boiling of surnatant after cell resuspension (6), surnatant after the centrifugation of boiling passage (7), pellet of centrifugation after ammonium sulphate fractionation (8), sample before purification by IE chromatography (9), main peak fractions (10, 11, 12), low molecular weight (LMW) markers (13). α-Syn purification by IE chromatography (B).

Figure 3.1.3 demonstrates that α-syn obtained after the ion exchange chromatography (IEC) is highly pure with this protocol. The eluted protein is then dialyzed against deionised water and lyophilized.

3.1.2 Cysteine mutants of alpha-synuclein

The same purification protocol is applied for α-syn cysteine mutants. No reducing agent is added to the protein purification mix prior to IE chromatography. Figure 3.1.4E shows as an example the chromatographic profile (which is analogous for all the variants) of the N-terminal Cys α-syn and SDS- PAGE analyses of the purification steps of E35C, CtM and NtM mutants. It can be noted the presence of a main peak at 55 minutes of retention time, which corresponds to the monomeric protein, and the presence of a second peak, which intensity depends on the position in the sequence of the mutant cysteine residue, and it corresponds with the covalent dimer of α-syn mutant. This assignment is confirmed by SDS-PAGE analysis: in Figure 3.1.4 the samples of each gel labelled (A) and (C) are dissolved in conventional sample buffer, which contains ditiothreitol (DTT) as reducing agent, the samples of gels labelled (B) and (D) are dissolved in sample buffer without any reducing agent. It can be easily detect which fractions contains protein monomers and which contain dimers.

At this point, the fractions can be held, dialyzed against water and lyophilized separately to obtain α-syn dimers. The yield of NtD (N-terminal Cys Dimer) is about 15 mg per litre of culture, while for CtD (C-terminal Cys Dimer) is about 8 mg. The difference is due to the lower tendency of CtM to form dimer, probably for the electrostatic repulsion between the highly acidic last 40 residues of α-syn. Otherwise, monomer and dimer can be mix together and incubated with DTT to reduce disulfide bonds. 20 minutes of incubation with ten fold molar excess of reducing agent DTT or Tris-carboxy-ethyl-phosphine (TCEP) is sufficient to completely reduce disulfide bonds. The purity of each protein stock was further improved by HPLC Using a C4 analytical column. The chromatographic profile is shown in Figure 3.1.5. A comparable level of purity was observed for each of the mutated protein produced.

It is important to check relative purity of stock proteins because they are used for experiments such as protein fibrillization or protein-protein interaction. The main contaminants of batch preparation are fragments of α-syn itself. Some fragments are believed to promote protein aggregation (Hoyer et al., 2004), so it is important to quantify such fragments to correlate potential differences in the aggregation propensities of the different

batch of protein to their compositing. This was done considering the area of HPLC peaks corresponding to the wt protein (Table 3.2).

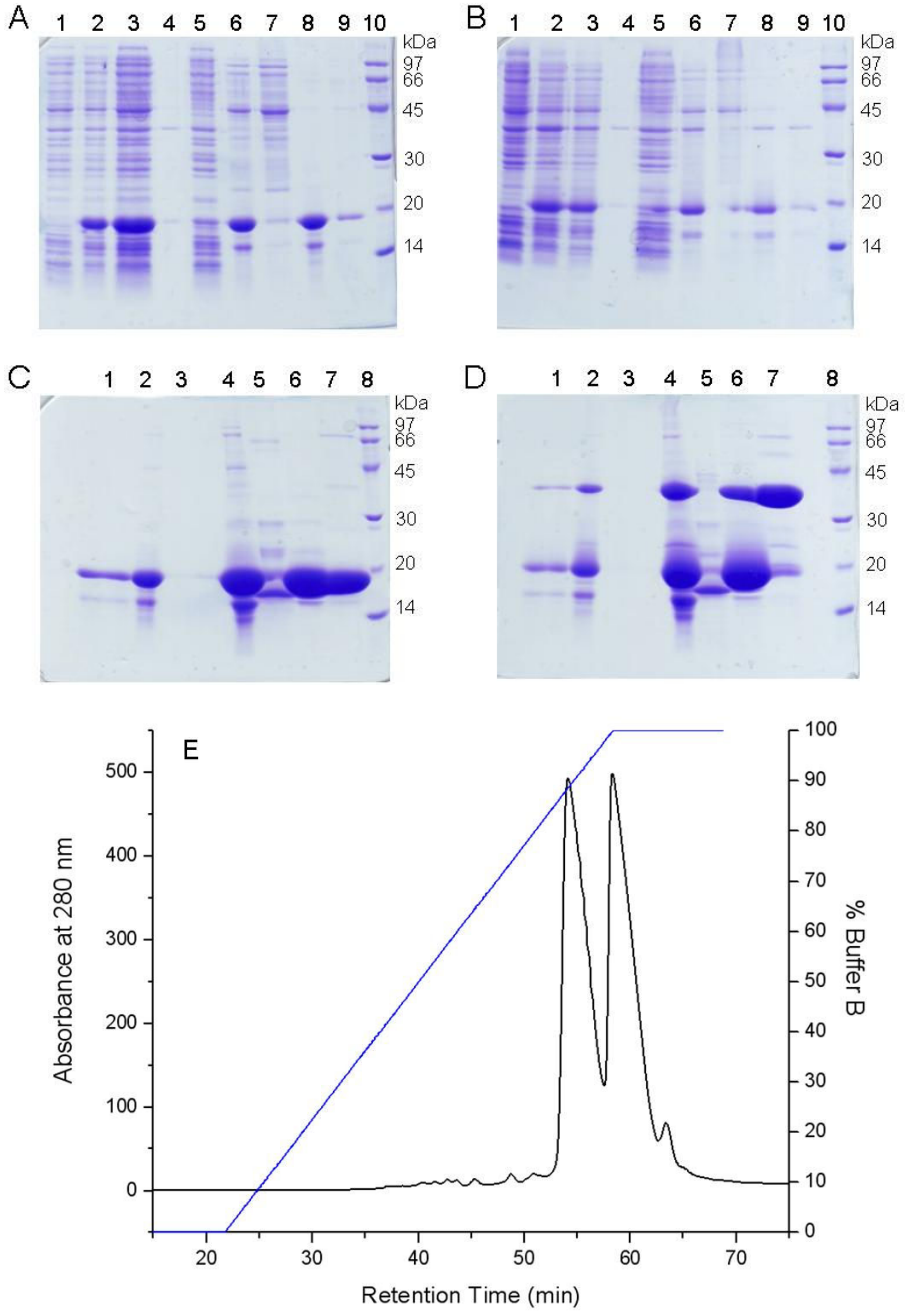

Figure 3.1.4: SDS-PAGEs of passages of expression and purification of α-syn N-terminal Cys mutant; samples loaded in (A) and (C) contain DTT to reduce disulfide bonds while samples in (B) and (D) do not contain any reducing agent. Loading order: not induced (1), induced (2), pellet (3) and surnatant (4) after osmotic shock, pellet (5) and surnatant (6) after cell resuspension in water, pellet (7) and surnatant (8) after boiling, pellet after the first fractionation ammonium sulphate passage (9), LMW markers (10) (A and B); surnatant after first amm. sulp. fractionation (1), pellet (2) and surnatant (3) after second ammonium

fractionation passage, sample before IE purification (4), peak at retention time (RT) 52 minutes (5), peak at 55 minutes RT (6), peak at 60 minutes RT (7), LMW markers (8). IE chromatogram of N-terminal Cys α-syn (E).

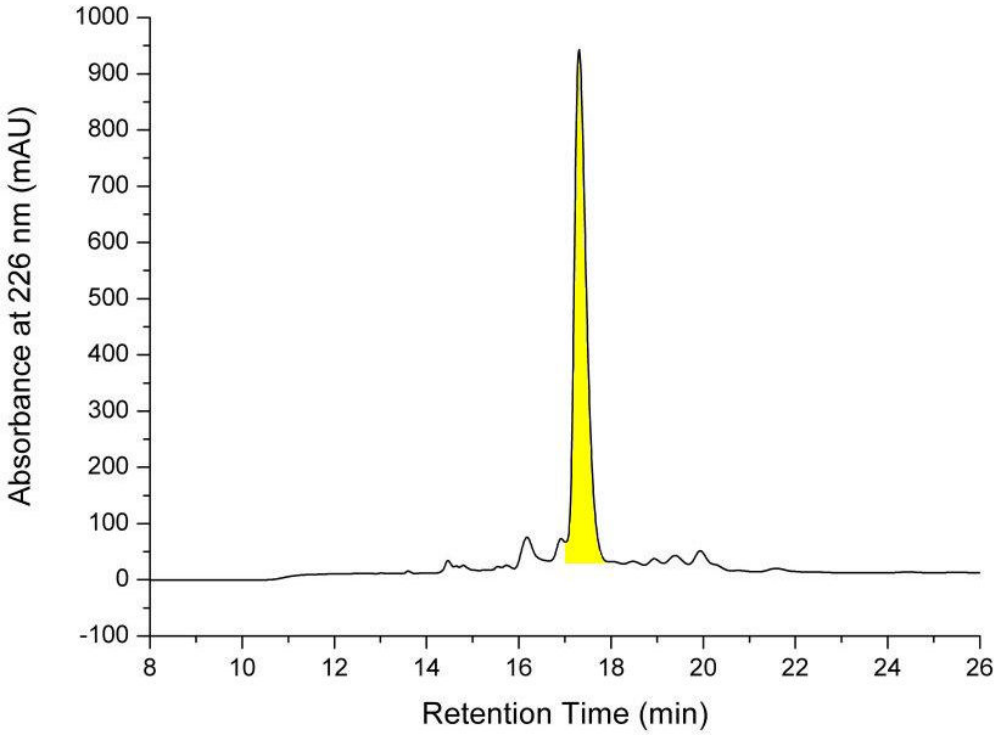

Figure 3.1.5: HPLC chromatogram of purified α-syn protein. The area under the peak considered for the calculation is coloured in yellow.

Intact α-syn is only the 50% in some batches, so it is necessary an additional purification step of the samples. To this purpose the lyophilized powder is dissolved and injected into a C18 preparative column (Figure 3.1.6). The eluted peak corresponding to α-syn is then lyophilized separately; the purity reached with this kind of purification is about 96%. Each batch of liophilyded powder was checked by mass spectrometry.

Table 3.2: Purity obtained for α-syn batches produced and stored.

α-Syn	*% purity*
Wild type α-syn	52%÷80%
A30P	87%
A53T	62%
E46K	70%
CtD	63%

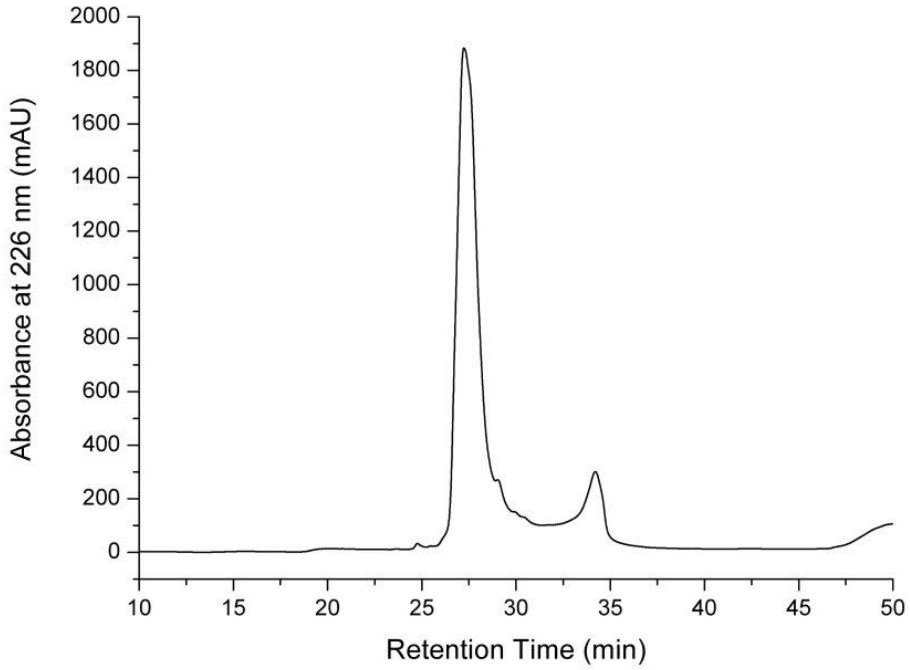

Figure 3.1.6: Final step in the purification of α-syn, chromatographic profile obtained with a preparative C18 column. Peak eluting at 27 min correspond to wild-type α-syn.

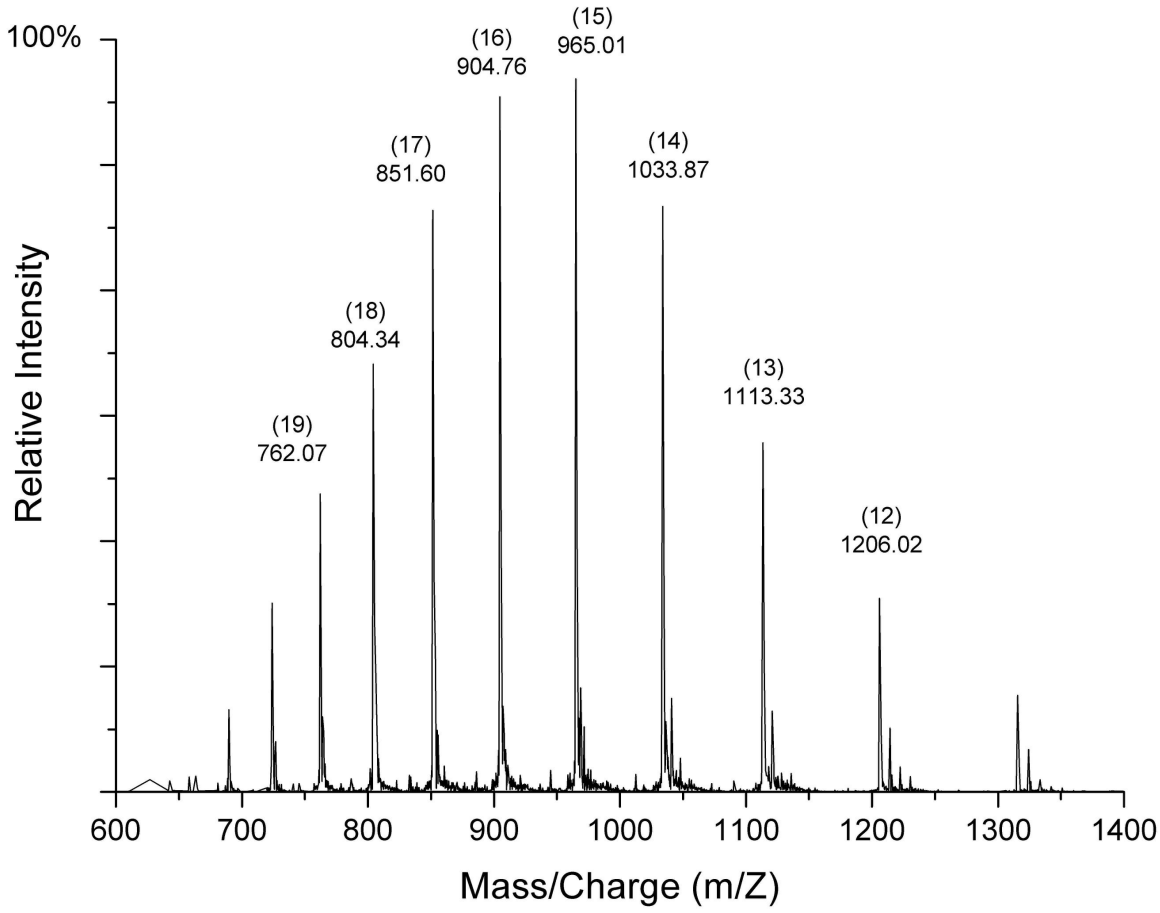

Figure 3.1.7: ESI mass spectra of wild type α-syn. Mass/charge value is reported for each peak while the charge of each specie is indicated within brackets.

3.1.3 Expression and purification of α-syn fragment 57-102

α-Syn fragment 57-102 is produced histidine-tagged. As this fragment is missing the C terminal, it is not conveyed to the periplasm, pelleted bacteria have to be sonicated to disrupt membrane and release proteins. The lysate is directly loaded into Co^{2+}-NTA resin in batch and eluted isocratically with a single step of elution buffer (150 mM imidazole, see § 2.2.3). The protein can be then lyophilized directly. The Histidine tag can be removed by digestion with thrombin.

3.1.4 Peptide purification

A series of peptides were designed by El-Agnaf and coworkers (2004) to test their ability to inhibit α-syn aggregation. Two of these peptides were used in fibrillogenesis experiments (see Section 3.4 of Results). The synthetic peptides named as ASI1 and ASI4 was synthesized by the laboratory of Dr. Barbara Biondi. The peptides was purified before the use by HPLC C18 preparative column, to separate the peptide from a contaminant peptides that are present in every preparation. Figure 3.1.8 shows the chromatographic profile of one of the peptide. The first peak corresponds to the desired peptide; ones eluted, it is lyophilized separately.

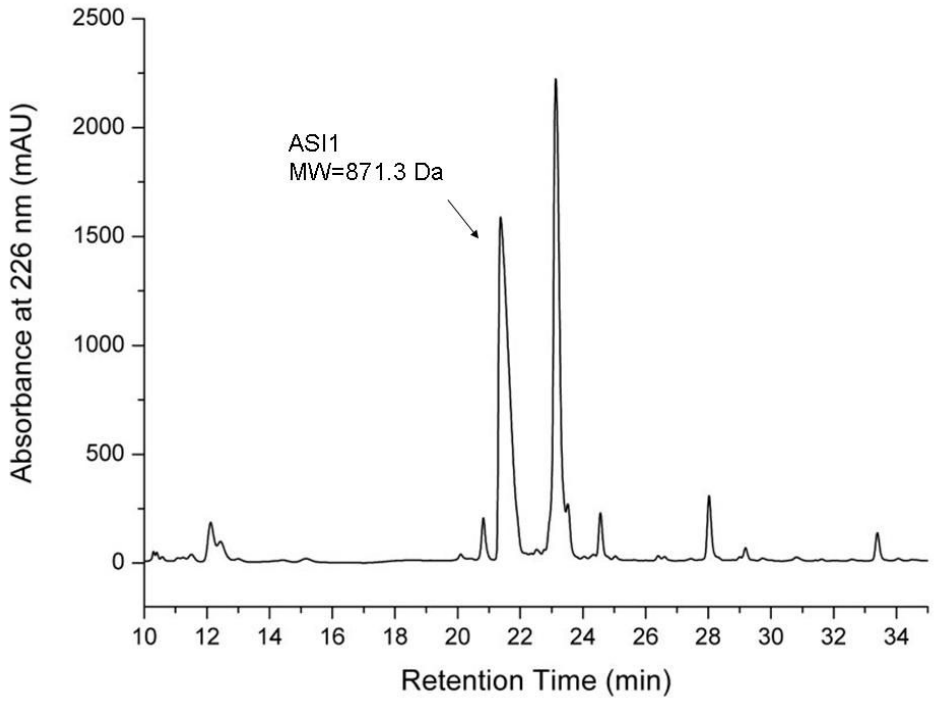

Figure 3.1.8: HPLC C18 preparative column of ASI1 peptide. Eluted peaks was analyzed by MS and it was found that the species eluted at RT 21.5 corresponds to ASI1 peptide while the other peaks was peptides with lower MW.

3.1.5 Conjugation, purification and characterization of fluorophores labelled alpha-synuclein

As α-syn primary structure does not contain any tryptophan, fluorescence studies are difficult to perform due to low absorption and quantum yield of tyrosines. Then, Cysteine mutants of α-syn were used for the conjugation with fluorescent molecules by maleimide chemistry.

2-(4-Maleimidophenyl)-6-methylbenzothiazole (MBT) was the first molecule chosen for this aim. The rational behind the choice of this molecule is its hydrophobicity, that would allow membrane interaction experiments, and its spectroscopic properties (λ_{ex}=337 nm, λ_{em}=390 nm), which made it a possible candidate to be the acceptor of FRET pair Trp/MBT, for protein-protein interaction purposes.

Chapter 2 describes the experimental conditions used for the conjugation reactions. Here HPLC chromatogram of reaction mixture after 2 h incubation of MBT maleimide with SynE35C (Figure 3.1.9A) or CtM (Figure 3.1.9B) is reported. These two proteins were used for preliminary experiments and characterization of α-syn labelled molecules.

As it can be deduced from the chromatographic profile, the reaction yield is different for the two kind of single point mutants: while for E35C the reaction is almost complete after 2 h of incubation, CtM reacts poorly with MBT maleimide. This is probably due to low solubility of the fluorescent molecule and high net charge of the C-termini of α-syn, where the cysteine residue is positioned. This can be compared with the low tendency of CtM to form dimers (§ 3.1.2). Also, it was observed that TCEP used for the reduction of disulfide bonds can compete for the reaction with maleimide (Shafer et al., 2000). In fact, a covalent adduct formed by MBT and TCEP was identified by ESI-MS (Figure 3.1.9B).

To solve low yield problem, a factorial experimental plan was set up using different condition: three temperature (25°, 37°C and 45°C) values and four TCEP concentration (0, 2, 3.5 and 5 molar excess), while length of reaction, α-syn and MBT concentration and buffer used was kept constant. Figure 3.1.10 shows that the best condition applicable to CtM reaction with MBT are 45°C in absence of TCEP. Reaction yield are calculated on the basis of the area of the peak corresponding to labelled protein in HPLC.

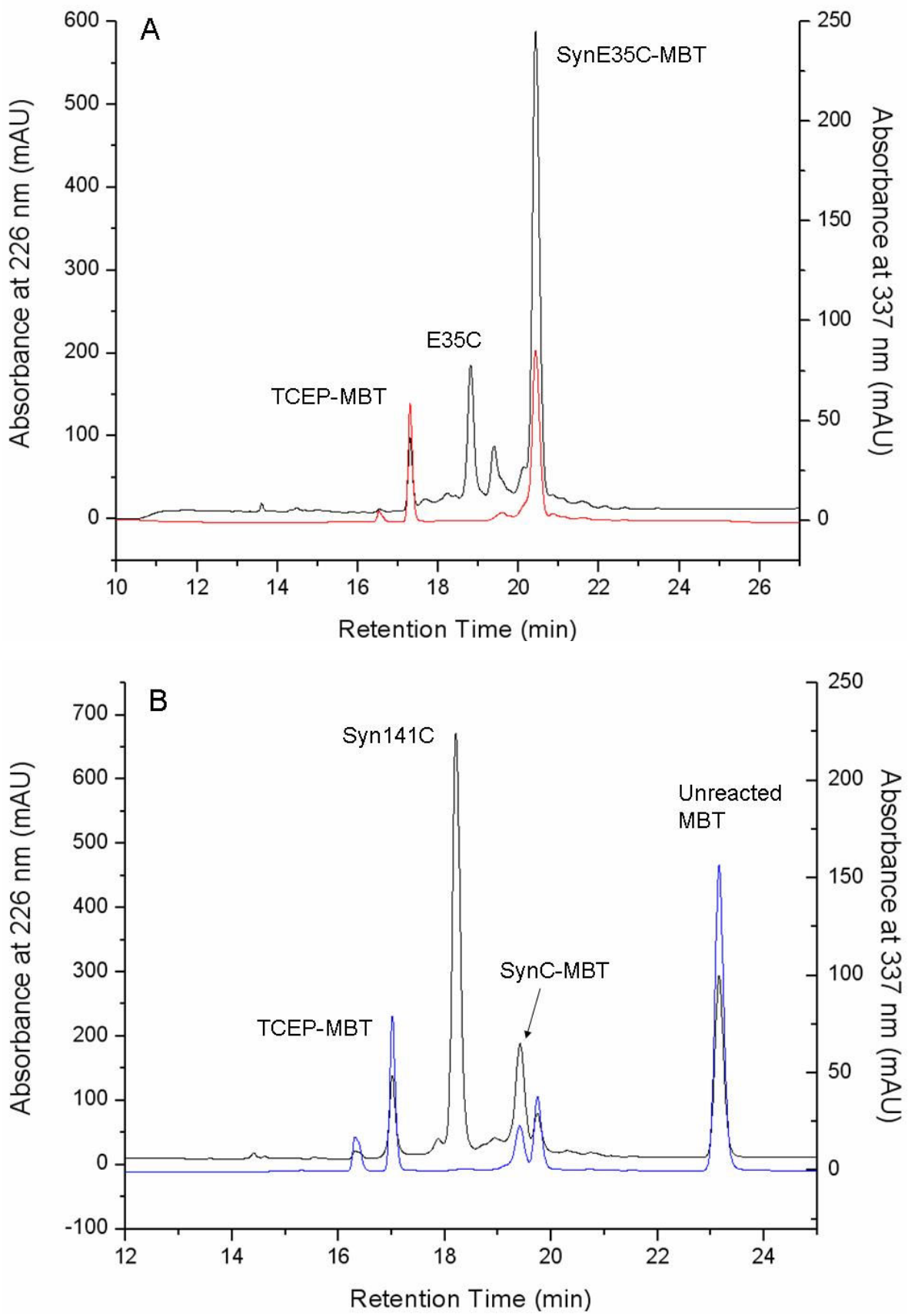

Figure 3.1.9: HPLC chromatogram of 2h incubation of α-syn E35C(A) or CtM (B) with MBT maleimide.

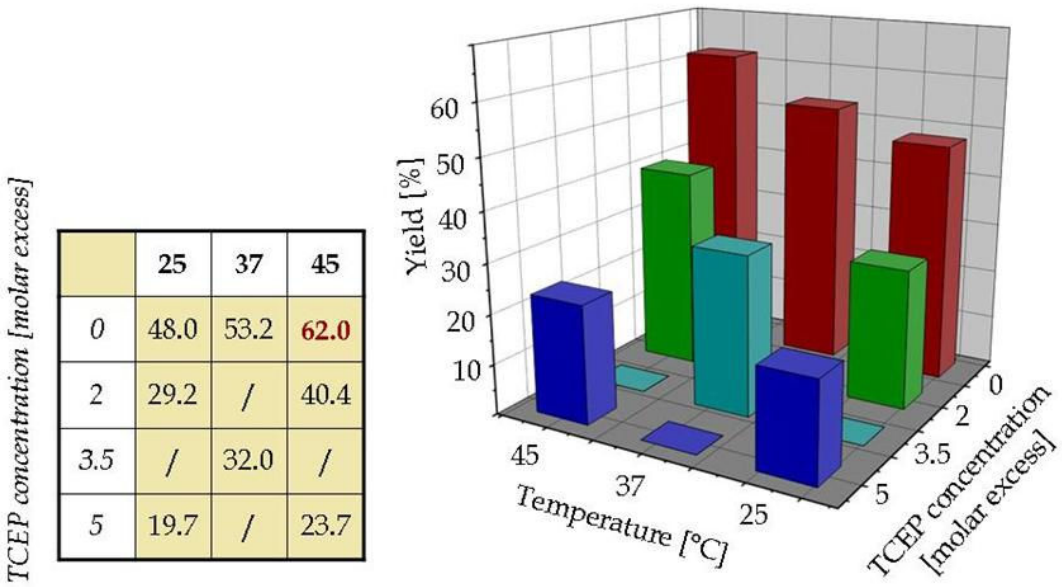

Figure 3.1.10: Factorial analysis of best experimental conditions for CtM reaction with MBT maleimide. Reaction yield are calculated on the base of the area of the peak corresponding to labelled protein in HPLC chromatogram, compared to unlabeled unreacted protein at starting time of the reaction.

The molecular mass of the labelled protein obtained (Figure 3.1.11) was verified by MS. The fluorescence spectra of the product is reported in Figure 3.1.12 and the evaluation of the lifetime of the molecule is reported in Figure 3.1.13. Figure 3.1.12 shows that the fluorophore bound to synuclein absorbs also at 295 nm, the wavelength used for selective excitation of Trp residues in proteins. This feature of MBT limits the use of this molecule in protein-protein interaction studies, because identification of FRET events between Trp and MBT is less straightforward in this case.

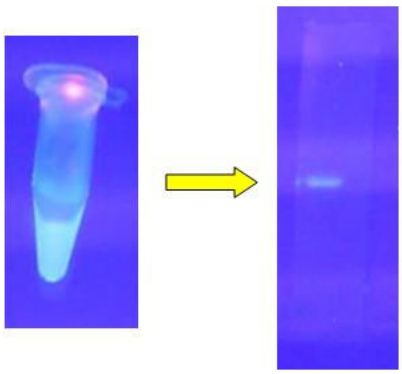

Figure 3.1.11: solution and SDS-PAGE containing α-syn labelled with MBT, upon UV excitation.

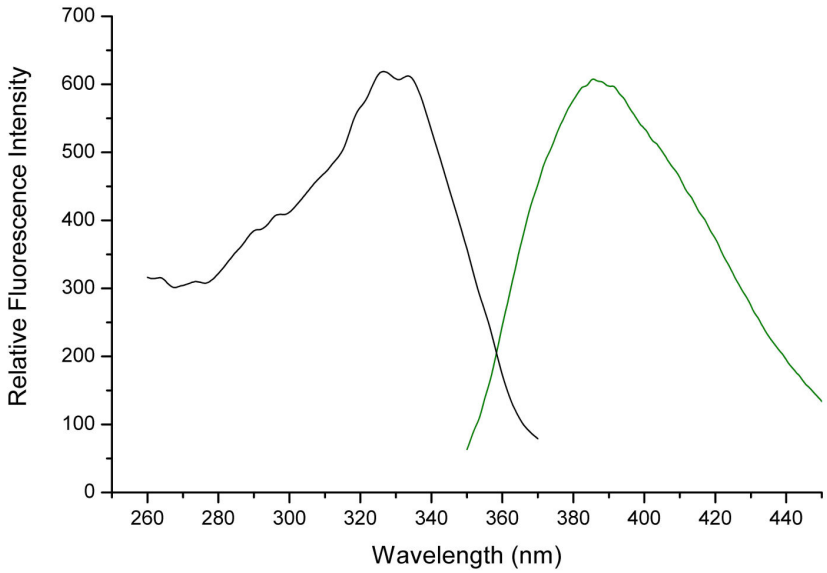

Figure 3.1.12: Fluorescence excitation and emission spectra of MBT labelled synE35C mutant. The concentration of the protein was 10µM. (λ_{ex}=334 nm, λ_{em}=390 nm).

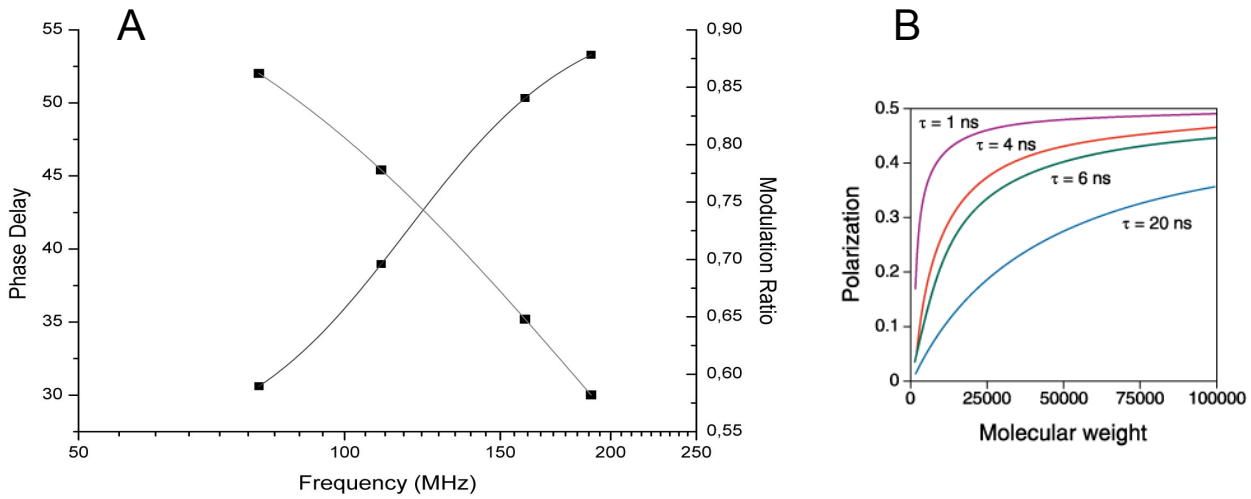

Figure 3.1.13: MBT fluorescence lifetime measured on a GREG200 fluorometer with phase-delay method (A). Relationship between fluorescence polarization, molecular weight and fluorescence lifetime of a fluorescent molecule (The Handbook, Molecular Probe – Invitrogen).

Fluorescence lifetime value calculated is 1.2 ns. This value limited fluorescence polarization sensibility to changes of molecular mass (Figure 3.1.14B), hence this molecule was not suitable for fluorescence polarization aggregation assay described in Section 3.4. In fact, when fluorophore with a short lifetime absorbs a photon, it does not have the time to re-orientate before the decay of the signal (see § 2.1.1). So, short lifetime fluorophores are not effective to detect events of molecular mass changes, like those occurring in protein

aggregation and protein interaction with large macromolecules like small unilamellar vesicles. Thus, it was important to use a fluorescent label characterized by a comparatively longer lifetime. In this frame, Oregon Green 488 (Molecular Probes, Invitrogen) was selected (Figure 3.1.15A). This molecule is an analogue of fluorescein (Figure 3.1.15B) with reduced photobleaching effect; the lifetime was documented to be 4.1 ns and extinction coefficient 81000 $M^{-1}cm^{-1}$ at 491 nm. Figure 3.1.15 both the structures OG and fluorescein together with the excitation and emission spectra of OG (The Handbook, Molecular Probes – Invitrogen).

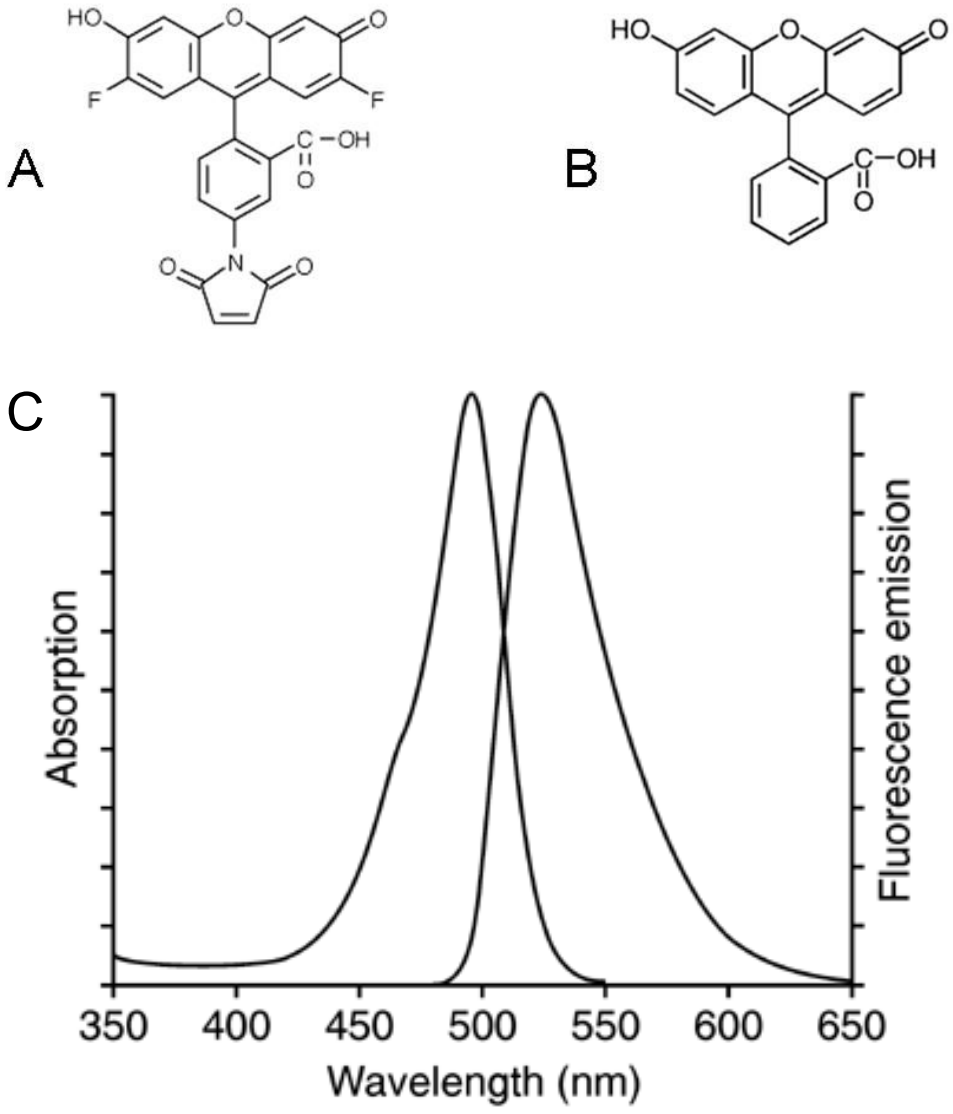

Figure 3.1.15: Oregon Green 488 maleimide structure (A). Fluorescein structure (B). Excitation and emission spectra of Oregon Green 488 (The Handbook, Molecular Probes – Invitrogen)(C).

The information on maleimide reactivity against α-syn cysteine residues was used for the conjugation to OG maleimide. OG maleimide was then mixed 1:10 to α-syn at 45°C, 5 molar excess TCEP, according to manufactures instructions and reaction yield obtained can be deduced from the chromatographic profile shown in Figure 3.1.11. The reaction was held till 4 hours, then labelled CtM purified by HPLC (Figure 3.1.16).

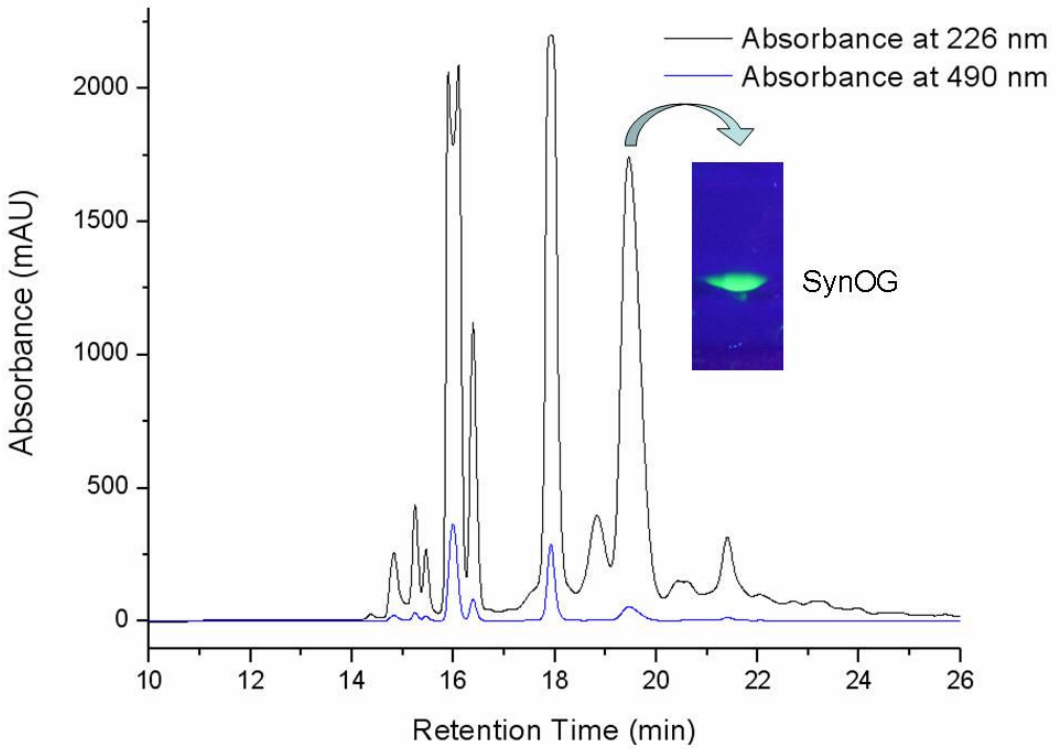

Figure 3.1.16: HPLC chromatogram of reaction mixture of syn CtM and Oregon Green 488 maleimide. Peak corresponding to 19.5 minutes retention time was identified as labelled α-syn from SDS-PAGE analysis put on UV lamp (insert) and ESI-MS.

OG labelled CtM (synOG) was identified as RT 19.5 of chromatogram shown in Figure 3.1.16 by ESI-MS. Then the eluted peak was dried in a Speed-Vac centrifuge and stored.

3.2 Interaction with membranes

The study of α-syn interaction with membranes is of great interest in the comprehension of α-syn interaction network and possibly the ethipatogenesis of PD. α-Syn was found to bind to synaptic vesicles (Clayton & George, 1999) even if it does not copurify

with them (Takamori et al., 2006). These and other evidences suggest that α-syn can be parted in the cell in a cytosolic pool and a vesicle associated pool. The equilibrium that regulates the transition between the two pools can be altered by toxic insults, mutation in α-syn interacting proteins, point mutation in α-syn itself and impairments in lipid metabolism. Such events can increase α-syn concentration in the cytoplasm, leading to a higher protein aggregation probability.

Investigation of α-syn monomer interacting with membranes was reported in detail in § 1.2.3. Several papers described also the ability of α-syn oligomers to interact with membranes, sometimes reporting heavy effects on membrane integrity (Zhu et al., 2003; Quist et al., 2005; Zakharov et al., 2007). These papers report on the capacity of α-syn oligomers to bind to membranes and pierce them. Pore like channels were observed (Quist et al., 2005) and ionic currents recorded (Zakharov et al., 2007). In particular, this latter work for the first time put forward the hypothesis that pores assemble on membranes as consequence of the applied membrane potential. Thus, it would be very interesting to investigate the behaviour of early aggregates forms of α-syn in contact with membranes. The α-syn dimers described in the previous section, were mixed with small unilamellar vesicles (SUVs) or with SDS micelles, to investigate whether the covalent constrain at the N-terminal or at the C-terminal of the polypeptide chain could alter the membrane binding properties of α-syn.

Figure 3.2.1 shows a schematic representation of α-syn dimers obtained as described in § 3.1.2.

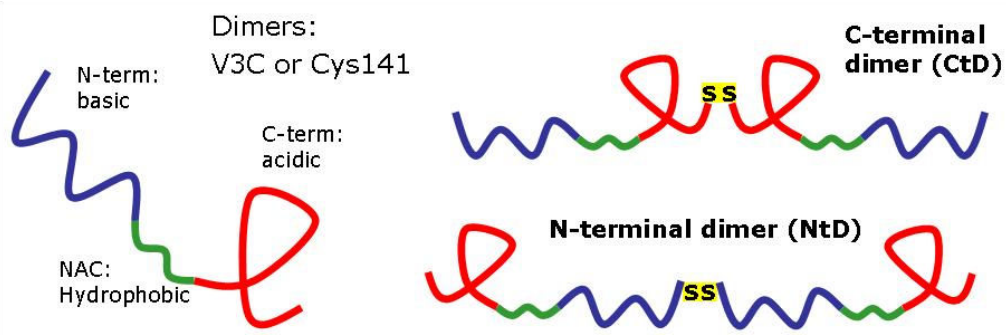

Figure 3.2.1: Schematic representation of α-syn dimers used in experiments in the presence of SDS micelles and acidic SUVs.

Figure 3.2.2 reports signals obtain from α-syn, monomeric and dimeric cysteine mutants in 20 mM sodium phosphate buffer, at pH 7.4. Spectra of monomer was recorded in the presence of 5 molar excess TCEP to prevent dimer formation. TCEP does not interfere with α-syn signals (data not shown). Although all the signals recorded can be assigned to a

majority of random polypeptide chain, the comparison of the monomeric and dimeric form of the C-terminal dimer reveal a difference in the 220 nm region.

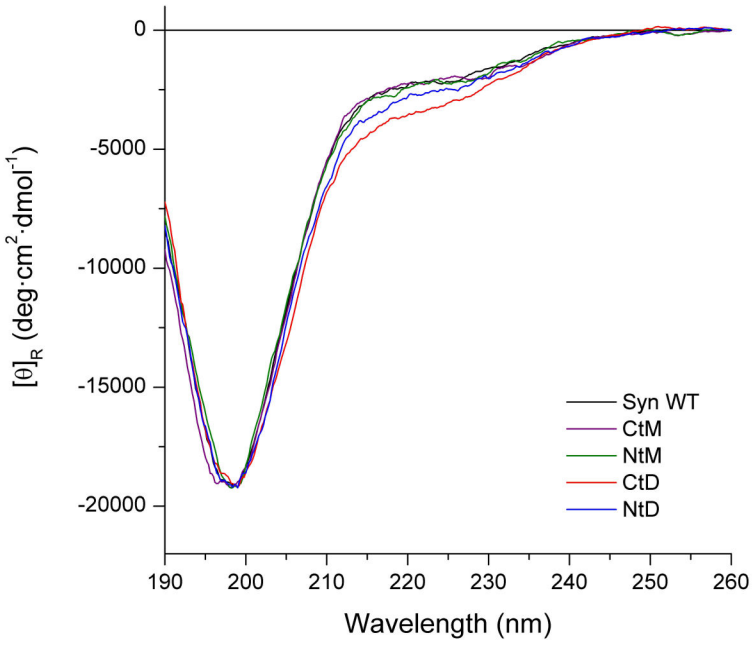

Figure 3.2.2: CD spectra of α-syn (black line), monomeric (purple) or dimeric (red) Cys C-terminal mutant, monomeric (green) or dimeric (blue) Cys N-terminal mutant. Spectra was recorded in 20 mM sodium phosphate buffer, at pH 7.4.

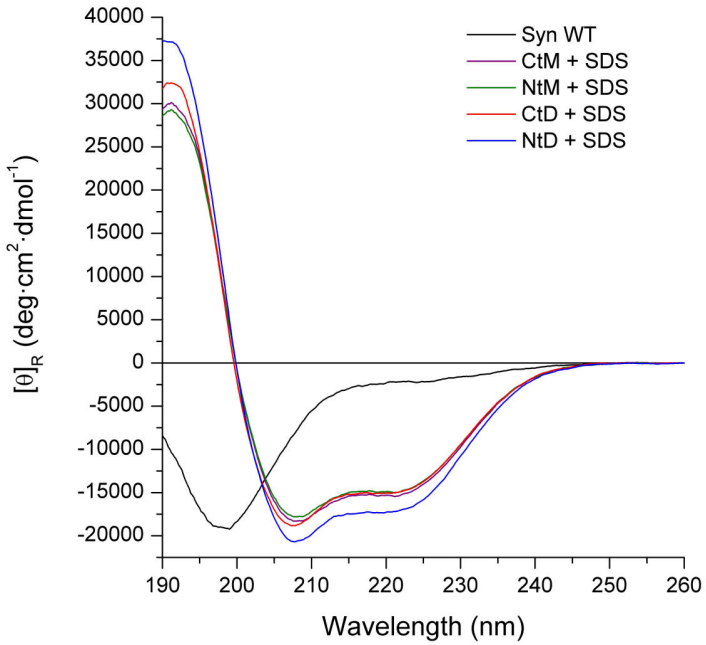

Figure 3.2.3: CD signals of: α-syn in buffer as reference (black line), monomeric (purple) or dimeric (red) Cys C-terminal mutant, monomeric (green) or dimeric (blue) Cys N-terminal mutant. Spectra of mutants were recorded in 20 mM Na phosphate buffer, at pH 7.4, in the presence of 10 mM SDS.

Figure 3.2.3 presents data obtained with α-syn monomers and dimers in the presence of SDS micelles. Spectra obtained show the formation of an α-helix, as it can be seen from minima at 208 and 222 nm. There are not significant differences between the species analyzed. A more interesting results came from the mixture of CtD with liposome obtained from 30 mM 50:50=PG:PC extruded with a 50 nm diameter membrane. The signal reported in the presence of SUVs in Figure 3.2.4 are different in comparison to those of the same samples in the presence of micelles, indicating the formation of a different distribution of α-helical structure. This observation may suggest that different dimention and therefore curvature of SUV and micelles may lead in the presence of the covalent constrain of the dimeric protein to either a distortion in the α-helixes or to a different distribution of structure for α-syn associated to the membrane. Further investigation are needed for to unravel the possible biological implications of this observation.

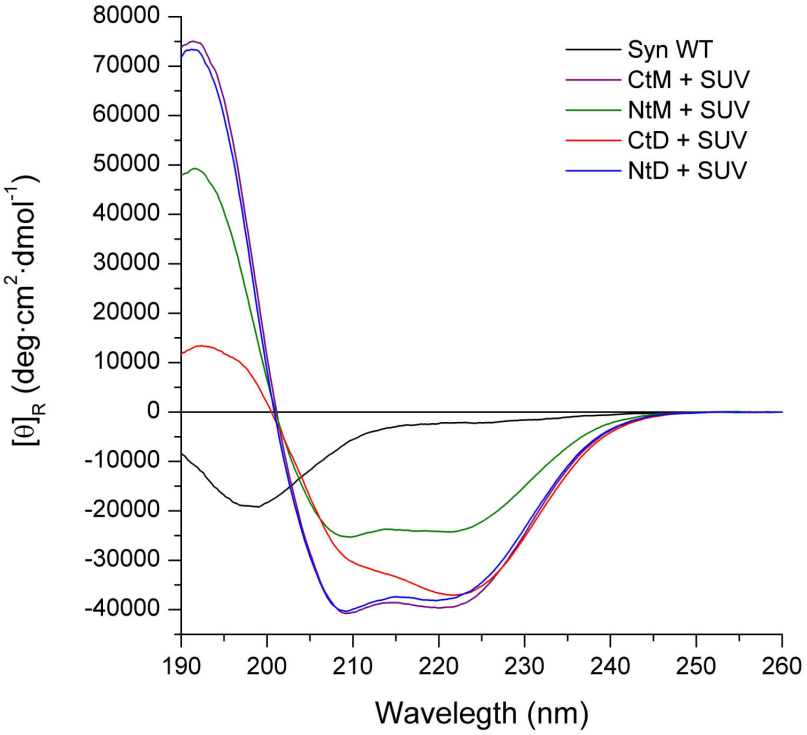

Figure 3.2.4: CD signals of α-syn (black line), monomeric (purple) or dimeric (red) Cys C-terminal mutant, monomeric (green) or dimeric (blue) Cys N-terminal mutant. Spectra was recorded in 20 mM Na phoshate buffer, at pH 7.4, in the presence of 10 mM SDS.

3.3 Interaction with proteins

3.3.1 Interaction with 3T protein

Two papers recently published by our laboratory in collaboration with University of Bologna (Sandal et al., 2008; Brucale et al., 2009) reported an analysis of the conformational properties of α-syn by Single Molecule Force Microscopy (SMFM). This method is a new development of Atomic Force Microscopy (AFM) in which single molecules can be selectively pulled to completely unfold its structure (Kellermayer et al., 1997; Forman & Clarke, 2007). The importance of this kind of experiments relies on the possibility of the study on single molecules and on the consequent possibility to detect rare events in proteins conformational distributions. To do this kind of experiments, chimeric proteins are needed, as α-syn per se is not suitable. To this aim, olecular chimeras were produced in our laboratory, flanking to both sides of an α-syn molecule three modules of I27 domain of human titin, which is a protein with well characterized elastic properties (Kellermayer et al., 1997). I27 domain contains only β-sheet secondary structure, which has the best characterized unfolding behaviour by SMFM. The chimeric protein is called 3S3 and the constructs used in SFMF experiments are shown in Figure 3.3.1.

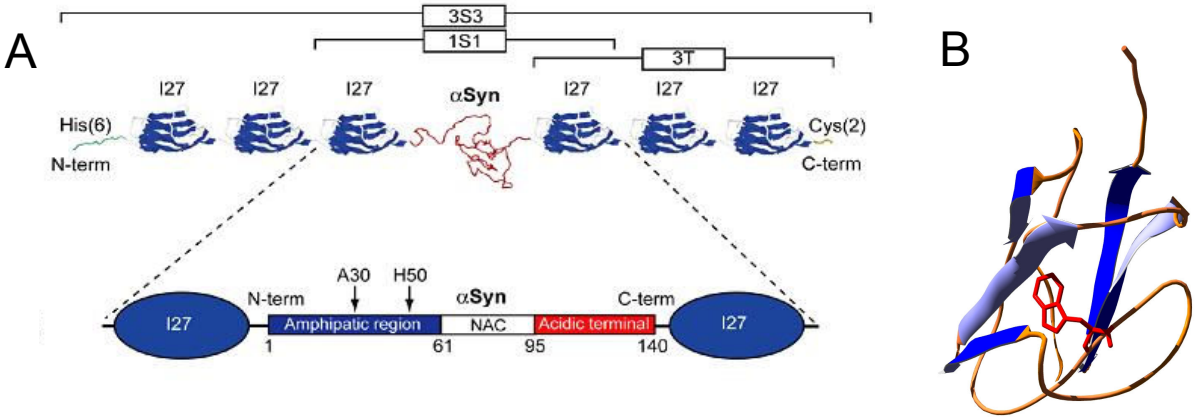

Figure 3.3.1: A) Chimera protein used in SMFM experiments on α-syn; at the N-terminal side Histidine tag allow an effective purification of the protein, the 2 Cys residues at the C-terminus are added to allow binding of the molecule on the gold surface of the sample holder. Adapted from Sandal et al. (2008). B) representation of the structure of the I27 module; Trp residue is evidenced in red (PDBcode: 1TIT).

Polypeptide chains are placed on a gold surface, to which protein bind by interaction of the two cys residues which are introduced by molecular biology at the and of aa sequence.

This binding has a high selectivity since both wt α-syn and I27 do not contain any Cys residue. Then, the cantilever passing on the surface pulls single molecules caught on (Figure 3.3.2). Resistance of the molecule to pull stress is detected and plotted vs distances (Figure 3.3.2B). Secondary structures and intramolecular interaction can be detected. While weak intramolecular interaction and α-helical secondary structures give poor resistance to pulling, β-sheet unfolding give a well defined signal due to the sudden disruption of several hydrogen bonds. The experimental set up allows for the measurement of a large number of curves, that a detailed statistical analysis allow to convert into a distribution of conformational. As this method is able to study single molecules, conformations that rarely occur in solution can be detected, in opposition to bulk analytical techniques in which rare conformers goes undetected below the multitude of the more frequent conformers.

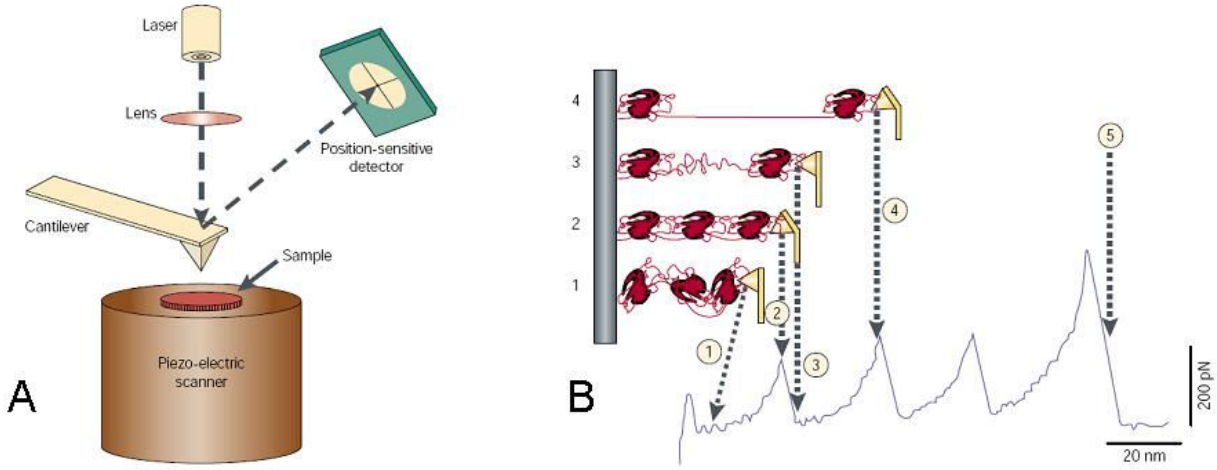

Figure 3.3.2: AFM apparatus: the sample is put on the gold surface, that is scanned by cantilever; piezo-electric scanner moves left and right to scan the surface and up and down to pull proteins that have bound to cantilever and; a laser ray point to the cantilever and a detector measures the difference in angle reflection of the light (A). Example of a pulling experiment on single molecule performed by SMFM: the protein is caught by the cantilever and pulled, relative resistance and bonding breakage is reported on a distances vs. forces graphic (B). Adapted from Bustamante et al. (2000).

Interesting results have been obtained on the α-syn conformation distribution as a function of high ionic strength (Sandal et al., 2008) or in the comparison of pathological mutants of α-syn linked to early onset Parkinson disease (Brucale et al., 2009).

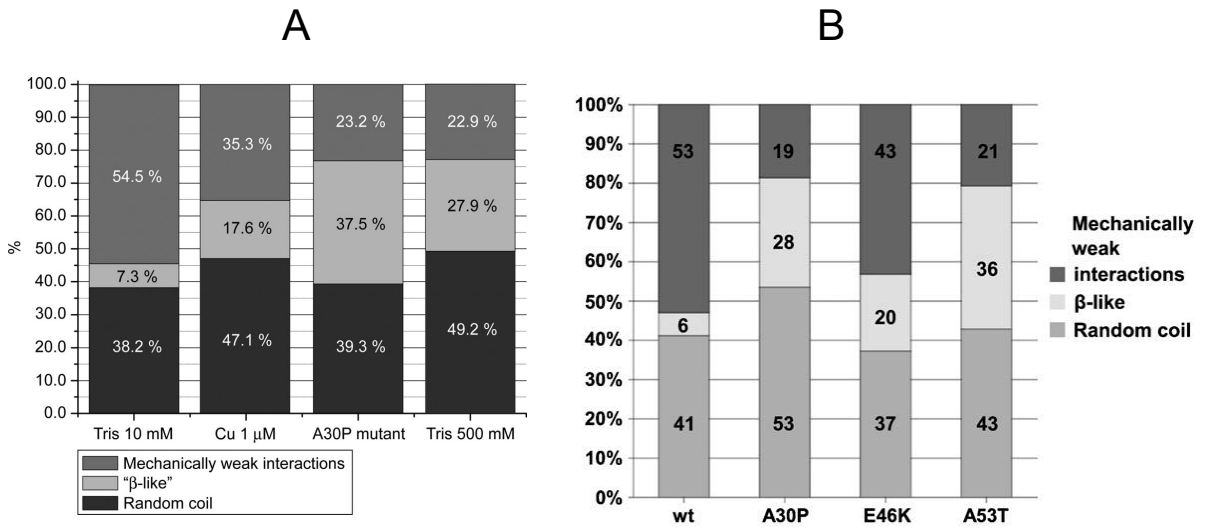

Figure 3.3.3: A) Conformational distribution analysis of 3S3 chimeric protein in 10 mM Tris, 10 mM Tris 1 µM Cu^{2+}, A30P mutant into 3S3 construct and 3S3 in 500 mM Tris; all measures was performed at pH 7.5 (Sandal et al., 2008). B) Conformational distribution of early onset pathological mutants inserted into 3S3 construct, performed in 10 mM Tris, pH 7.5 (Brucale et al., 2009).

The conformation distribution in Figure 3.3.3B shows the presence of three species in solution, characterized by a distinct behaviour to pulling events: random coil, which gives no resistance to pulling; weak intramolecular interactions characterized by the presence of a weak resistence, and β-like structure, which presents a SMFM signal analogous to β-sheet unfolding. 3S3 construct shows different distributions in random coil, weak interaction and β-like conformation in dependence of experimental condition. The presence of Cu^{2+}, high ionic strength and single point mutations linked to early onset PD enhance the presence of β-like forms. In particular, β-like structures account for about 30% of A30P and A53T conformers detected in solution, while wt α-syn presents only 6% β-sheet like containing forms. This findings are relevant because β-sheet conformation is believed to be the first event in protein aggregation leading to fibrillogenesis, and for 3S3 chimera β-sheet formation was estimated to involve the 2/3 of α-syn polipeptide chain, beyond I27 modules (Sandal et al., 2008).

Some controls were needed to test the presence of aspecific interactions between α-syn and I27 modules and eventually to characterize them. Previous CD and fluorescence experiments showed that α-syn within the construct 1S1 (a shorter form of chimera constituted by α-syn flanked with a single I27 module) is able to interact with titin modules

(Figure 3.3.4). Figure 3.3.4A shows that α-syn signal obtained by subtraction of the contribution of I27 in the 1S1 CD signal, revels the presence of an α-helix content. Therefore intramolecular interaction between α-syn and I27 modules can enhance the natural propensity of α-syn to adopt α-helical structure. This is probably due to interaction between the negative charged surface of titin modules and lysine residues of α-syn N-terminal part (Sandal et al., 2008).

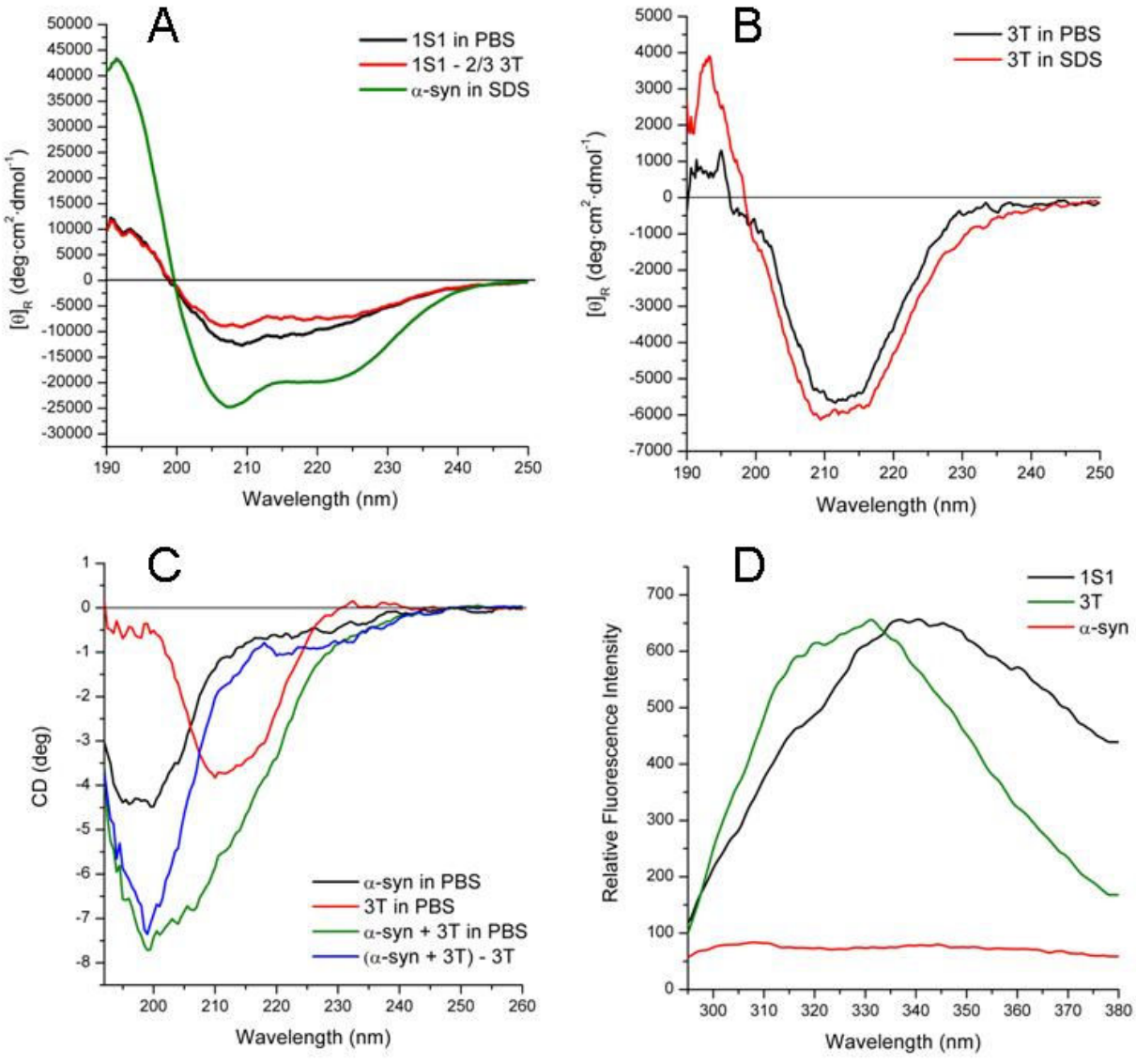

Figure 3.3.4: CD spectra of 1S1 construct in PBS (black line), α-syn in 250 molar excess SDS (green line), 2/3 of 3T signal substracted to 1S1 spectrum (red line) (A). 3T signals in PBS (black line) and 250 molar excess SDS (red line) (B). CD spectra of α-syn (black line), 3T (red line), 1:1=α-syn:3T (green line) and the subtraction of 3T signal to the one of the mixture (blue line), all spectra was recorded in PBS (C). Trp emission spectra of 1S1 (black line), 3T (green line) and α-syn (red line) (D).

However, when wt α-syn is mixed with 3T protein (a chimera constituted by three modules of I27), the CD signals is simply the sum of the contributions of the α-syn random structure and of the 3T β-sheet conformation (Figure 3.3.4B and C). Also I27 Tryptophanes emission shows a red shift in 1S1 construct, revealing a conformational change in I27 module that change Trp exposure to solvent compared to Trp emission of 3T protein (Figure 3.3.4D).

To further verify that this kind of interaction is only due to intramolecular constrain and not to a specific interaction, α-syn labelled with MBT (§ 3.1.5) was used to investigate whether Forster Resonance Energy Transfer (FRET) occurs between Trp and MBT fluorophore.

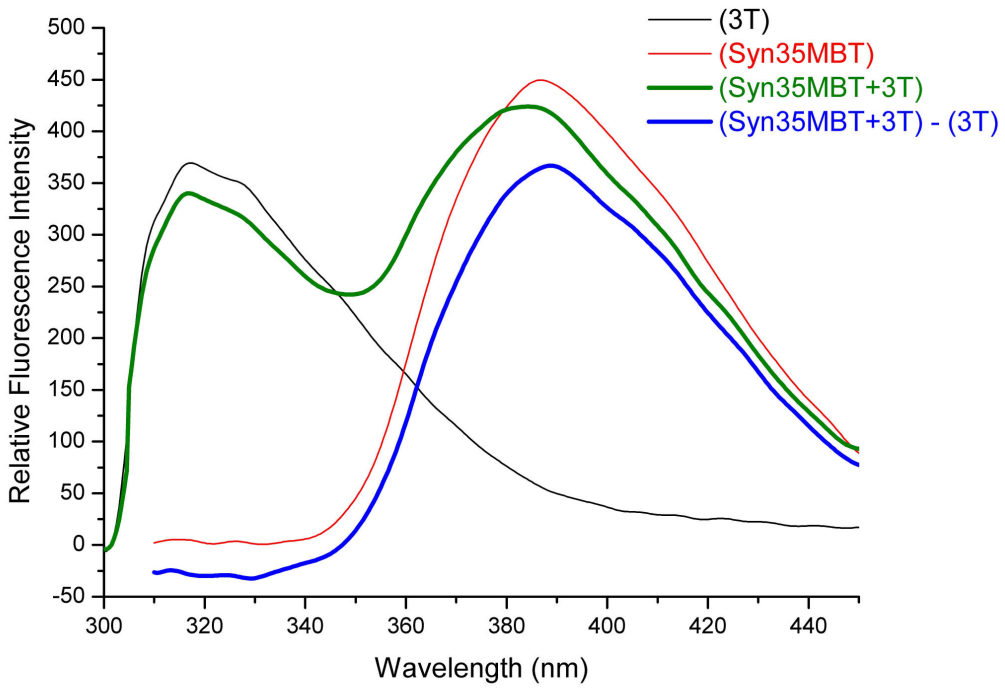

Figure 3.3.5: Fluorescence emission spectra of synMBT and 3T protein.

Figure 3.3.5 shows fluorescence spectra obtained for 3T protein (black line), synMBT (red line) and 1:1 mixture of the two proteins (green line). Signals was obtained in PBS, with 295 nm as excitation wavelength. Note that MBT is also excited at 295 nm. However, no enhancement of MBT fluorescence emission is obtained, and fluorescence signal of the mixture is the sum of the signals recorded for the two proteins alone (grey line). Also note that no red shift is detectable for 3T protein emission with the addition of α-syn, indicating that no conformational changes occur in this case. Being a negative result, this esperiment did not contribute to the definition of the purported interaction between 3T and α-syn.

3.3.2 Interaction with 14-3-3 proteins

14-3-3 proteins is a family of acidic regulatory molecules of about 30 kDa expressed in eukariotic cells. They bind to several different signalling proteins, including kinases, phosphatases and transmembrane receptors. 14-3-3s are present as seven isoforms in humans and can form homo and eterodimers. A specific combination of dimer formation may influence which of the 14-3-3 interacting protein could be brought together. Over 200 proteins have been shown to interact with 14-3-3 specifically and some of them are involved in neurodegenerative disease (Aitken, 2006). Of note, 14-3-3s are molecular chaperones, and 14-3-3η is also found in Lewy bodies (Kawamoto et al., 2002). So, the study of the interaction of 14-3-3 proteins, in particular isoform η, is relevant for the comprehension of α-syn interaction network.

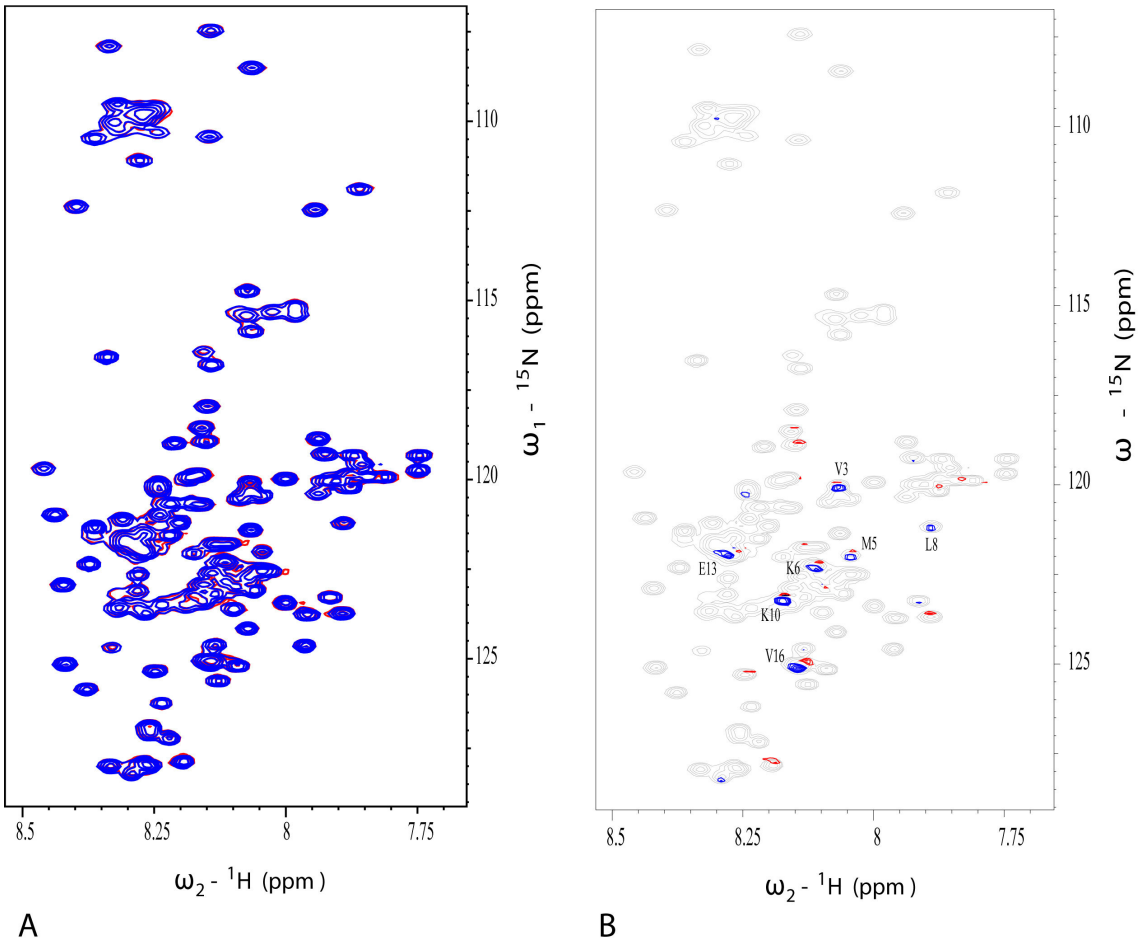

Figure 3.3.6: Overlay (A) and difference map (B) of ^{15}N-labelled α-syn [^{1}H–^{15}N] HSQC spectra recorded with (red) or w/o (blue) 3 molar excess of 14-3-3η.

HSQC (Heteronuclear Single Quantum Coherence) spectra of ^{15}N labelled α-syn was performed by Dr. Francesca Munari of our research group in the presence or the absence of three molar excess 14-3-3η protein. Figure 3.3.6A shows only small differences in the chemical shifts values of α-syn residues. Panel B reveals some changes in relative intensities, however, no interaction between α-syn and 14-3-3η protein was detected.

As Sato et al. (2006) reported direct interaction of 14-3-3η with parkin (K_d = 4.2 nM) and α-syn (K_d=1.1 μM) measured by Surface Plasma Resonance binding of 14-3-3η chaperone with Histidine tagged α-syn functionalized chip was tested. Figure 3.3.7 shows no differences between the signal of 14-3-3η injected on α-syn conjugated chip or on reference cell, even injecting increasing concentration of 14-3-3η (data not shown). The increase in response units is probably due to aspecific interaction between chip surface and 14-3-3η. Hence, these data do not show evidence of interaction between α-syn and 14-3-3η protein.

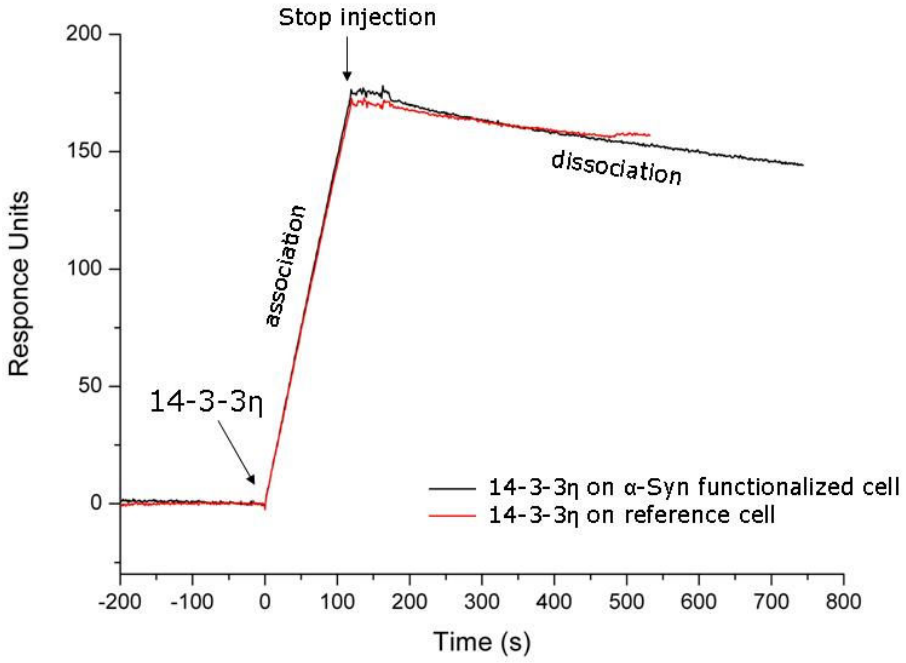

Figure 3.3.7: SPR signal of 1.3 μM 14-3-3η injection (black arrow) on α-syn functionalized chip (black line) or reference empty cell (red line). No difference between the two signals can be detected.

However, these negative results that suggest no interaction between α-syn and 14-3-3η become very interesting in the contest of the aggregation experiments (that will be described in Section 3.4) in which the 14-3-3η is competent to slow down the aggregation rate of α-syn (Figure 3.4.17). Suggesting that the interaction occurs between the chaperone and α-syn in its oligomeric state

3.3.3 Interaction with NAC derived peptides

Dr Francesca Munari also performed HSQC spectra of ^{15}N labelled α-syn in the presence of 2 molar excess ASI1 peptide. Figure 3.3.8 compares the spectra obtained. Merged signals (Figure 3.3.8C) shows no evidences of chemical shifts modification, suggesting that the reported effect of the peptide on the aggregation process may derive from an iteraction that occurs with aggregated form of α-syn.

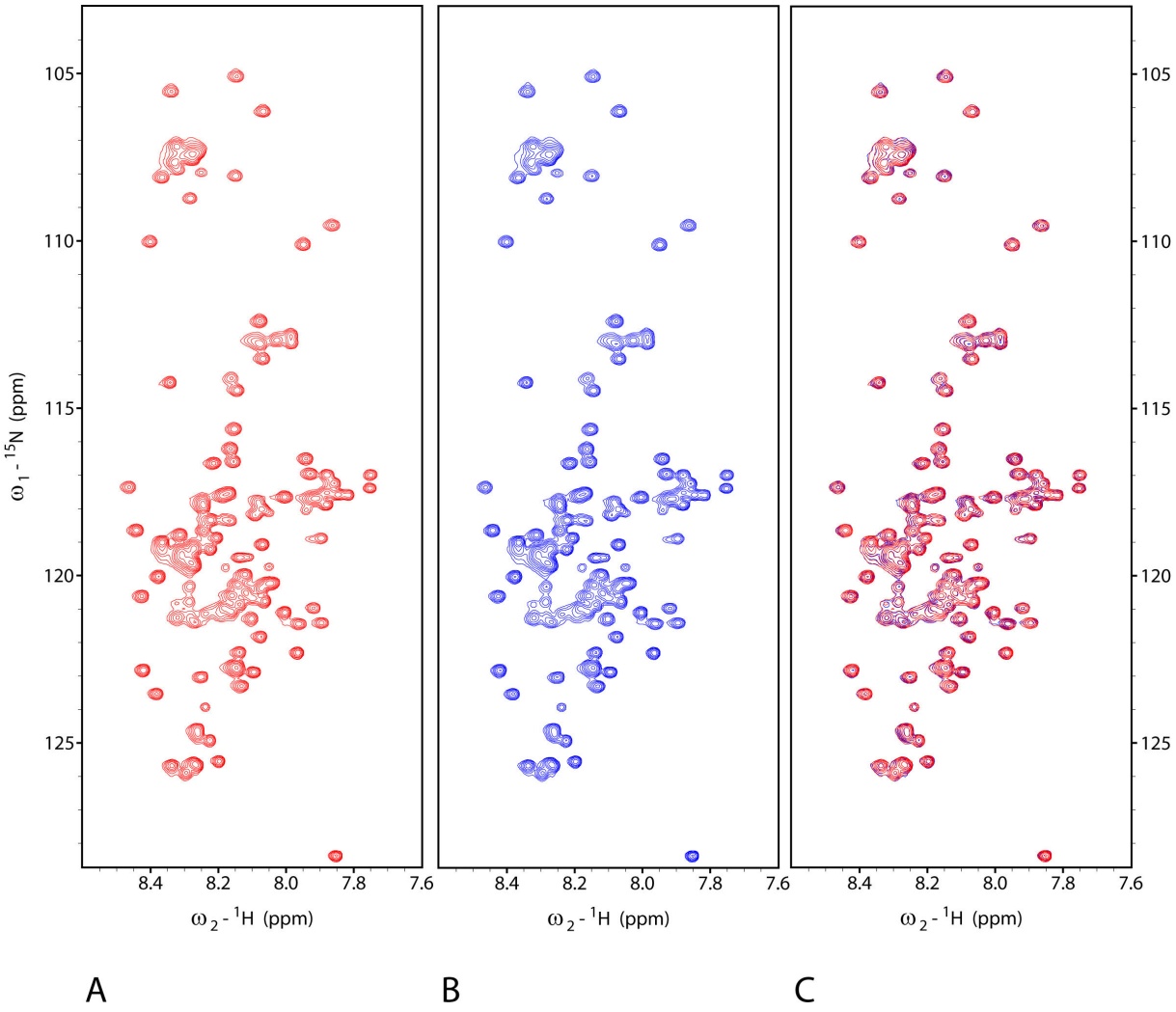

Figure 3.3.8: HSQC spectra of 0.13 mM α-syn (A), α-syn and 2 molar excess ASI1 peptide (B) and merged peaks (C). No modification of α-syn residues chemical shifts can be observed.

3.4 Self-interaction

3.4.1 Surface Plasmon Resonance self-interaction experiments

In the first experiment the self-interaction of whole α-syn molecules was tested. The Histidine-tagged α-syn was bound to the Ni-chip, then free α-syn solution was injected onto functionalized and reference cell at increasing concentrations. No interaction was detected between the free α-syn injection and the α-syn attached to the chip (data not shown).

In a second experiment the Ni-Chip was functionalized with the Histidine tagged NAC peptide (the 57-102 region). In this case the addition of α-syn resulted in a significant response reported in Figure 3.4.1.

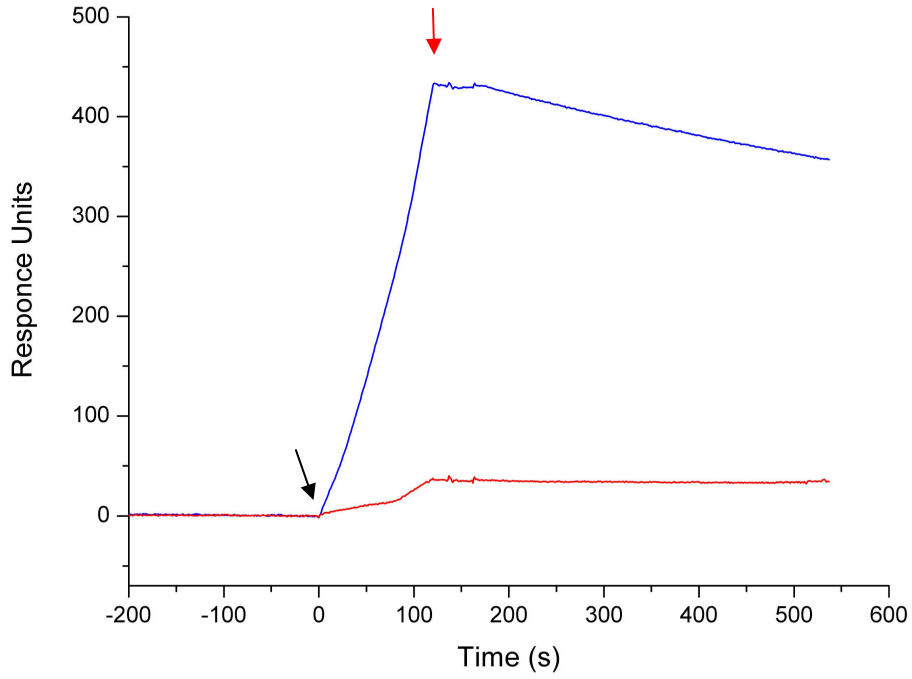

Figure 3.4.1 SPR signal of α-syn injection on NAC functionalized Ni^{2+} NTA Sensor Chip. The black arrow indicate the injection of α-syn on Histidine Tagged NAC functionalized Ni^{2+} activated NTA Sensor Chip (blue signal) or on reference cell (red signal), while the red arrow point the end of the injection and then the start of dissociation phase.

The difference in response units between the two signals in Figure 3.4.1 is proportional to the quantity of material that binds to chip surface. However, good dose/response relationship can not be obtained experimentally probably as a consequence of the low solubility of NAC used to functionalize the Ni^{2+}-NTA Sensor Chip (Figure 3.4.2 A and B). Moreover, the curves obtained can not be fitted with an exponential curve suggesting that binding do not occur as simple Langmuir binding of one molecule to another.

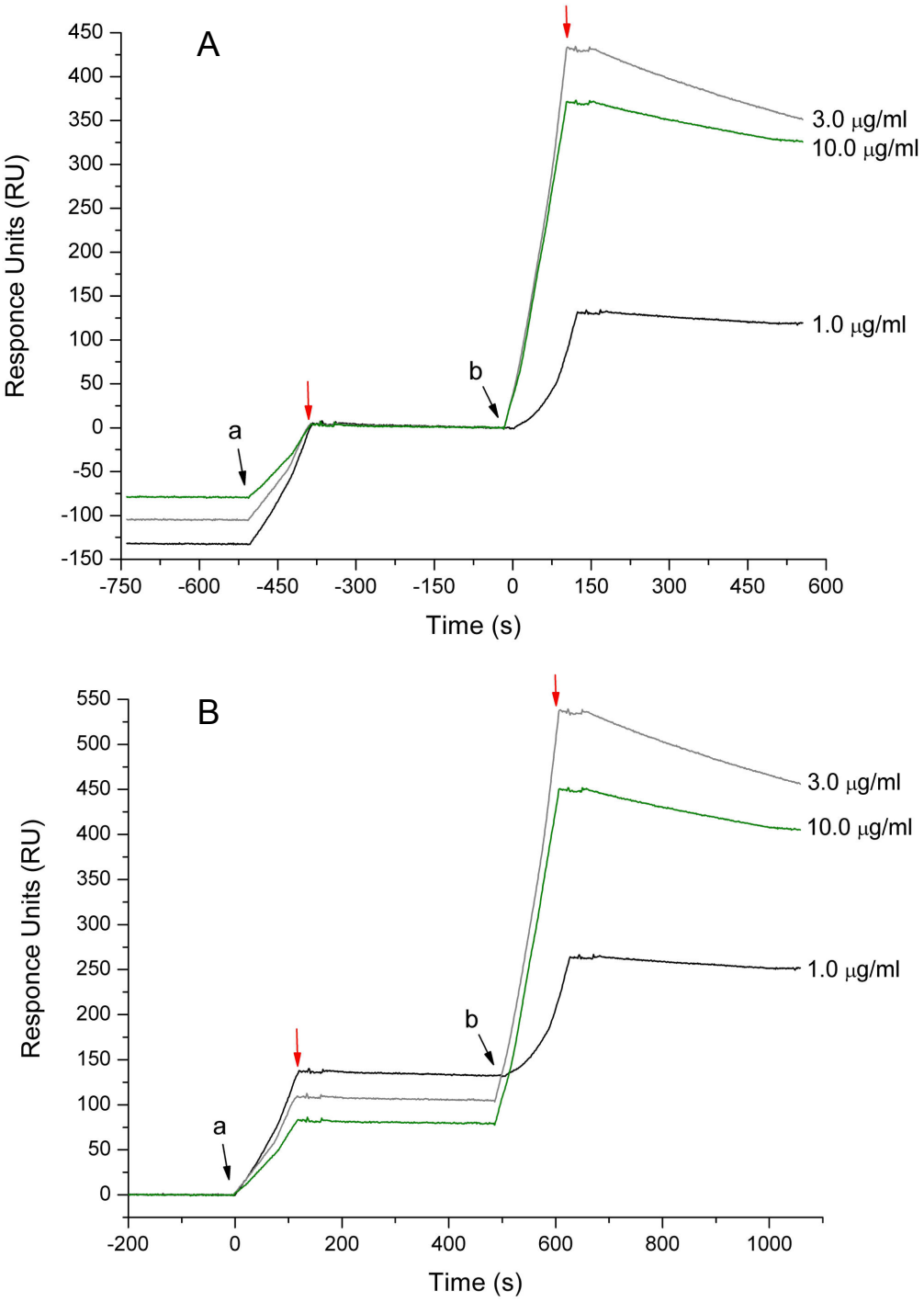

Figure 3.4.2: Dose/response relationship of α-syn on NAC activated chip. Figure A and figure B shows different alignments of the same graphic, starting from the injection of 2 µg/ml Histidine Tagged NAC on Ni^{2+} activated NTA cell (a) or from the injection of wild type α-syn (a) at different concentrations. Black arrows indicate the start of a sample injection, so the beginning of association phase, then red arrows point the end of injection and then the beginning of dissociation phase.

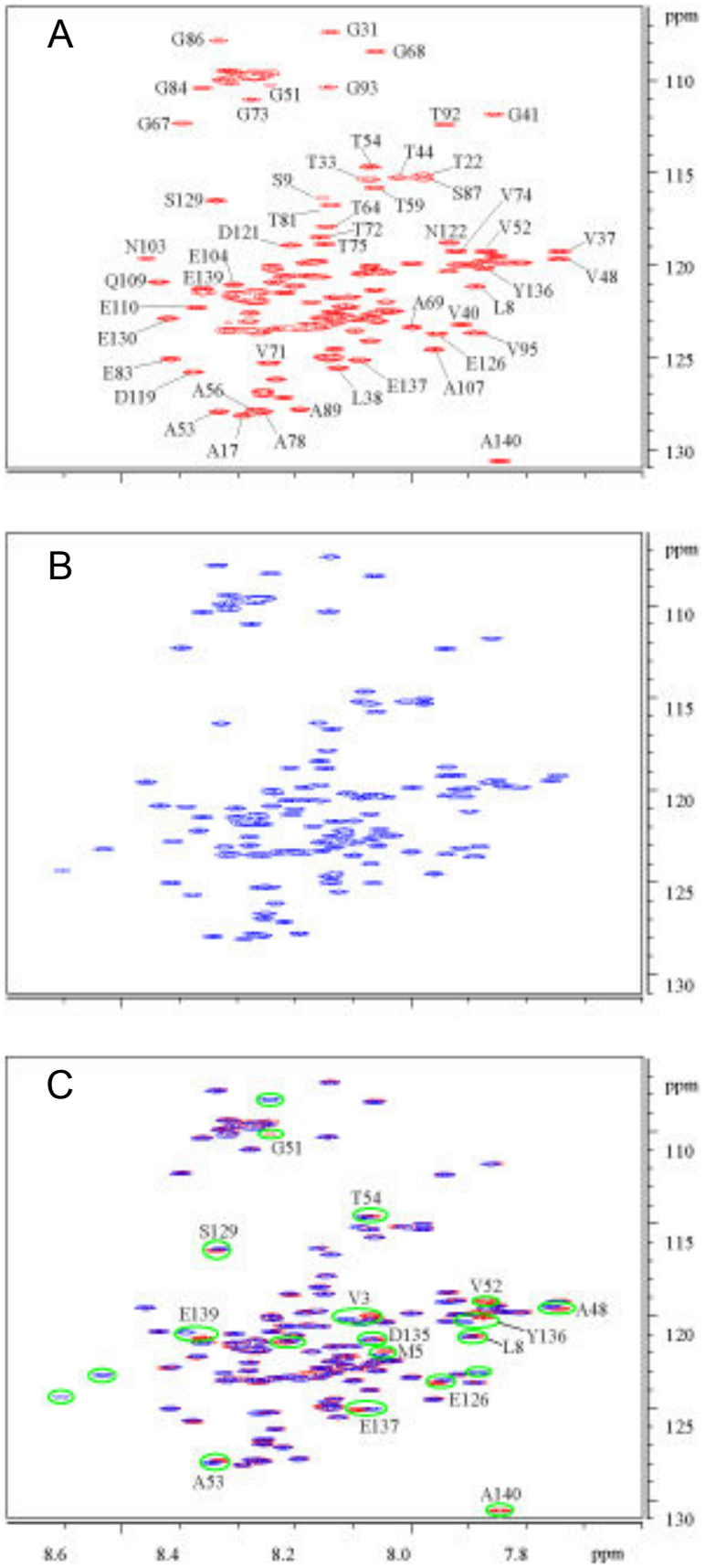

Figure 3.4.3: HSQC spectra of the monomeric protein (A), covalent dimer (B) and merged peaks (C). In green are highlighted the main differences in chemical shifts that involve C-terminal residues. Spectra acquisition was carried out by Dr. Marco Bisaglia of our lab.

3.4.2 NMR alpha-synuclein cysteine C-terminal dimer

The C-terminal Cys mutant of α-syn described in the previous sections, was used to evaluate the structural effects of the covalent constrain in C-term region posed by dimer formation. The interaction between the two molecule of the dimer were investigated by NMR. To this aim, C-term dimer was formed by mixing 80% (^{14}N)syn-Cys with 20% (^{15}N)syn-Cys. This ratio was chosen to maximize the probability to obtain a dimer formed by a molecule of ^{15}N isotope enriched α-syn and a ^{14}N molecule. With such sample intramolecular interaction can be effectively investigated by NMR. Figure 3.4.3 shows that the main chemical shifts modifications observed are related to residues in the C-terminal region. No relevant difference is observed between the spectrum of the "hetero" covalent dimers and that of the corresponding monomer.

3.4.3 Aggregation experiments

The aggregation kinetic experiments resulted to be poorly reproducible and this is likely due to a the large number of uncontrolled experiential variables. One of these, variables is the presence of α-syn fragments that are known to promote the aggregation of the whole protein. In this frame it is important to check and eventually improve, samples purity before starting a fibrillization kinetic study. Every protein batch used for aggregation incubation was loaded into a HPLC C4 column and chromatogram obtained analysed for the presence of unexpected peaks (see Chapter 3.1). In the case of α-syn most of the contaminants are fragments of the protein itself. As a procedure, a α-syn protein batch that resulted to be contaminated by fragments were further purified by preparative HPLC.

The competence to aggregate into amyloid fibrils is a property of every polypeptide chain, as reviewed by Dobson (1999). However, it is of particular interest the case of proteins involved in pathological events, such as β-amyloid (Joachim & Selkoe, 1989), Prion protein (Hope et al., 1986), tau (Bancher et al., 1987) and α-syn in neurodegenerative disease (Spillantini et al., 1997 and 1998). In particular, as single point mutations in the sequence of α-syn have been linked to the early onset Parkinson's disease (Polymeropoulos et al., 1997; Kruger et al., 1998; Zarranz et al., 2004), the role of such sequence differences in protein aggregation was investigated.

Several articles report important differences in the aggregation properties between early onset mutants of α-syn and wild-type protein. In particular, A53T and E46K mutants form fibrils faster than wild-type α-syn (Conway et al., 1998), A30P instead shows a slower kinetic of fibrils formation and accumulation of large amounts of oligomers (Conway et al.,

2000; Greenbaum et al., 2005). Since no progress has been made in the development of drugs capable to block α-syn fibrillogenesis or oligomerization, and since protein aggregation is not a fully understood phenomenon due to the difficulty in studying the intermediates of the process, every experiments that helps in the comprehension of this purported pathological process is welcome. In particular, I focused my attention on differences between wild-type α-syn and single point mutants, and on the possibility that some peptides by interacting with the part of the protein involved in protein self-interaction, may block the progression of amyloid fibril elongation.

There are several difficulties in the study of the process of fibrillogenesis, among which the precipitation of mature fibrils, as they are not soluble. This fact hampers the possibilities to study fibrils with methods used to investigate objects in solutions. Also oligomers are problematic to study because they generally represent a small fraction of the material in solution and likely they are a distribution of object of different dimensions. So, the unique parameter that can be quantify in a fibrillation kinetic is the loss of monomer in solution, that can be monitored by UV absorbance decrease. Another way to follow a kinetic of fibrillation is Thioflavin T (ThT) fluorescence. However, this is a method poorly reproducible and semiquantitative, and consequentially the kinetic data obtained are not always reproducible and therefore comparable.

Several research groups are trying to define the structure of mature fibrils, but those can not be studied with high resolution methods as NMR or X-ray crystallography due to huge dimension and the fibrillar structure. Hydrogen/Deuterium exchange, Fourier Transformed InfraRed spectroscopy, electron microscopy and atomic force microscopy are techniques currently used for the analysis of the structure of amyloid fibrils, but they can not solve 3D structure. The identification of the residues that govern the aggregation process is one of the main step for the comprehension of fibrillogenesis. These residues correspond to the region which drives protein-protein interaction, and its identification would allow to make several considerations on aggregation, the forces involved and the design of strategies to hamper the process. This could eventually lead to compound with a potential in slowing down the progression of the neurodegenerative disease.

Among the strategies proposed to block aggregation, one is based on peptides able to interact with aa engaged in fibril elongation, blocking the hydrogen bonding formation (Kapurniotu et al., 2002) or inserting flexibility and dynamic enhancements (Soto et al., 2000; El-Agnaf et al., 2004; Chalifour et al., 2003). The peptides described is these papers competes for amyloid formation binding region and inhibit fibril elongation or simply protein-protein

interaction. In particular, El-Agnaf and coworkes found that the region involved in α-syn self-interaction are residues 69-72 (El-Agnaf et al., 2004). A library of 7-residues peptide was created and screened. The library is composed of 7-amino acid peptides overlapped residues by residues which cover the whole α-syn sequence. Region comprising amino acid 68-72 resulted to able to interact the most with α-syn. The residues of this region are GAVVT; this motif was also found as aggregation leader also in other studies, among which Giasson et al. (2001). The authors used this peptide and some variants to see whether it was able to compete for α-syn fibril formation. The peptides used for aggregation kinetic modulation are flanked by arginine residues to improve solubility. They differ from each other of one residue by substitution or deletions, so ideally it is possible to unravel the features that are really involved in the interaction that lead to fibrillogenesis of α-syn, or possibly they cover the region implicated in protein-protein interaction. Their small molecular weight make them very dynamic. Maybe this one of the key reason for the hampering of protein aggregation in α-syn. If we consider protein-protein interaction as a rare event, the use of such peptides competes for the formation of NAC self-interaction, but the small dimension do not allow a stable interaction. Three among the peptides tested were found to decrease fibrils formation rate, a fourth one was instead an enhancer. Probably, the high hydrophobicity of the latter peptide overcome the factors that lead to inhibition of the fibril formation in the case of the other peptides.

To confirm published data and eventually extend the same approach to early onset pathological mutants, preliminary experiments were set with one of El-Agnaf's inhibitor peptides and the enhancer one. The peptides was produced by synthetic chemistry and purified (see Materials and Method section). The amino acid sequence of the peptide used is reported:

Name	Sequence	MW (Da)
ASI1	RGGAVVTGR-NH_2	871
ASI4	RGAVVGR-NH_2	713
NAC (α-syn 68-75)	GAVVTGVT	702

Then, aggregation kinetic was performed incubating 1.8 mg/ml α-syn in PBS in the presence or absence of five molar excess ASI1 or ASI4. The experiments was carried out at 37°C, under 150-200 rpm orbital shaking. Aliquots was taken at different times for analyses with ThT assay and Transmission Electron Microscopy (TEM) (Figure 3.4.4 and 3.4.5).

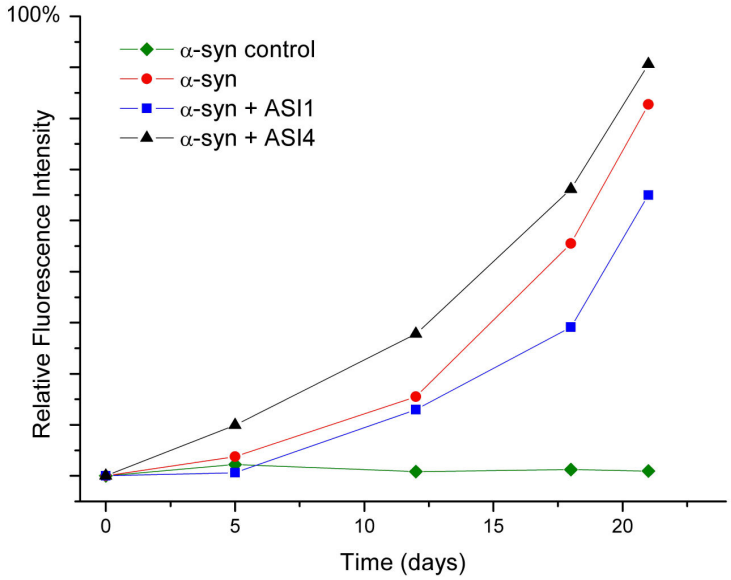

Figure 3.4.4: ThT fluorescence assay on aliquots taken from α-syn incubation in presence or absence of ASI1 or ASI4. Signals of α-syn wild type protein (circles), α-syn mixed with 5 molar excess ASI1 (squares), α-syn mixed with 5 molar excess ASI4 (triangles) and a control (wild type α-syn kept at 4°C) are shown. The green line is a negative control corresponding to α-syn kept at 4°C in absence of shaking.

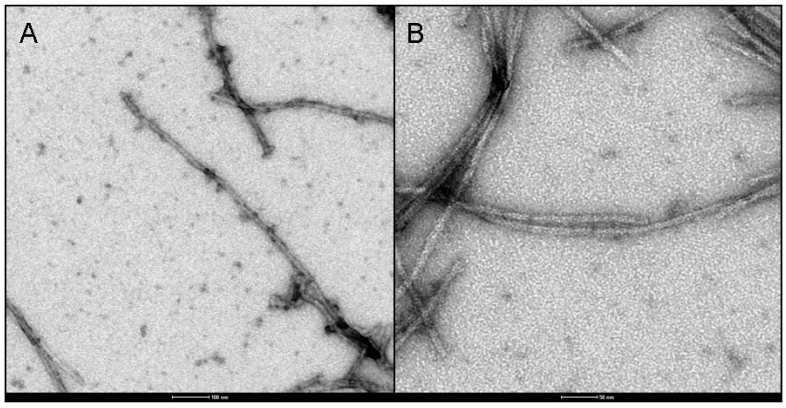

Figure 3.4.5: TEM images of 12 days incubation α-syn in presence of ASI1 (A) or 18 day incubation α-syn in presence of ASI4 (B). Fibrils have a diameter of about 16 nm for the sample with ASI1 and 12 nm for the sample with ASI4.

The kinetic was stopped before reaching a plateau, but some differences can be observed. However, because no statistic analysis can be done on these samples, the significance of the observed enhancement of fibrillation rate by ASI4 and inhibitor by ASI1 remain to be proved. TEM images on aliquots taken for ThT assay can be seen in Figure 3.4.5. Figure 3.4.4 and 3.4.5 indicate the presence of amyloid fibrils even in the sample containing inhibitor peptide ASI1.

To study the formation of oligomers, a new kinetic was prepared. α-Syn was incubated 1.8 mg/ml in PBS, at 37°C with 300 rpm shaking, in the presence or in the absence of five molar excess ASI1 or ASI4. The kinetic was monitored by gel filtration (GF) chromatography, to observe the formation of oligomers and isolate them. Every day an aliquot was taken and loaded into FPLC connected Superdex 200 HR chromatographic column pre-equilibrated with PBS. As it can be seen in Figure 3.4.6, a decrease in the area of the peak corresponding to α-syn monomer was observed, but no formation of oligomeric species at the expected earlier eluting time (Figure 3.4.6D), and no differences was observed between the evolution of GF chromatograms in the presence or in the absence of ASI1 or ASI4. The HPLC analysis of each peak of the monomer eluted from gel filtration chromatography reveals no strong interaction between α-syn and inhibitors peptide, as it was not present in the HPLC chromatogram the peak corresponding to peptide (Figure 3.4.7).

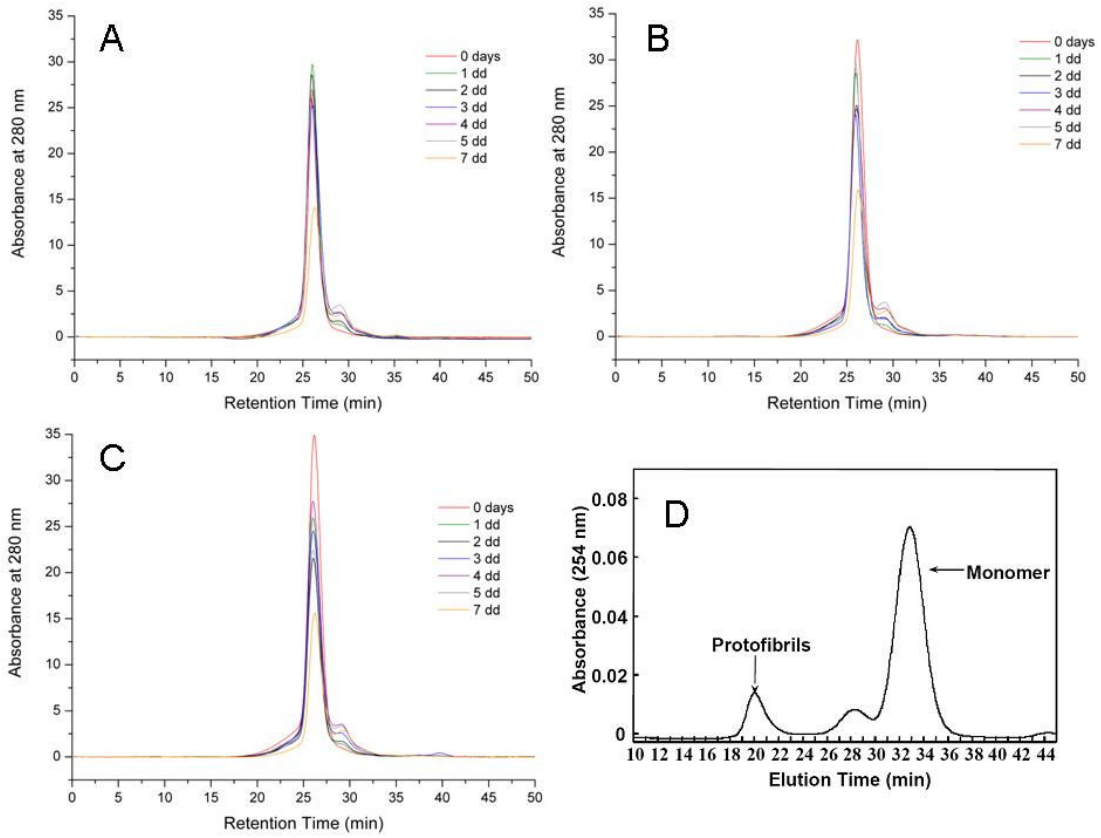

Figure 3.4.6: Gel filtration chromatography on 1mg/m α-syn samples incubated at 37°C, under 300 rpm shaking, in PBS (A), in presence of 5 molar excess of ASI1 (B) or ASI4 (C). Reference chromatogram adapted from Lashuel et al. (2002) showing chromatographic profile of α-syn solution containing protofibrillar forms at RT 20 min; dimer elute at 28 min while monomer at 33 min. Experimental conditions of GF analysis are reported in § 2.4.1.

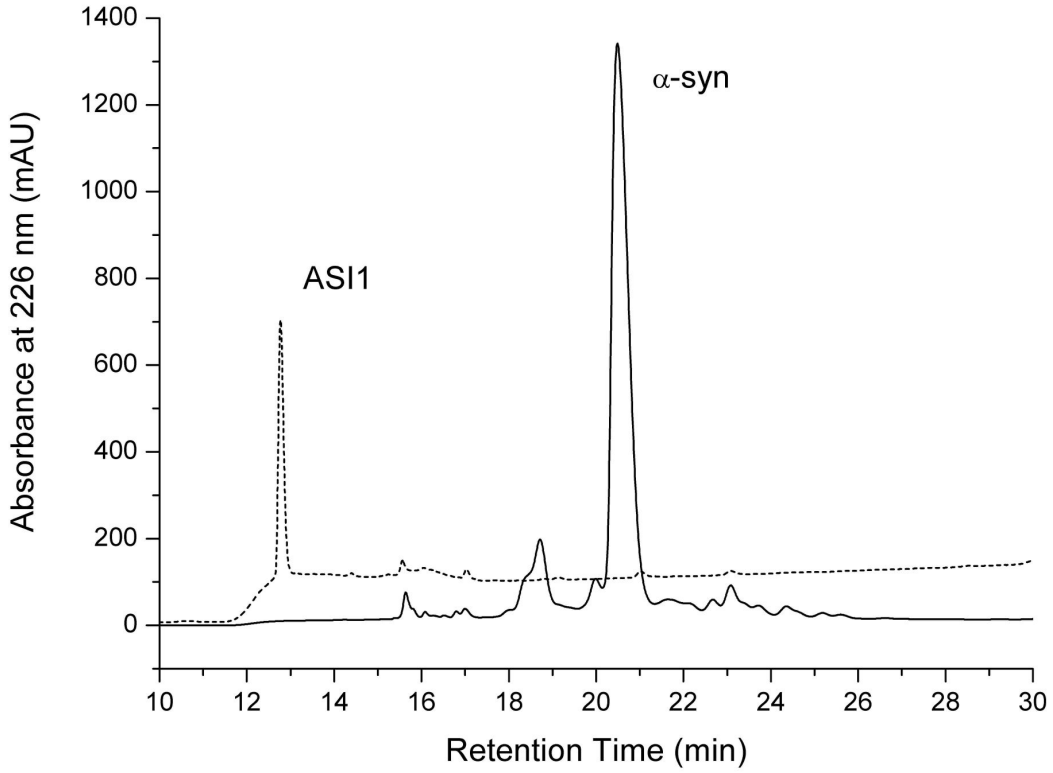

Figure 3.4.7: HPLC analysis of peak eluted from gel filtration chromatography (continuous line) and simple peptide solution injection (dashed line). α-Syn elutes at 20.5 min, while ASI1 and ASI4 peptides elute at 13 min. The analysis was performed on C4 analytical column (see Materials and Methods section).

The sample corresponding to each peak eluted from gel filtration column was analysed by HPLC using a C4 column, but no trace of peptide ASI1 or ASI4 was observed, implying no stable interaction between α-syn and peptides. Moreover, no shift in retention times in of the peak in the gel filtration chromatographic profile was recorded. These results allow to exclude the possibility of oligomers formation and of degradation. Furthermore, the consistency of the elution profile in the C4 column allow to exclude the possibility of chemical modification like oxidation for the protein.

ThT assay was performed, as shown in Figure 3.4.8. As observed in the previous kinetic, also in this experiment ASI1 did not hamper the formation of amyloid fibrils. TEM images of aliquots taken from incubated samples show the presence of fibrils (Figure 3.4.9).

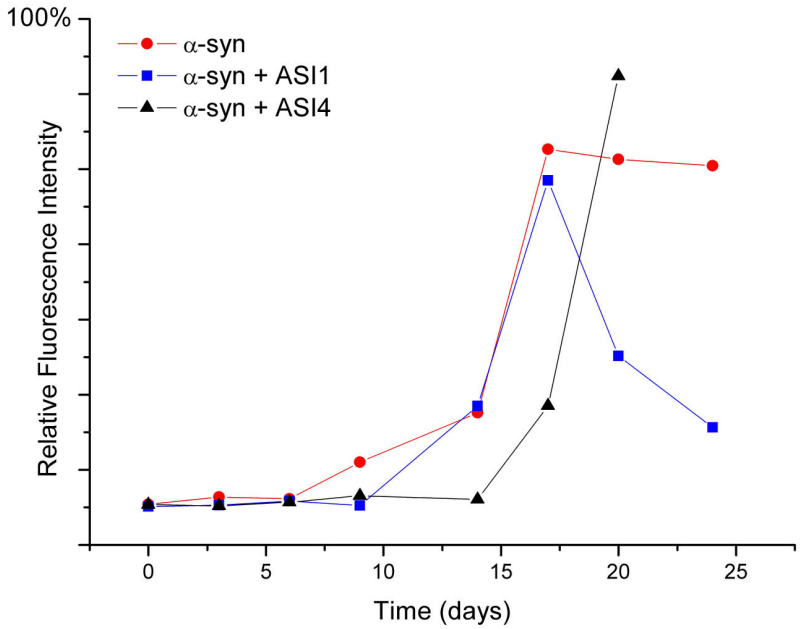

Figure 3.4.8: ThT fluorescence assay of α-syn incubated in the presence or in the absence of 5 molar excess ASI peptides.

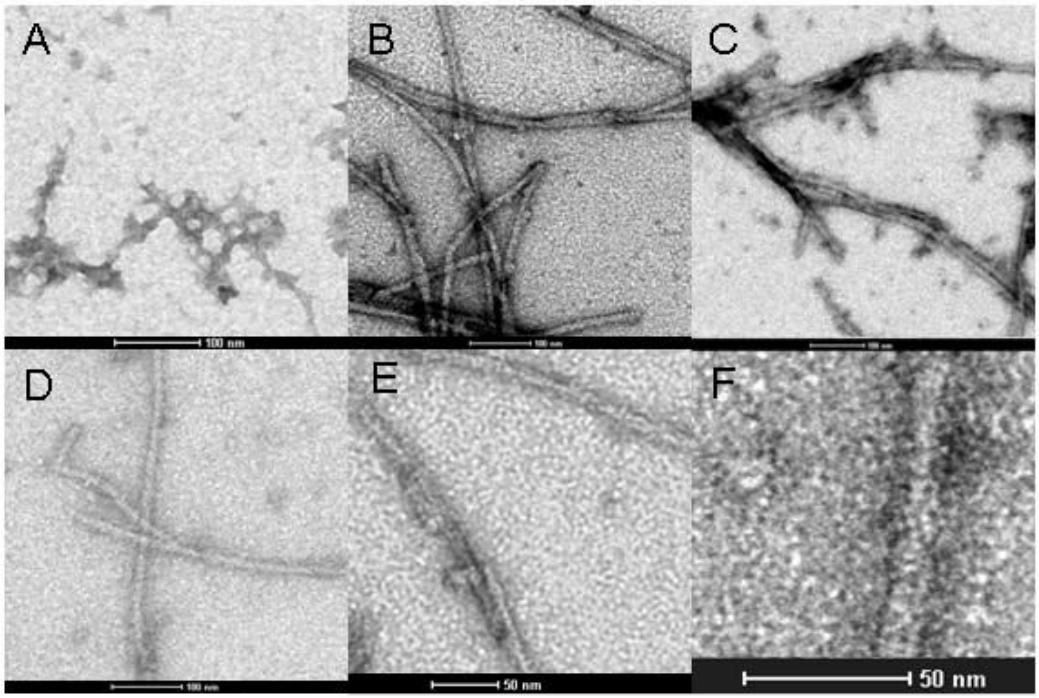

Figure 3.4.9: TEM images of aliquots taken during α-syn incubating in absence or presence of ASI1 or ASI4 peptides. (A) 9 days incubated α-syn; (B) 14 days incubation α-syn; (C) 17 days incubation α-syn; (D) 14 days incubation α-syn in presence of five molar excess ASI1; (E) 14 days incubation α-syn in presence of five molar excess ASI4; (F) zoom on a fibril obtained in 14 days incubation α-syn in presence of five molar excess ASI1, the diameter measured is about 15 nm.

To further elucidate the mechanisms of fibril formation and search for differences in the aggregation properties among pathological mutants, an aggregation kinetic was curried out to compare α-syn wild type protein and the mutants A30P, A53T and E46K. In the same experiment, the fibrillation behaviour of Cys C-term dimer (CtD) was also monitored. The proteins were incubated in PBS, at 37°C, under 500 rpm shaking. Aliquots was taken at different times and ThT assay and CD measurements performed. ThT fluorescence assay results are shown in Figure 3.4.10.

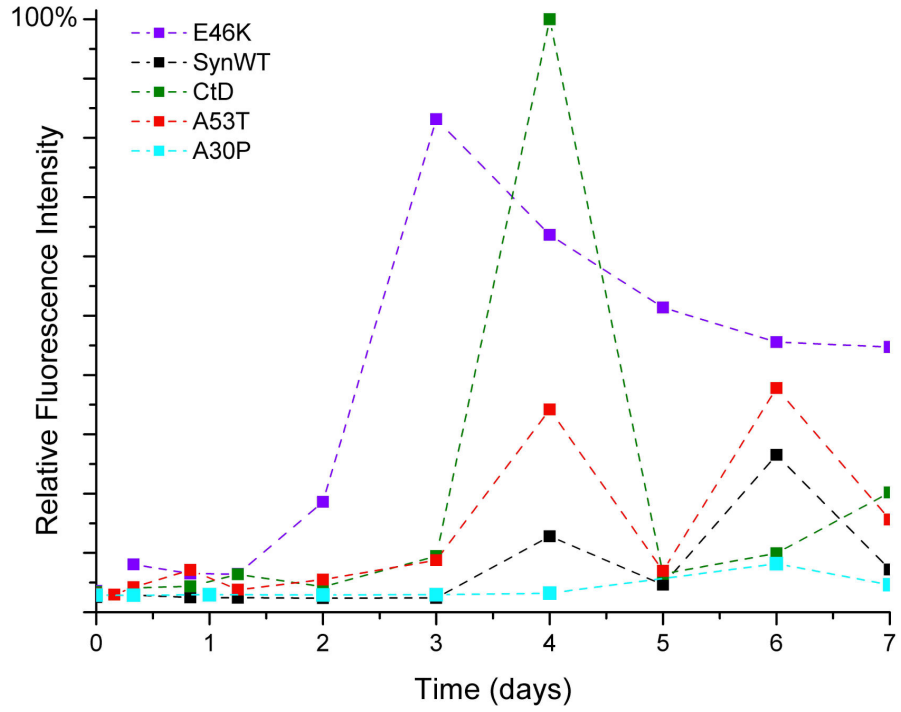

Figure 3.4.10: Fibrillation rate of α-syn, pathological mutants and CtD shown with ThT assay.

Looking at Figure 3.4.10, some considerations are due:

- pathological mutant E46K and A53T fibrillate faster than α-syn wild type protein. A30P have a slower fibrillation rate. These data are confirmed by literature (Conway et al., 1998; Greenbaum et al., 2005))

- the C-terminal dimer of α-syn forms fibrils faster than α-syn.

CD spectra of the proteins after 2 (Figure 3.4.11) and after 7 (Figure 3.4.12) days of incubation were measured. Signals obtained in Figure 3.4.11A are typical of random polypeptide chains. Some difference can be detected for E46K mutant, that present also a higher baseline in UV spectra (Figure 3.4.11B), probably due to light scattering in the sample.

Of note, E46K mutant shows an increase in ThT fluorescence after 2 days of incubation, compared to the other mutants and wild type protein.

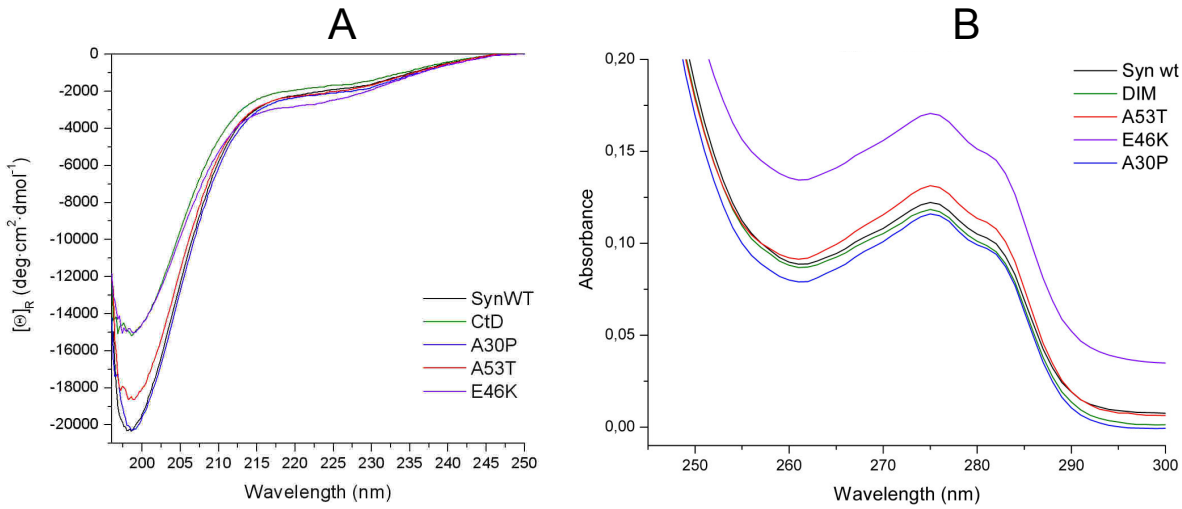

Figure 3.4.11: CD spectra (A) and UV absorbance (B) of 2 days incubation aggregation kinetic of α-syn, CtD and pathological mutants.

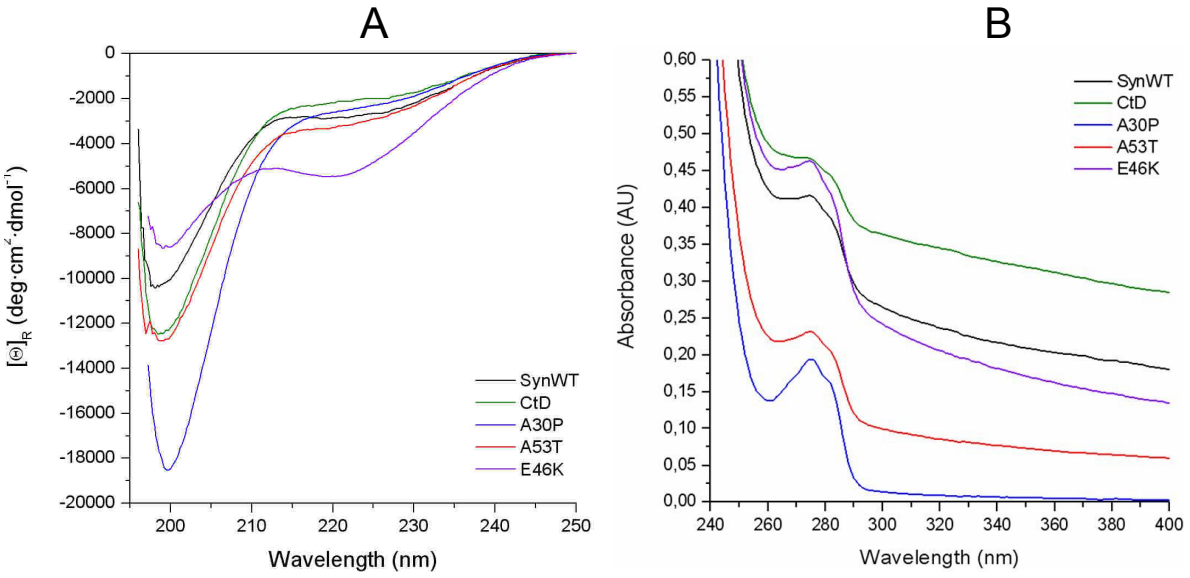

Figure 3.4.12: CD spectra (A) and UV absorbance (B) of 7 days incubation aggregation kinetic of α-syn, CtD and pathological mutants.

CD signals obtained after 7 days of incubation shows marked differences between samples (Figure 3.4.12A). However, scattered UV spectra was recorded. Light scattering contribution was subtracted from spectra considering absorbance signal as the sum of three component:

$$A = A_{baseline} + A_{lightscattering} + A_{sample}$$

where $A_{baseline}$ corresponds to the baseline signal of recorded spectrum due to instrumental factors and it is a constant value at all wavelength; A_{sample} is the absorbance of protein chromophores; $A_{lightscattering}$ is the contribution of large particles. This last contribution cn be evaluated using the relationship below:

$$A_{lightscattering} = \left(\frac{400}{\lambda}\right)^{n} \cdot \left(A_{400} - A_{baseline}\right)$$

where λ is the wavelength independent variable; A_{400} is absorbance value at 400 nm; $A_{baseline}$ is the constant contribution of baseline; n is an value that depend on the molecular dimensions and features of the object in solution. The scatterin g curve is fitted to overlap the experimental curve in a region of the spectrum where proteins chromophores do not contribute to absorption (see Figure 3.4.13). When the fitting parameters are indentified, scattering contribution is subtracted to experimental signal and the protein concentration is calculated from this processed signal.

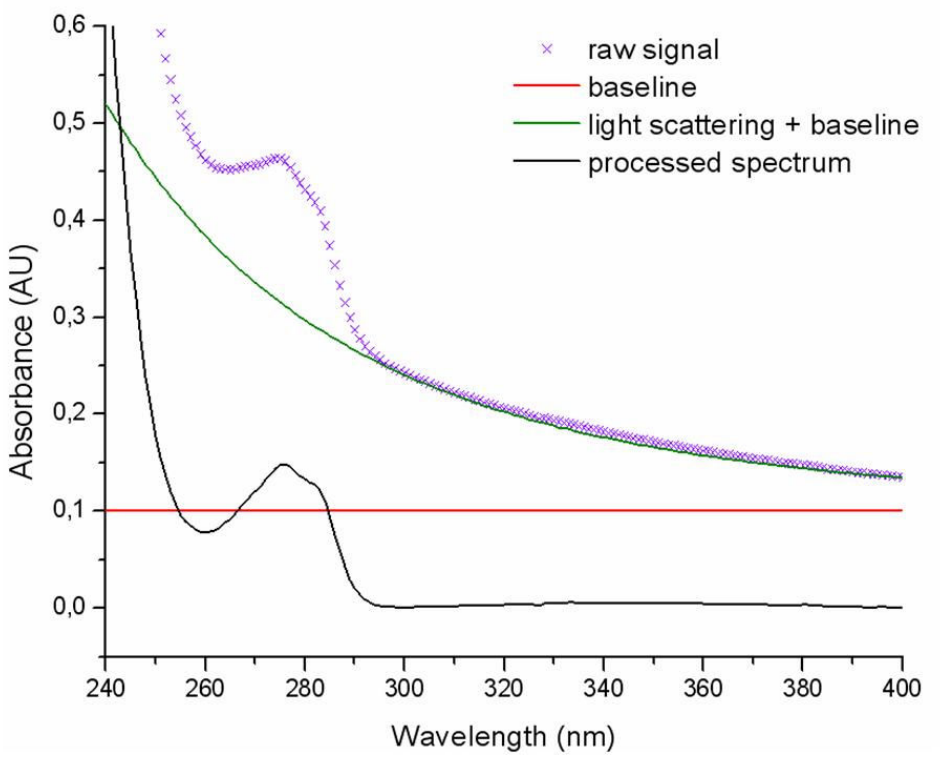

Figure 3.4.13: Example of signal processing to subtract light scattering contribution and estimate protein absorbance at 280 nm.

Protein concentration deduced according to the procedure described above is used to a more precise normalization of dichroic signals. Looking at Figure 3.4.12A, only E46K mutant

seems to present some β-sheet structure content, while signals obtained from the other samples appears only as loss of random polypeptide chain contribution. Figure 3.4.10 reveals that after 7 days of incubation all the samples should be amyloid fibrils. So, the CD spectra shown in Figure 3.4.12A must belongs to soluble α-syn in the sample, and data reveal that the majority of polypeptide chain remains random even after the trigger of fibril elongation. E46K mutant has a faster conformational transition to β-sheet structure as regards wild type α-syn, and this finding is in agreement with previous observations by Greenbaum and coworkers (2005).

Of note, as Glu is an amino acid that hosts the formation of β-sheet structure, E46K mutation was supposed to fibrillate faster than wild type protein and A53T mutant. Greenbaum et al. (2005) reported a faster conversion into β-sheet containing structure for E46K as regards to wild type α-syn, but in this paper authors reported that A53T is the mutation with the higher rate of fibrillogenesis; Choi et al. (2004) instead, reported an analogous increase of ThT fluorescence for A53T and E46K. Our findings seem to agree with the observation that E46K should increase fibril formation rates.

Interesting observation came from conformational distribution analysis performed with SMFM (§ 3.3.1). Data reported by Brucale et al. (2009) reveal that A30P and A53T has the highest propensity for the formation of β-sheet like structures in solution compared to wild type α-syn. E46K mutant presents intermediate characteristics, in contrast with the faster fibril formation rate reported in Figure 3.4.10. However, it should be underlined that single tendency for β-sheet structure acquisition could not be parallel to a high propensity in fibril elongation. Also, oligomers and aggregates formation propensity has to be distinguished from fibril elongation tendency, as it is not clear yet whether structures and self-interaction involved in one case or in the other are the same, or whether they are the same for wild type α-syn and PD linked mutants. In other terms, equilibria that regulate the passage from one species to another can be different for different syn proteins.

A satisfactory and reproducible ThT sigmoidal fibrillation curves was never obtained. ThT assay, especially on the case of α-syn, never retained the higher fluorescence value reached as fibrillation progresses, that is, it never maintained the plateau value expected for a sigmoid curve which describe the kinetic of fibrils formation. Maybe this fact was due to fibrils precipitation and disruption or to light scattering. So, ThT assay is not really suitable for the study of α-syn aggregation.

Luk et coworkers developed a protocol to monitor α-syn aggregation based on fluorescence polarization (Luk et al., 2007, see Materials and Methods section).

α-Syn samples were incubated 1 mg/ml in PBS, at 37°C, in a 96 wells plate, under 1000 rpm shaking. This method allows the comparison of different samples and conditions, and it avoid the problems due to aliquot sampling. Kinetics was performed in triplicate, and the plate was directly introduced in a plate reader. The instrument was equipped with filters and polarisers for the detection of fluorescence emission of fluorescein and analogues like Oregon Green 488. C-term Cys OG labeled α-syn is mixed in a fixed ratio (1:100) with wild type α-syn, mutants and dimers.

Results from the first kinetic performed are shown in Figure 3.4.14. In this experiment, OG labeled and unlabeled α-syn were incubated at different molar ratios. This experimental design allow to explore the correlation between the size of the oligomers and the intensity of the FP signal. Higher synOG/α-syn ratio, will result in a higher probability to include a labelled molecule in the growing oligomer. However, it is no clear what is the size of the oligomer that start to give a FP signal. A furthere consideration that should be made regard the OG molar extinction coefficient, that is 81000 $M^{-1}cm^{-1}$, in our solution conditions, posing the risk, when the fraction of labelled α-syn molecules is too high of a inner filter effect.

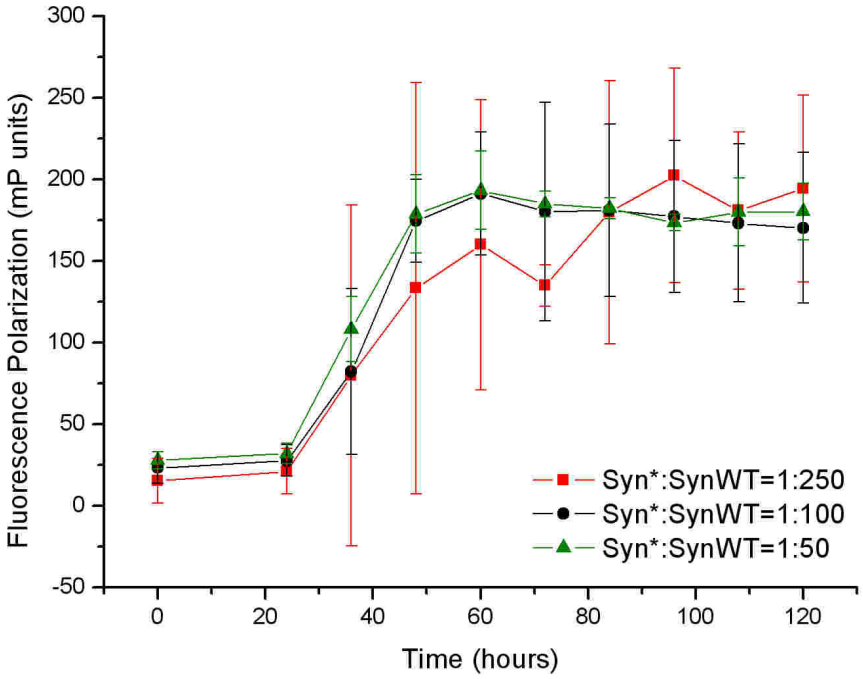

Figure 3.4.14: FP kinetic of 1 mg/ml α-syn incubated with different ratios of syn-OG. SynOG is incubated with α-syn in different ratios (1:50, 1:100, 1:250).

However, Figure 3.4.14 shows only little differences between different samples, and high errors bars do not allow to speculate on the observed differences.

The same experiment was also performed to compare α-syn with early onset PD mutants, to overcome problems found in ThT fluorescence assay. The experimental conditions are different from those used in the fibrillation kinetic monitored with ThT (Figure 3.4.10), however, it should be mentioned that FP method detects aggregates while ThT binds to mature fibrils. FP data obtained in this experiment show a faster aggregates formation by α-syn wild type protein, although E46K reaches higher values of FP, indicating the presence of larger aggregates. A30P have a longer lag phase and still do not reach a plateau even after 200 hours of incubation, and the data on the A53T mutant can not be fitted with a simple sigmoidal trend.

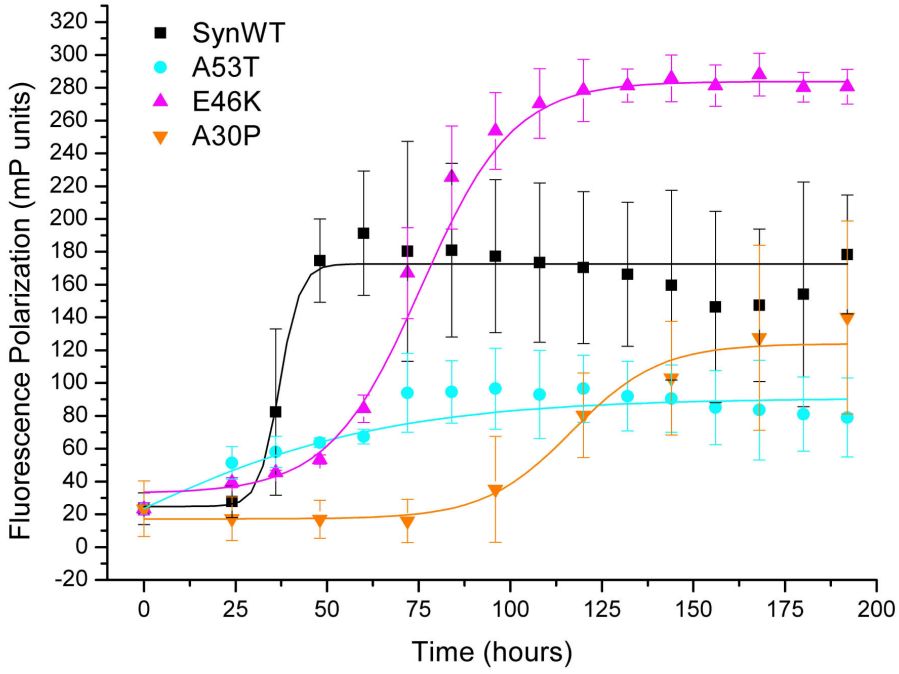

Figure 3.4.15: FP kinetic of 1 mg/ml α-syn or early onset pathological mutant of PD. SynOG/unlabelledSyn ratios (1:100).

Interesting results came from the comparison between α-syn, CtD and NtD. Figure 3.4.16 presents the aggregation kinetic of the three molecules mixed 100:1 with synOG. Data indicate that CtD has a faster aggregation rate than α-syn and also aggregates formed are larger, while NtD variant has a four fold increased lag phase.

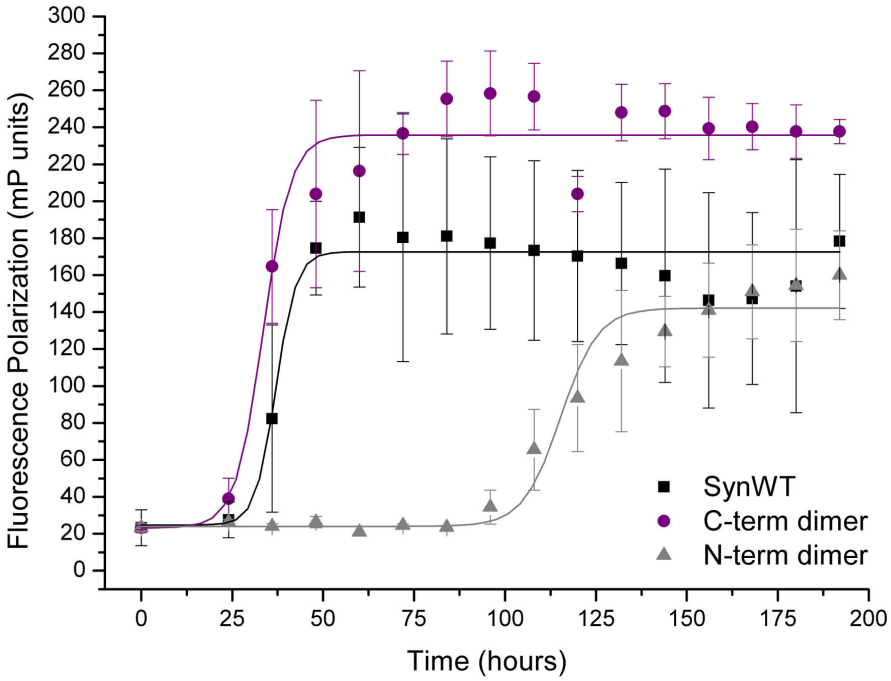

Figure 3.4.16: FP kinetic of 1 mg/ml α-syn or N-term and C-term dimers. SynOG/unlabelledSyn ratios (1:100).

Moreover, the incubation of the mixture of 1:1 α-syn with 14-3-3η shows that the chaperone is able to slow down α-syn aggregation (Figure 3.4.17). 14-3-3η increases lag phase and decrease the slope of FP increase, indicating an inhibitor effect of this protein.

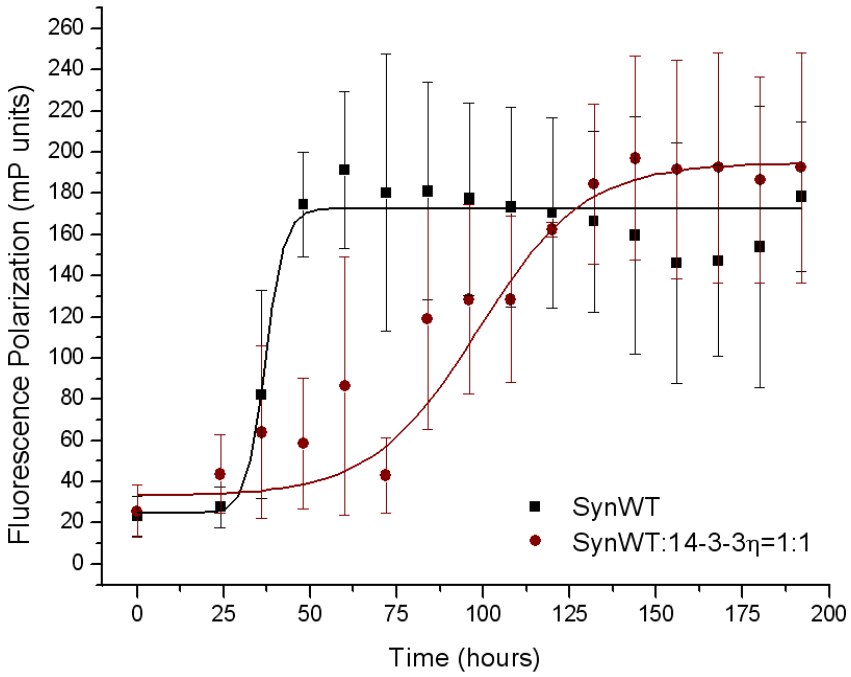

Figure 3.4.17: FP kinetic of 1 mg/ml α-syn incubated with 1:1 14-3-3η. SynOG/unlabelledSyn ratios (1:100).

As results presented in Chapter 3.3 do not evidence a direct interaction between α-syn and 14-3-3η, it can be supposed that the chaperone is able to interact with some conformations of α-syn, maybe those implied in oligomerization, or directly with α-syn growing oligomers.

It can be noted that error bars in FP experiments presented are large and can compromise the possibility to make conclusive considerations on the kinetic parameters obtained, specially for the first part of the sigmoidal curve. Experiments was performed again and FP increase was analyzed well by well. The use of glass beads spring of the phenomenological observation that the latter are very effective in decreasing the variability among the replication of the individual aggregation experiments (Giuseppe Legname personal communication). α-Syn was put 1 mg/ml in PBS, pH 7.4, 0.05% sodium azide to prevent microbial degradation, at 37°C at 1000 rpm shaking. SynOG was added 1:100 in every sample. To reduce variability due to sampling, a single mix solution of α-syn and synOG was prepared and then divided among the different wells of the plates. Different α-syn:14-3-3η ratios was tested, to investigate the possibility of a dose effect on aggregation. Also, a 14-3-3η mutant (kindly provided by Dr. Francesca Munari of our research group) unable to dimerize was tested, to investigate whether a different effect can derive from the use of 14-3-3η in monomeric or dimeric form. The mixture with other two proteins was tested. The first one is chimeric construct 3T (§ 3.3.1), which was used as negative control for unspecific molecular crowding effects. The second one is DJ1, a redox sensitive protein whose biological role is still poorly defined, but associated to genetics forms of PD (Bonifati et al., 2003). Recently, it has been proposed that DJ-1 acts as redox-dependent chaperone that inhibits protein aggregation in vitro, and intracytoplasmic inclusions (including those of α-syn) in vivo. (Shendelman et al., 2004). In this work authors propose that the presence of native DJ-1 inhibited the fibrillation of α-syn at 37 °C, based on Congo red binding, and decreased the formation of larger material (attributed to protofibrils) on incubation at 55 °C, based on SDS gels. Thus, these two proteins were mixed together with α-syn, to test their effect on aggregates formation rate of α-syn.

Each sample condition the kinetic of aggregation was replicated in four wells. No increase of synOG FP values was observed in controls done for all the samples tested, when synOG was incubated alone or in the presence of putative interacting proteins but no unlabelled α-syn. The approach for FP kinetic analysis was different in this case, and the aggregation kinetics in each well was analyzed separately. The reason for this approach was

the observation that high error bars were due to the fact that FP values started to increase in each well at different times, id est, lag phase of aggregation curves were different even if samples were the very same same simple put in distinct wells. Figure 3.4.18 shows an example of the data analyzed plotting mean values of FP measurements recorded for two plates incubated in parallel:

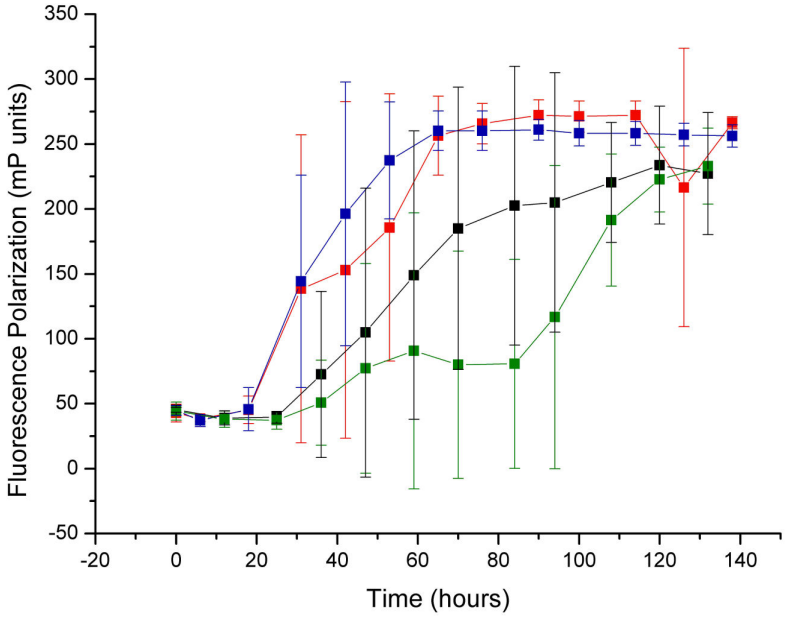

Figure 3.4.19: α-syn incubated in the presence (green and blue lines) or in the absence (red and black lines) of 5 mM DTT. Each line corresponds to mean FP values calculated from 4 samples measurements in 2 distinct and plates.

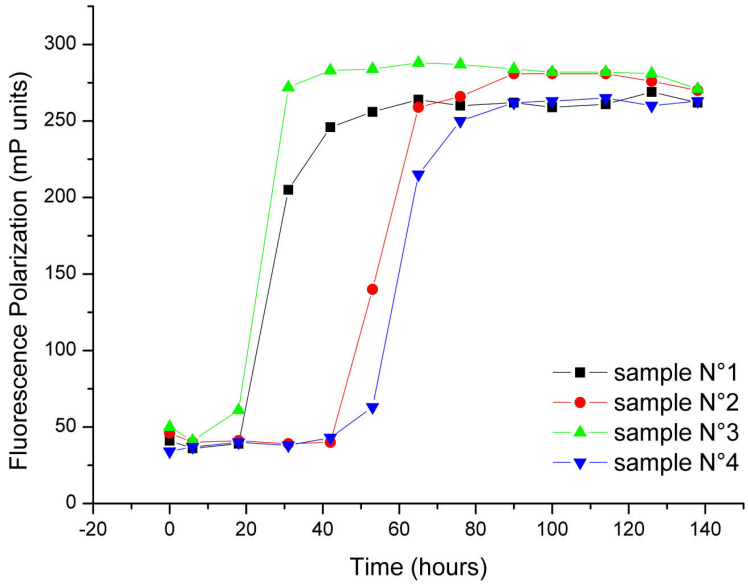

Figure 3.4.20: FP increase of 1 mg/ml α-syn incubated in four distinct wells in the same plate.

Figure 3.4.20 is the representation of single kinetic behaviour of distinct samples. Of note, lag phase of different samples are different, while sigmoid slope is the same for all the samples.

As samples increase of FP can be fitted with a sigmoid, the curve can be described with parameters as asymptotes, time at which the signal has reaches the half of the highest FP value (t50) and curve slope at t50 (Figure 3.4.21).

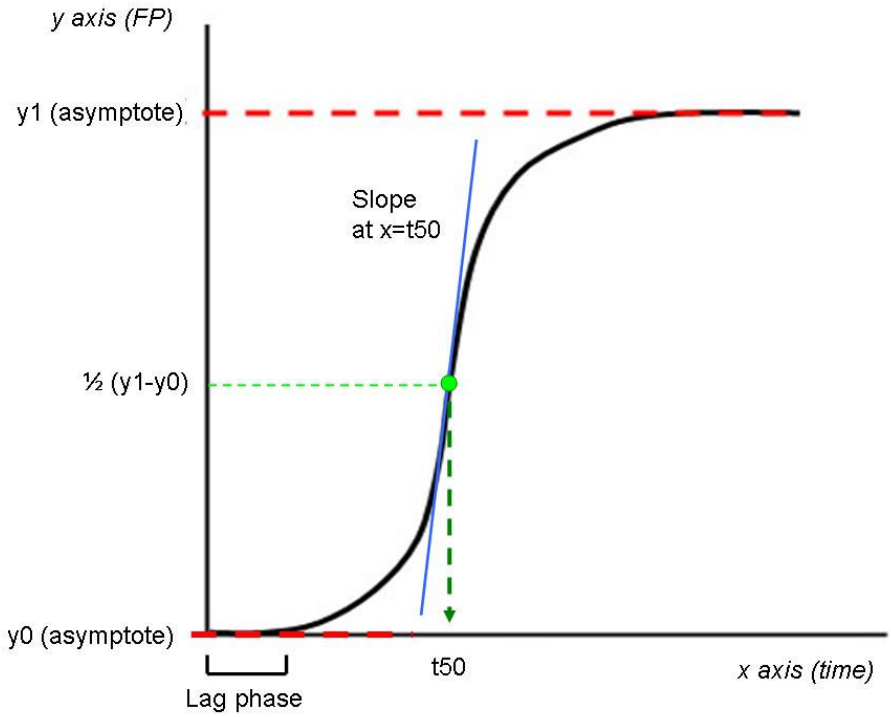

Figure 3.4.21. Parameters that define a sigmoidal lineshape. Asymptotes are reported with dashed red lines, while blue line indicate the linear fit of thetime point in the t50 region (green spot and green arrows) whose slope is indicative of oligomers enlargement rate.

Curve slope is linked to the growing rate of aggregates. The lag phase is defined instead as the initial period of time during which it can not be observed FP increase, probably associated to the early aggregation events that generates oligomeric form that do not lead to a variation of the FP properties. As the curves obtained do not allow to define a precise lag phase, t50 has been chosen to be the parameter that partially indicate relative times at which aggregation formation is triggered to compare different samples. t50 values reports on both lag phase and slope of the rising part of the curve. Thus, in the following kinetic experiments we chose to increase the number of time point in the expected lag phase period, to better

describe this parameter and correlate different curves in a straight forward way. Moreover, as these data are very recent, an electron microscopy characterization of oligomers obtained become necessary. SynOG is 1/100 of α-syn molecules, so in very broad statistical terms then oligomers should be detectable after they reach a size that correspond to the incorporation of several α-syn molecules. Hence, as the aim of this experiment is the detection of early events in α-syn aggregation process, it is not yet possible to establish whether the lag phase in FP curves is indicative of lag phase in oligomer formation or result from a slow equilibrium between monomeric forms of which only few can aggregate. Consequentially, a an interpretation of the lag pahse has to await for the definition of a stringent correlation between FP values and oligomers dimensions .

Every sample was then analyzed in terms of t50 and slope; asymptotes resulted equal for all the curves, with minor differences (Figure 3.4.22). This may signify that objects has the same mobility in solution at the end of aggregation experiment.

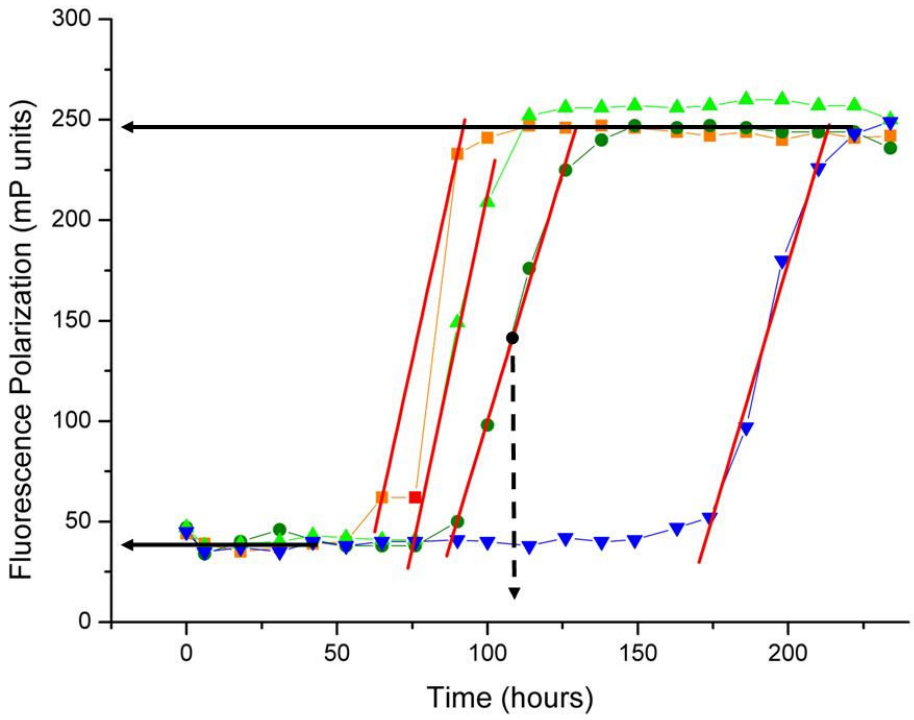

Figure 3.4.22: Example of curve parameter extrapolation. Black arrows indicate asymptotes, then the black spot is positioned on t50 point from which is extrapolated the correspondent value on x axis (dashed black arrow) and calculated slope (red lines fitting the curves).

Sample tested and results obtained are listed in table 3.3. Samples in italics contain 5 mM DTT.

Table 3.3: Slope and t50 values deduced with sigmoid parameter analysis on curve obtained in FP experiments. 14-3-3η monomer and dimer are indicated respectively as (m) or (d).

Sample	Slope (ΔmP units/hours)	t50 (hours)
α-syn	8.2±1.3	53±26
α-syn 5 mM DTT	*7.5±0.9*	*60±35*
α-syn + beads	7.9±1.0	29±4
α-syn + beads	*5.3±2.2*	*38±9*
α-syn:3T=1:1	4.7±0.8	63±35
α-syn:3T=1:1	*2.7±0.4*	*68±9*
α-syn:14-3-3η(m)=1:8	*6.3±1.1*	*110±30*
α-syn:14-3-3η(m)=1:4	*5.5±0.9*	*95±48*
α-syn:14-3-3η(m)=1:1	*5.1±0.9*	*165±52*
α-syn:14-3-3η(d)=1:8	*5.4±1.0*	*104±31*
α-syn:14-3-3η(d)=1:4	*5.8±0.5*	*115±30*
α-syn:14-3-3η(d)=1:1	*4.7±0.9*	*136±45*
α-syn:DJ1=1:1.5	8.0±3.3	74±32
α-syn:DJ1=1:1.5	*6.8±4.2*	*127±52*
A30P	1.6±0.6	105±15
A53T	3.0±2.1	55±10
E46K	2.9±1.2	93±18
CtD	10.0±3.5	33±3
NtD	2.4±0.9	123±11

Better comparison can be done in histogram plots that are reported below. Slope can be referred as variation of FP units in function of time (hours).

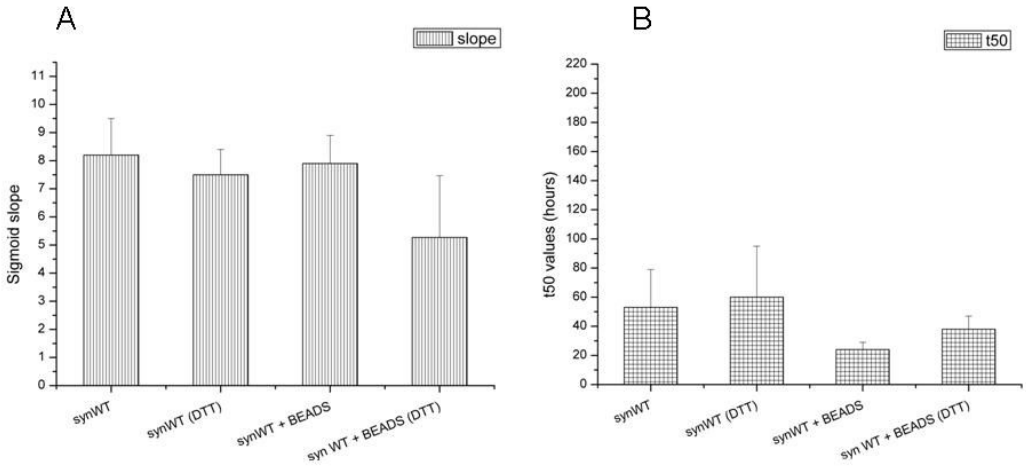

Figure 3.4.23: Slope (A) and t50 (B) comparison between sample of 1 mg/ml α-syn incubated in the presence or in the absence of 5 mM DTT, with or without glass beads.

The comparison between samples shows again that α-syn has the higher aggregation propensity as regards the other proteins tested. In particular, the introduction of a glass bead into the well during the incubation was found to reduce errors in t50 values for all the sample tested (see Table 3.3), being equal values of slopes, the increase of t50 can assigned to a variation in the value of the lag phase. The presence of DTT in the incubation buffer was found to have no effect on aggregation properties of α-syn.

Looking at Figure 3.4.24, data obtained in Figure 3.4.15 was confirmed. Mutants have a slower aggregation rate compared to α-syn; in addition, t50 is shifted for A30P and E46K mutants, even if no lag phase analysis can be reported. Of note, for A30P and A53T mutants, asymptote of final FP value reached is significantly different compared to all the other samples tested: 141±48 for A30P, 138±48 for A53T and 197±16 for E46K, while α-syn reached a final FP value of 244±24.

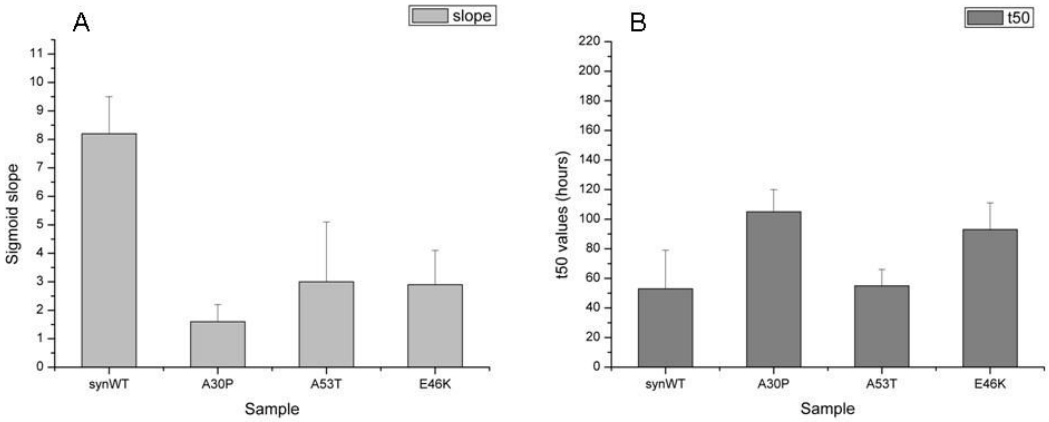

Figure 3.4.24: Slope (A) and t50 (B) comparison between sample of 1 mg/ml α-syn compared to early onset PD mutants.

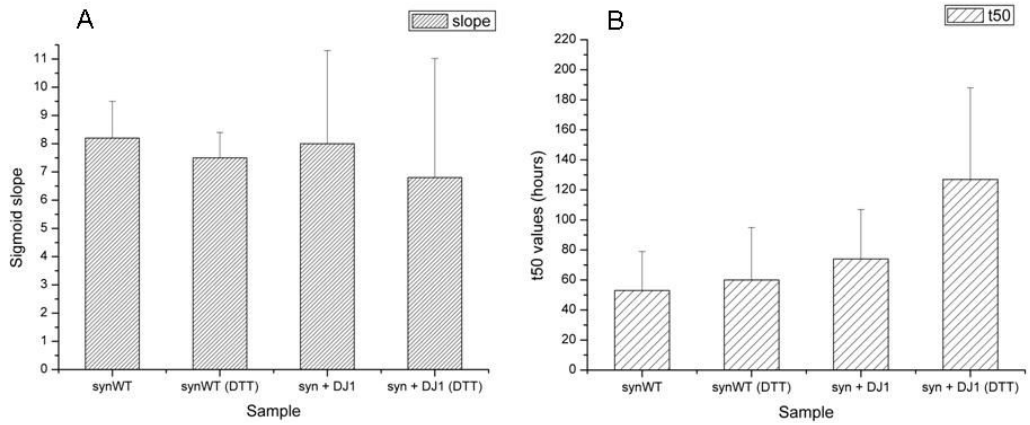

Figure 3.4.25: Slope (A) and t50 (B) comparison between sample of 1 mg/ml α-syn incubated in the presence or in the absence of 2 mg/ml DJ1, in the presence or in the absence of 5 mM DTT.

Figure 3.4.25 reports sigmoid parameter of aggregation kinetic curves achieved from α-syn:DJ1 mixture 1:1.5. No significant differences can be observed for the sigmoid slopes of samples incubated in the presence or in the absence of DJ1, in oxidizing or reducing solution. The great variability of t50 values does not allow the evaluation of a delay in α-syn aggregation due to DJ1 in solution.

On the other hand, 14-3-3η protein is able to decrease oligomer enlargement rate (Figure 3.4.26A) and to extend t50 values (Figure 3.4.26B). Some degree of dose dependence can be observed, as the higher 14-3-3η:α-syn ratio has the heaviest effect, in the case of both monomers and dimers. However, a large errors suggest further experiments to demonstrate the proposed interaction.

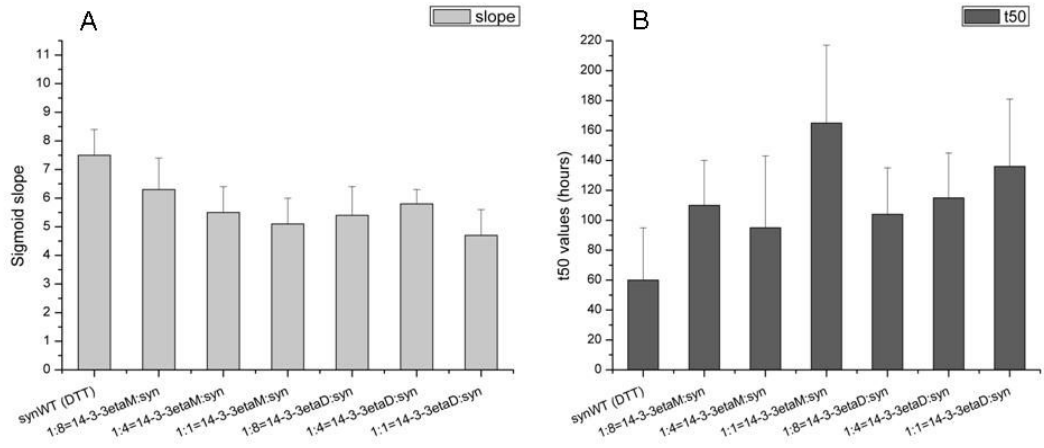

Figure 3.4.26: Slope (A) and t50 (B) comparison between sample of 1 mg/ml α-syn incubated in the presence or in the absence of increasing amounts of 14-3-3η monomer (14-3-3etaM) or dimer (14-3-3etaD). Molar ratios are indicated in tick labels. For 14-3-3η dimer, the molar ratio is expressed in terms of quantity of monomer, thus the concentration expressed in terms of mg/ml is the same.

The incubation with 3T protein influenced sigmoid slopes (Figure 3.4.27), with no effect on t50 instead. Such effect was not expected, as 3T protein was not expected to interact with α-syn (§ 3.3). Maybe, non specific electrostatic interaction occurs between negative charged surface of 3T protein and N-terminal part of α-syn, which is included in aggregation formation. Thus, it seems that 3T protein does not have an influence on the probability to start oligomerization, as t50 are similar, but the influence on aggregation rate is proved by the decrease of sigmoid slopes of α-syn FP units in the presence of 1:1 3T protein.

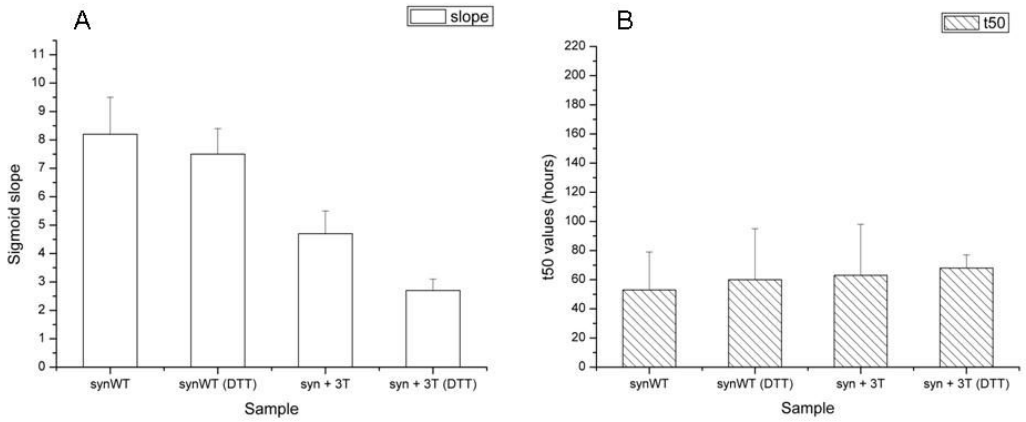

Figure 3.4.27: Slope (A) and t50 (B) comparison between sample of 1 mg/ml α-syn incubated in the presence or in the absence of 1:1 molar ratio 3T chimera protein, and in the presence or absence of 5 mM DTT.

Results for the aggregation kinetics of the CtD and NtD are reported in Figure 3.4.28. It is clear that structural constrain in NtD protein inhibits aggregation formation and enlargement.

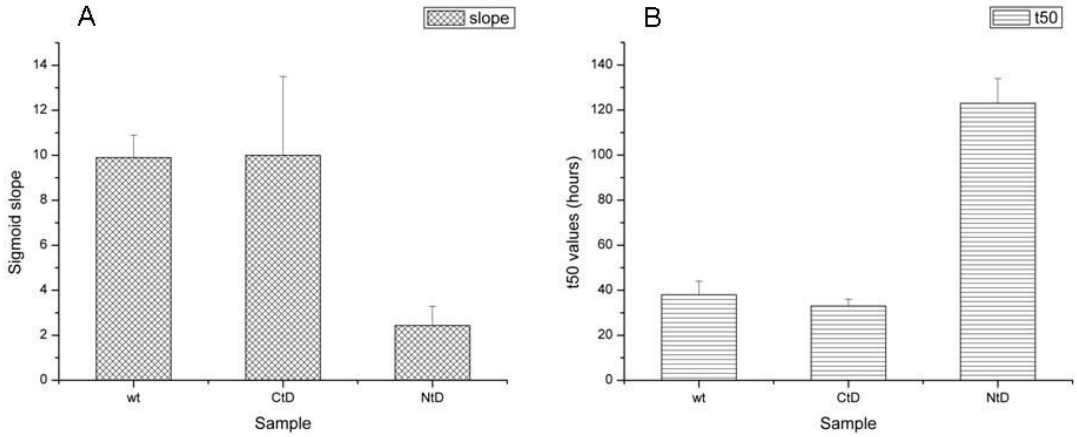

Figure 3.4.28: Slope (A) and t50 (B) comparison between sample of 1 mg/ml α-syn compared to 1 mg/ml CtD or NtD.

Finally, TEM imaging was performed on α-syn samples taken at 25 h and 31 h of incubation (Figure 3.4.29) from two distinct wells. This two samples were chosen for microscopic analysis as they presented different values of FP: 42 mP units for sample taken at 25 h of incubation, and 205 mP units for the sample of 31 h of incubation. Of note, mature fibrils were not detected in different fields of the first sample (25 h, Figure 3.4.29A); only the presence of oligomers was documented. On the contrary, the second sample (Figure 3.4.29B, C and D) showed first evidences of small fibrils, in rare field in the same specimen, in addition to the analogous presence of oligomers detected for 25 h incubation α-syn sample.

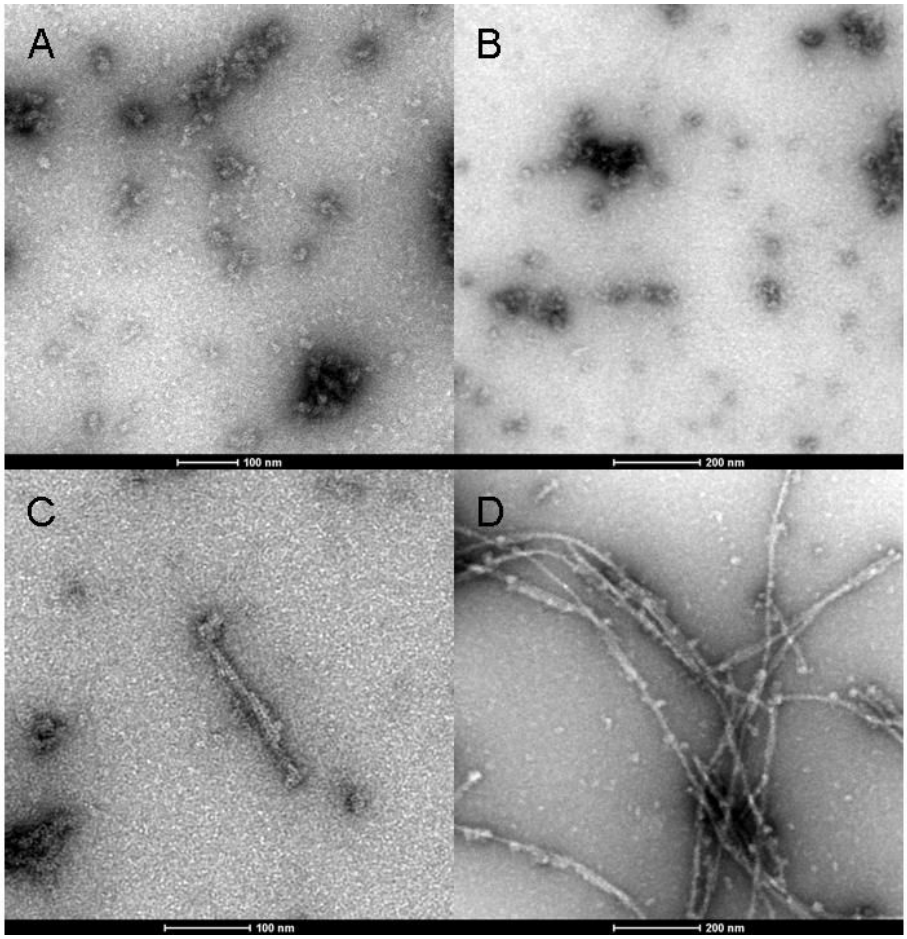

Figure 3.4.29: TEM images of 1 mg/ml α-syn incubated in PBS, at 37°C, 1000 rpm shaking, taken at 25 h (A) and 31 h (B, C and D) of incubation. B, C and D are different view of the same preparation.

In conclusion, FP method seems to be a good technique for α-syn aggregation kinetic study. Further investigations are needed to improve the capacity of the technique to detect early oligomers formation and sigmoidal curves suitable for conclusive analysis. Moreover, the introduction of glass beads into the wells can help to reduce errors bars, levelling t50 values within experimental replica. A correlation between oligomer dimensions and FP values is required. However, this technique seems to be promising for the screening of compounds able to inhibit protein aggregation, and for the identification of proteins able to enhance or inhibit α-syn fibril formation.

Discussion

α-Syn plays an evident role in the ethiopathogenesis of PD since two proofs link it to PD: LB composed mainly of α-syn are the hallmark of PD in brains of patients and misfolding and aggregation properties α-syn are implied in LB formation. The second evidence is that three single point mutations in α-syn aa sequence have been linked to early onset PD. These mutants present some structural differences in comparison to wild type protein and certified enhanced aggregation proprieties (§ 1.3.4).

In this PhD thesis, a grat relevance was given to the investigation of the interaction network of α-syn. In fact, unravelling the molecular partners and equilibria that sequester α-syn from cytosol is important for the comprehension of the causes that lead to protein fibrillogenesis. At the same time, the analysis of the first steps of α-syn aggregation is relevant to unravel the molecular mechanism of the elusive aggregation process. Both lines of research can provide insights useful for the design of new therapeutic strategies based on the prevention, or eventually reversion, of molecular causes of that lead to neuronal loss.

A large part of the work presented in this thesis consisted in the preparation of materials. Proteins were cloned, expressed and purified, and the purity certified. Molecular mass was checked by MS, to detect the presence of oxidized, modified or heterogeneous samples. Then α-syn interaction with membranes was tested. In particular, the behaviour of α-syn dimers formed by disulfide bond between Cys at the C-terminal (CtD) or at the N-terminal (NtD) part of the molecule was analyzed by CD.

α-Syn cys monomers and dimers showed signals proper to random coil polypeptide chains in sodium phosphate buffer, at pH 7.4 (Figure 3.2.2). CD spectra of the same sample documented the transition of the protein to α-helical structure in the presence of SDS micelles (Figure 3.2.3). Interesting differences to CtD signal can be observed in the presence of

50:50=PG:PC SUVs (Figure 3.2.4). In this case CtD α-helical spectra does not overlap with the signals obtained in the case of monomers or NtD. It is probable that the covalent constrain that links the C-terminal end of α-syn is responsible for an α-helix distortion, that it is not present in the case of NtD. Also, liposome dimension, ore more likely the curvature of the vescicle surface, is likely to be implied in such a result as SDS micelles do not produce such structural modification.

Referring to Figure 1.2.7 that replicates a cartoon proposed by Jao et al. (2008), it is possible that NtD dimer forms a continuous α-helix that fits on liposome surface. In the case of CtD the acidic part of the molecule forms a 80 residues break between the amphipathic helix formed by N-terminus of α-syn. This region does never acquire any kind of structure, as it contains several prolines and it is rich in acidic residues. Moreover, electrostatic repulsion can occur between this part of the molecule and negative charged phospholipid headgroups. Structural details remain to be investigated, nevertheless, this preliminary results encourage to go on with the study of α-syn dimers binding to membranes.

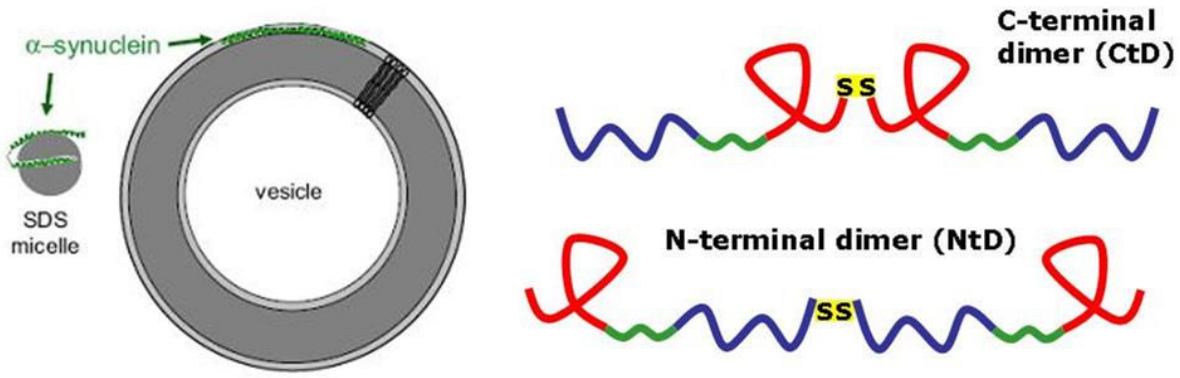

Figure 4.1: Dimers structure and relationship with SDS micelles and SUV dimension (adapted from Jao et al., 2008).

The attention was also focused on protein-protein interaction. α-Syn was reported to interact with a lot of proteins in literature by evidences of co-immunopreciptation or affinity column, but in most of the cases results were not confirmed and measured by high "resolutive" methods like NMR or SPR. As previous experiments from our laboratory led to the observation of an interaction between α-syn and I27 modules in the chimeric protein 3S3 (§ 3.3.1), we investigated the interaction of the separate proteins in solution. However, CD and fluorescence spectra do not provide evidences of any kind for contacts between α-syn and 3T protein (Figures 3.3.4 and 3.3.5), suggesting that interaction observed in 3S3 is aspecific and mainly due to the covalent bond that link the two proteins.

A more interesting investigation, due to the biological relevance of the two "subjects", was made on the interaction between 14-3-3η and α-syn. The binding of these two proteins was tested by SPR and dissociation constant measured (1.1 μM) (Sato et al., 2006). In the attempt to reproduce this experimental data, no evidences of an interaction between the two proteins observed by SPR in our experimental set up (Figure 3.3.7). It is true that conditions applied in the two experiments were different, mainly for the conjugation method applied. However, in the paper published by Sato et al. (2006), α-syn was randomly conjugated to a CM5 carboxymethyldextran matrix of a chip by covalent coupling of amino groups. Since α-syn contains 11 lysine residues in addition to the amino terminus, and since it has a random coil conformation which potentially can expose all Lys residues in the same extent, the approach used from Sato & coworkers produces a randomly functionalized sensor chip, in other words, α-syn bound to CM5 chip exposes different parts of the molecule, in relationship with relative reactivity of the individual lysines. In the method used in the experiments described in this thesis, α-syn was bound to the chip by the His-tag positioned at the N-terminus of the protein. Hence, every α-syn conjugated to Ni^{2+}-NTA Sensor Chip has the same orientation, id est, the C-terminus is exposed and floating in the analysis cell while the N-terminal part is employed in the binding to the chip. This implies a consideration: whether the interaction between the two proteins would involve the N-terminal part of α-syn, it can not be detected by this method because it could be hindered.

To define the molecular features that govern the interaction between α-syn and 14-3-3η HSQC NMR spectra were recorded on a sample of ^{15}N labelled α-syn in a 2 fold molar excess of 14-3-3η. No modification of the values chemical shifts of the α-syn residues was detected (Figure 3.3.6), excluding the possibility of a stable interaction between the two proteins. Nor interaction was detected between α-syn and ASI1 peptide (Figure 3.3.8) proved by HSQC spectra of 15N α-syn recorded in the presence of 2 fold molar excess of ASI1.

Finally, self-interaction of α-syn was analysed. First of all, interesting results came from SPR analysis of NAC binding to NTA Sensor Chip, which was able to capture α-syn injected into analysis cell (Figure 3.4.1). Although SPR is a sensible and precise method the quantification of the interaction was not possible due to low solubility of NAC, that do not allow to obtain a good dose-response calibration, and to the shapes of SPR signals, that do not fit with 1:1 Langmuir binding model.

Searching for strategy that could prevent α-syn aggregation and/or fibrillogenesis, α-syn fibril formation was performed in the presence or in the absence of two peptides. ASI 1

was proposed to inhibit fibril formation while ASI 4 was suggested to act as an enhancer (El-Agnaf et al., 2004). ThT kinetic was performed on α-syn incubated at 37°C in the presence or in the absence of five molar excess ASI1, but no significant differences were observed between the samples. In particular, the presence of fibrils in TEM images of α-syn mixture with ASI 1 peptide was documented (Figures 3.4.5 and 3.4.9), in contrast with El-Agnaf and coworkers findings.

The comparison between fibrillogenesis rate of α-syn and early onset PD mutant was done. ThT kinetic was first performed (Figure 3.4.10), and this experiment evidences that E46K mutant and CtD dimer have a faster fibril formation rate compared to wild-type α-syn. A30P mutant shows instead a slower fibril formation rate, in agreement with literature (Conway et al., 2000).

To to improve the quality of the aggregation kinetic data a new methodology was applied. This technique was set up by Lük and coworkers (2007) and is based on fluorescence polarization. The incorporation of a fluorescent labelled molecule of α-syn into a growing oligomer is detected by the increase of FP signal (§ 2.1.1). As this technique is able to detect aggregates and not mature fibrils, it can monitor early step of aggregation process, that are the least characterized in literature, in contrast with ThT fluorescence assay that detect prevalently mature fibrils.

Results obtained show a disagreement with ThT curves, as FP experiments report α-syn as the fastest species (Figure 3.4.15 and 3.4.24). Of note, experimental conditions were different, as protein concentration was 1.5 mg/ml for ThT fluorescence assay, with 500 rpm shaking, while for FP measurements protein concentration was 1 mg/ml with 1000 rpm shaking. However, the behaviour of the protein and of all its variants can be compared within the same experimental procedure. Thus, since the two methods are different and detect different species, it can be supposed that wt α-syn has a lower propensity for the formation of mature fibrils in comparison with the pathological mutants while it can form oligomeric species very rapidly.

However, as FP experiments were all performed in the same conditions, data can be compared and some considerations can be done:

- PD associated mutants have a slower rate of aggregates formation in comparison to the wt protein (Figure 3.4.15 and 3.4.24). As synOG is 1/100 of total α-syn present in solution, it is possible that α-syn can form large aggregates very easily in solution. PD α-syn mutants show a different oligomerization kinetic for two possible reasons. The first is that the binding of the monomers to the growing oligomers may be less

efficient as a consequence of the mutation. The second implies a distribution of the monomers among conformers that may or may not be competent to bind to the growing oligomers resulting in a apparently reduce active concentration of aggregating monomer. The second argument has a strong support in the different distribution in conformers population observed in a recent AFM study by Brucale et al. (2009) in collaboration with our group. Of course the possibility remains that both effect act concomitantly on the aggregation process.

- Although 3T interaction with α-syn was tested and produced no evidence of a distinct and stable binding between the two proteins, 1:1=3T:α-syn mixture in solution shows a slower rate of aggregates enlargements, as sigmoid slope is significantly smaller than FP data of α-syn incubated alone (Figure 3.4.27). It is possible that some electrostatic interactions may occur between 3T protein and α-syn oligomers. The nature of this interaction should be aspecific and occur between negatively charged surface of 3T and α-syn lysines of its first 100 residues.
- Zhu et al. (2006) reported an inhibition of α-syn fibril formation in the case of α-syn and oxidized DJ1 mixed together. Although there is no statistic relevance, FP kinetics seem to accomplish to opposite hypothesis: oxidized DJ1 does not influence α-syn aggregation, while the reduced form is able to slow down oligomer formation rate (Figure 3.4.25). As Zhu and coworkers monitored protein aggregation with ThT fluorescence assay, the same considerations mentioned above for early onset PD mutants of α-syn can be reported here. A comparison will be done once parallel ThT and FP assays will be performed.
- The effect of 14-3-3η protein in fibril formation rate is evident (Figure 3.4.26). 14-3-3η is able to affect both slope and t50 of FP sigmoid. However, no differences between 14-3-3η monomer or dimer can be observed. It is interesting to correlate HSQC and SPR data that did not reveal detectable interaction between α-syn and 14-3-3η. Since 14-3-3η is a chaperone, it is tempting to suggest that the interaction between the two proteins occurs only when some α-syn conformers expose hydrophobic NAC, which are relatively rare in solution (§ 1.2.3). Otherwise, 14-3-3η can bind selectively to α-syn oligomers inhibiting formation and enlargement of aggregates.
- NtD has lower aggregation tendency in comparison to α-syn and CtD. The increase in FP is slowed down and t50 is delayed. It is interesting to observe that while the covalent attachment of C-terminal tail modifies α-syn membrane binding proprieties,

the N-terminal constriction influences self-assembly. This finding can be important for the comprehension of molecule topology required for oligomer formation.

Thus looking at interaction network proposed in Figure 4.2, results obtained in this PhD thesis can be reported. In particular, 14-3-3η is able to inhibit aggregation formation, and also structural imposition due to disulfide bond in NtD. CtD seems to have aggregation properties analogous to those of α-syn, while it shows a faster amyloid fibril formation rate (Figure 3.4.10). Consideration for what concerns early onset pathological mutants require further investigations on oligomers dimension of different sample.

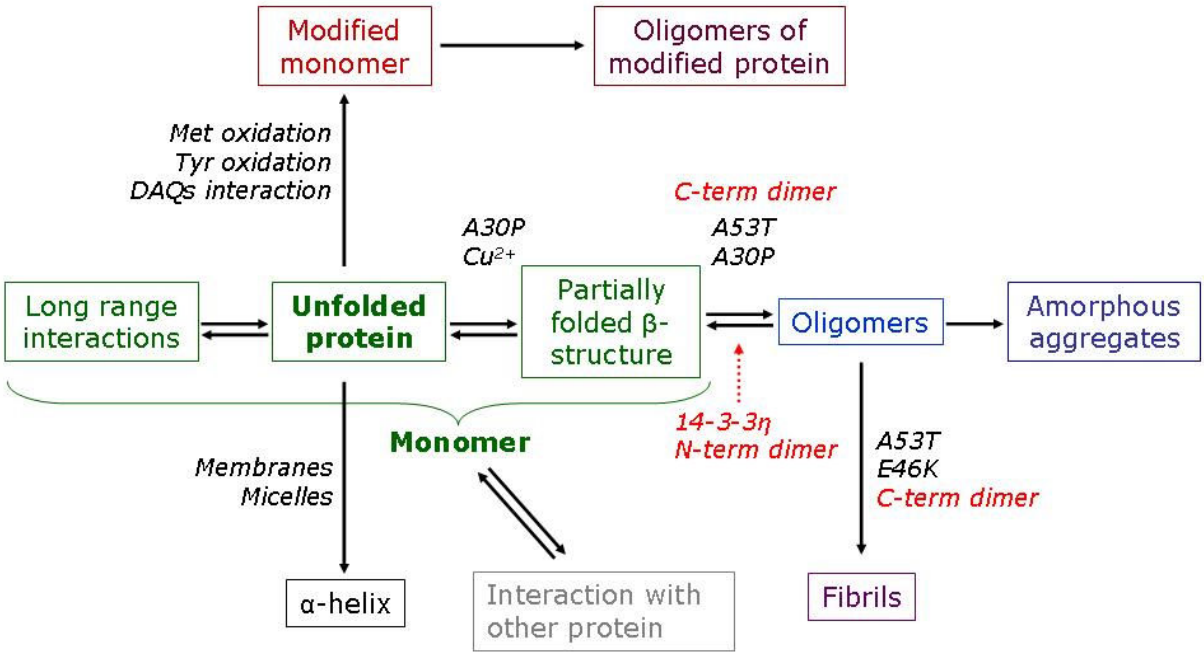

Figure 4.2: Findings (red labels) reported in this PhD thesis on α-syn interaction network.

Finally, FP based aggregation assay appears to be a good method for the analysis of α-syn aggregation kinetic. TEM images show the presence of oligomers in solution (Figure 3.4.29), and a more detailed correlation between FP values and aggregates dimensions is required. Also, glass beads were found to decrease variability in t50 values of proteins incubated, while they have no effects on sigmoid slope. Whether the t50 advance will be common for all the sample tested, glass beads will be systematically used in all FP kinetics experiments. Moreover, as this method allows the use of 96 well plates, sample replication can be done providing statistical significance to these studies, and a plethora of different conditions and proteins can be tested. The aim in future project will be the identification of lead compounds that can block α-syn aggregation.

Bibliography

Abeliovich A., Schmitz Y., Fariñas I., Choi-Lundberg D., Ho W. H., Castillo P. E., Shinsky N., Verdugo J. M., Armanini M., Ryan A., Hynes M., Phillips H., Sulzer D. & Rosenthal A. (2000) Mice lacking alpha-synuclein display functional deficits in the nigrostriatal dopamine system. *Neuron* 25, 239–252.

Aitken A. (2006) 14-3-3 protein: a historic overview. *Semin Cancer Biol* 16, 162–172.

Alim M. A., Hossain M. S., Arima K., Takeda K., Izumiyama Y., Nakamura M., Kaji H., Shinoda T., Hisanaga S. & Ueda K. (2002) Tubulin seeds alpha-synuclein fibril formation. *J Biol Chem* 277, 2112–2117.

Anfinsen C. B. (1973) Principles that govern the folding of protein chains. *Science* 181, 223–230.

Bancher C., Lassmann H., Budka H., Grundke-Iqbal I., Iqbal K., Wiche G., Seitelberger F. & Wisniewski H. M. (1987) Neurofibrillary tangles in Alzheimer's disease and progressive supranuclear palsy: antigenic similarities and differences. Microtubule-associated protein tau antigenicity is prominent in all types of tangles. *Acta Neuropathol* 74, 39–46.

Bandopadhyay R., Kingsbury A. E., Cookson M. R., Reid A. R., Evans I. M., Hope A. D., Pittman A. M., Lashley T., Canet-Aviles R., Miller D. W., McLendon C., Strand C., Leonard A. J., Abou-Sleiman P. M., Healy D. G., Ariga H., Wood N. W., de Silva R., Revesz T., Hardy J. A. & Lees A. J. (2004) The expression of DJ-1 (PARK7) in normal human CNS and idiopathic Parkinson's disease. *Brain* 127, 420–430.

Berg D., Holzmann C. & Riess O. (2003) 14-3-3 proteins in the nervous system. *Nat Rev Neurosci* 4, 752–762.

Bernheimer H., Birkmayer W., Hornykiewicz O., Jellinger K. & Seitelberger F. (1973) Brain dopamine and the syndromes of Parkinson and Huntington. Clinical, morphological and neurochemical correlations. *J Neurol Sci* 20, 415–455.

Bertini I., Gupta Y. K., Luchinat C., Parigi G., Peana M., Sgheri L. & Yuan J. (2007) Paramagnetism-based NMR restraints provide maximum allowed probabilities for the different conformations of partially independent protein domains. *J Am Chem Soc* 129, 12786–12794.

Bertoncini C. W., Jung Y. S., Fernandez C. O., Hoyer W., Griesinger C., Jovin T. M. & Zweckstetter M. (2005) Release of long-range tertiary interactions potentiates aggregation of natively unstructured alpha-synuclein. *Proc Nat Acad Sci USA* 102, 1430–1435.

Bertoncini C. W., Fernandez C. O., Griesinger C., Jovin T. M. & and Zweckstetter M. (2005b) Familial mutants of alpha-synuclein with increased neurotoxicity have a destabilized conformation. *J Biol Chem* 280, 30649–30652.

Binolfi A., Rasia R. M., Bertoncini C. W., Ceolin M., Zweckstetter M., Griesinger C., Jovin T. M. & Fernández C. O. (2006) Interaction of alpha-synuclein with divalent metal ions reveals key differences: a link between structure, binding specificity and fibrillation enhancement. *J Am Chem Soc* 128, 9893–9901.

Bisaglia M., Tessari I., Pinato L., Bellanda M., Giraudo S., Fasano M., Bergantino E., Bubacco L. & Mammi S. (2005) A topological model of the interaction between alpha-synuclein and sodium dodecyl sulfate micelles. *Biochemistry* 44, 329–339.

Bisaglia M., Schievano E., Caporale A., Peggion E. & Mammi S. (2006) The 11-mer repeats of human alpha-synuclein in vesicle interaction and lipid composition discrimination: a cooperative role. *Biopolymers* 84, 310–316.

Bisaglia M., Mammi S. & Bubacco L. (2009) Structural insights on the physiological functions and pathological effects of alpha-synuclein. *FASEB J* 23, [Epub ehead of print].

Bonifati V., Rizzu P., Squitieri F., Krieger E., Vanacore N., van Swieten J. C., Brice A., van Duijn C. M., Oostra B., Meco G. & Heutink P. (2003) DJ-1 (PARK7), a novel gene for autosomal recessive, early onset parkinsonism. *Neurol Sci* 24, 159–160.

Bustamante C., Macosko J. C. & Wuite G. J. (2000) Grabbing the cat by the tail: manipulating molecules one by one. *Nat Rev Mol Cell Biol* 1, 130–136.

Brucale M, Sandal M., Di Maio S., Rampioni A., Tessari I., Tosatto L., Bisaglia M., Bubacco L. & Samorì B. (2009) Pathogenic mutations shift the equilibria of alpha-synuclein single molecules towards structured conformers. *Chembiochem* 10, 176–183.

Bucciantini M., Giannoni E., Chiti F., Baroni F., Formigli L., Zurdo J., Taddei N., Ramponi G., Dobson C. M. & Stefani M. (2002) Inherent toxicity of aggregates implies a common mechanism for protein misfolding diseases. *Nature* 416, 507–511.

Bukau B. & Horwich A. L. (1998) The Hsp70 and Hsp60 chaperone machines. *Cell* 92, 351–366.

Bussell R. Jr & Eliezer D. (2001) Residual structure and dynamics in Parkinson's disease-associated mutants of alpha-synuclein. *J Biol Chem* 276, 45996–46003.

Bussell R. Jr & Eliezer D. (2003) A structural and functional role for 11-mer repeats in α-syn and other exchangeable lipid binding proteins. *J Mol Biol* 329, 763–778.

Bussell R. Jr & Eliezer D. (2004) Effects of Parkinson's disease-linked mutations on the structure of lipid-associated alpha-synuclein. *Biochemistry* 43, 4810–4818.

Bussell R. Jr, Ramlall T. F. & Eliezer D. (2005) Helix periodicity, topology, and dynamics of membrane-associated alpha-synuclein. *Protein Sci* 14, 862–872.

Canet-Aviles R. M., Wilson M. A., Miller D. W., Ahmad R., McLendon C., Bandyopadhyay S., Baptista M. J., Ringe D., Petsko G. A. & Cookson M. R. (2004) The Parkinson's disease protein DJ-1 is neuroprotective due to cysteine-sulfinic acid-driven mitochondrial localization. *Proc Natl Acad Sci USA* 101, 9103-9108.

Caughey B. & Lansbury P. T. Jr (2003) Protofibrils, pores, fibrils, and neurodegeneration: separating the responsible protein aggregates from the innocent bystanders. *Annu Rev Neurosci* 26, 267–298.

Chalifour R. J., McLaughlin R. W., Lavoie L., Morissette C., Tremblay N., Boulé M., Sarazin P., Stéa D., Lacombe D., Tremblay P. & Gervais F. (2003) Stereoselective interactions of peptide inhibitors with the β-amyloid peptide. *J Biol Chem* 278, 34874–34881.

Chandra S., Chen X., Rizo J., Jahn R. & Sudhof T. C. (2004) A broken alpha-helix in folded alpha-synuclein. *J Biol Chem* 278, 15313–15318.

Chandra S., Gallardo G., Fernández-Chacón R., Schlüter O. M. & Südhof T. C. (2005) Alpha-synuclein cooperates with CSPalpha in preventing neurodegeneration. *Cell* 123, 383–396.

Chen M., Margittai M., Chen J. & Langen R. (2007) Investigation of alpha-synuclein fibrils structure by site-directed spin labeling. *J Biol Chem* 282, 24970–24979.

Chiti F., Stefani M., Taddei N., Ramponi G. & Dobson C. M. (2003) Rationalization of the effects of mutations on peptides and protein aggregation rates. *Nature* 424, 805–808.

Choi W., Zibaee S., Jakes R., Serpell L. C., Davletov B., Crowther R. A. & Goedert M. (2004) Mutation E46K increase phosholipid binding and assembly into filaments of human alpha-synuclein. *FEBS Lett* 576, 363–368.

Chung K. K., Zhang Y., Lim K. L., Tanaka Y., Huang H., Gao J., Ross C. A., Dawson V. L. & Dawson T. M. (2001) Parkin ubiquitinates the alpha-synuclein-interacting protein, synphilin-1: implications for, Lewy-body formation in Parkinson disease. *Nat Med* 7, 1144–1150.

Clayton D. F. & George J. M. (1998) The synucleins: a family of proteins involved in synaptic function, plasticity, neurodegeneration and disease. *Trends Neurosc*i 21, 249–254.

Clayton D. F. & George J. M. (1999) Synucleins in synaptic plasticity and neurodegenerative disorders. *J Neurosci Res* 58, 120–129.

Conway K. A., Harper J. D. & Lansbury P. T . Jr (1998) Accelerated in vitro fibril formation by a mutant alpha-synuclein linked to early onset Parkinson's disease. *Nature Med* 4, 1318–1320.

Conway K. A., Lee S.-J-. Rochet J.-C., Ding T. T., Williamson R. E. & Lansburt P. T. Jr (2000) Acceleration of oligomerization, not fibrillation, is a shared property of both alpha-synuclein mutations linked to early-onset Parkinson's disease: implications for pathogenesis and therapy. *Proc Nat Acad Sci USA* 97, 571–576.

Conway K. A., Rochet J. C., Bieganski R. M. & Lansbury P. T.Jr. (2001) Kinetic stabilization of the alpha-synuclein protofibril by a dopamine-alpha-synuclein adduct. *Science* 294, 1346–1349.

Cookson M. R. (2005) The biochemistry of Parkinson's disease. *Annu Rev Biochem* 74, 29–52.

Crowther R. A., Jakes R., Spillantini M. G. & Goedert M. (1998) Synthetic filaments assembled from C-terminally truncated alpha-synuclein. *FEBS Lett* 436, 309–312.

Darios F., Corti O., Lucking C. B., Hampe C., Muriel M. P., Abbas N., Gu W. J., Hirsch E. C., Rooney T., Ruberg M. & Brice A. (2003) Parkin prevents mitochondrial swelling and cytochrome c release in mitochondria-dependent cell death. *Hum Mol Genet* 12, 517–526.

Davidson W. S., Jonas A., Clayton D. F. & George J. M. (1998) Stabilization of alpha-synuclein secondary structure upon binding to synthetic membranes. *J Biol Chem* 273, 9443–9449.

Dedmon M. M., Lindorff-Larsen K., Christodoulou J., Vendruscolo M. & Dobson C. M. (2005) Mapping long-range interactions in alpha-synuclein using spin-label NMR and ensamble molecular dynamic simulations. *J Am Chem Soc* 127, 476–477.

Ding T. T., Lee S. J., Rochet J. C. & Lansbury P. T. Jr. (2002). Annular alpha-synuclein protofibrils are produced when spherical protofibrils are incubated in solution or bound to brain-derived membranes. *Biochemistry* 41, 10209–10217.

Di Fonzo A., Rohe C. F., Ferreira J., Chien H. F., Vacca L., Stocchi F., Guedes L., Fabrizio E., Manfredi M., Vanacore N., Goldwurm S.,Breedveld G., Sampaio C., Meco G., Barbosa E., Oostra B. A. & Bonifati V. (2005) A frequent LRRK2 gene mutation associated with autosomal dominant Parkinson's disease. *Lancet* 365, 412–415.

Dobson C. M. (1999) Protein misfolding, evolution and disease. *Trends Biochem Sci* 24, 329–332.

Dobson C. M. (2001) The structural basis of protein folding and its links with human disease. *Phil Trans R Soc Lond B* 356, 133–145.

Dobson C. M. (2003) Protein folding and misfolding. *Nature* 426, 884– 890.

Drescher M., Veldhuis G., van Rooijen B. D., Milikisyants S., Subramaniam V. & Huber M. (2008) Antiparallel arrangement of the helices of vesicle-bound alpha-synuclein. *J Am Chem Soc* 130, 7796–7797.

Duda J. E., Giasson B. I., Gur T. L., Montine T. J., Robertson D., Biaggioni I., Hurtig H. I., Stern M. B., Gollomp S. M., Grossman M., Lee V. M.-Y. & Trojanowski J. Q. (2000) Immunohistochemical and biochemical studies demonstrate a distinc profile of alpha-synclein permutations in multiple system atrophy. *J Neuropathol Exp Neurol* 59, 830–841.

Duda J. E., Giasson B. I., Chen Q., Gur T. L., Hurtig H. I., Stern M. B., Gollomp S. M., Ischiropoulos H., Lee V. M. & Trojanowski J. Q. (2000b) Widespread nitration of pathological inclusions in neurodegenerative synucleinopathies. *Am J Pathol* 157, 1439–1445.

Duffy P. E. & Tennyson V. M. (1965) Phase and electron microscopic observation of Lewy bodies and melanin granules in the substantia nigra and locus coeruleus in Parkinson's disease. *J Neuropathol Exp Neurol* 24, 398–414.

El-Agnaf O. M., Paleologou K. E., Greer B., Abogrein A. M., King J. E., Salem S. A., Fullwood N. J., Benson F. E., Hewitt R., Ford K. J., Martin F. L., Harriott P., Cookson M. R. & Allsop D. (2004) A strategy for designing inhibitors of alpha-synuclein aggregation and toxicity as a novel treatment for Parkinson's disease and related disorders. *FASEB J* 18, 1315–1317.

Eliezer D., Kutluay E., Bussell R. Jr & Browne G. (2001) Conformational properties of alpha-synuclein in its free and lipid-associated states. *J Mol Biol* 307, 1061–1073.

Engelender S., Kaminsky Z., Guo X., Sharp A. H., Amaravi R. K., Kleiderlein J. J., Margolis R. L., Troncoso J. C., Lanahan A. A., Worley P. F., Dawson V. L., Dawson T. M. & Ross C. A. (1999) Synphilin-1 associates with alpha-synuclein and promotes the formation of cytosolic inclusions. *Nat Genet* 22, 110–114.

Forman J. R. & Clarke J. (2007) Mechanical unfolding of proteins: insights into biology, structure and folding. *Curr Opin Struct Biol* 17, 58–66.

Fredenburg R. A., Rospigliosi C., Meray R. K., Kessler J. C., Lashuel H. A., Eliezer D. & Lansbury P. T. Jr (2007) The impact of the E46K mutation on the properties of alpha-synuclein in its monomeric and oligomeric states. *Biochemistry* 46, 7107–7118.

Fujiwara H., Hasegawa M., Dohmae N., Kawashima A., Masliah E., Goldberg M.S., Shen J., Takio K. & Iwatsubo T. (2002) Alpha-Synuclein is phosphorylated in synucleinopathy lesions. *Nat Cell Biol* 4, 160–164.

Gardino A. K., Smerdon S. J. & Yaffe M. B. (2006) Structural determinants of 14-3-3 binding specificities and regulation of subcellular localization of 14-3-3-ligand complexes: a comparison of the X-ray crystal structures of all human 14-3-3 isoforms. *Semin Cancer Biol* 16, 173–182.

Georgieva E. R., Ramlall T. F., Borbat P. P., Freed H. J. & Eliezer D. (2008) Membrane-bound alpha-synuclein forms an extended helix: long-distances pulsed ESR measurements using vesicles, bicelles and rodlike micelles. *J Am Chem Soc* 130, 12856–12857.

Giasson B. I., Duda J. E., Murray I. V., Chen Q., Souza J. M., Hurtig H. I., Ischiropoulos H., Trojanowski J. Q. & Lee V. M. (2000) Oxidative damage linked to neurodegeneration by selective alpha-synuclein nitration in synucleinopathy lesions. *Science* 290, 985–989.

Giasson B. I., Murray I. V., Trojanowski J. Q. & Lee V. M. (2001) A hydrophobic stretch of 12 amino acid residues in the middle of alpha-synuclein is essential for filament assembly. *J Biol Chem* 276, 2380–2386.

Gilks W. P., Abou-Sleiman P. M., Gandhi S., Jain S., Singleton A., Lees A. J., Shaw K., Bhatia K. P., Bonifati V., Quinn N. P., Lynch J., Healy D. G., Holton J. L., Revesz T. & Wood, N. W. (2005) A common LRRK2 mutation in idiopathic Parkinson's disease. *Lancet* 365, 415–416.

Glaser C. B., Yamin G., Uversky V. N. & Fink A. L. (2005) Methionine oxidation, alpha-synuclein and Parkinson's disease. *Biochim Biophys Acta* 1703, 157–169.

Goedert M. (2001) Alpha-synuclein and neurodegenerative disease. *Nature Rev Neurosci* 2, 492–501.

Goers J., Manning-Bog A. B., McCormack A. L., Millett I. S., Doniach S., Di Monte D. A., Uversky V. N. & Fink A.L. (2003) Nuclear localization of alpha-synuclein and its interaction with histones. *Biochemistry* 42, 8465–8471.

Greenbaum E. A., Graves C. L., Mishizen-Eberz A. J., Lupoli M. A., Lynar D. R., Englander S. W., Axelsen P. H. & Giasson G. I. (2005) The E46K mutantion in alpha-synuclein increases amyloid fibril formation. *J Biol Chem* 280, 7800–7807.

Greggio E., Lewis P. A., van der Brug M. P., Ahmad R., Kaganovich A., Ding J., Beilina A., Baker A. K. & Cookson, M. R. (2007) Mutations in LRRK2/dardarin associated with Parkinson disease are more toxic than equivalent mutations in the homologous kinase LRRK1. *J Neurochem* 102, 93–102.

Hardesty B. & Kramer G. (2001) Folding of a nascent peptide on the ribosome. *Prog Nucleic Acid Res Mol Biol* 66, 41–66.

Harper J. D., Wong S. S., Lieber C. M. and Lansbury P. T. (1997) Observation of metastable Abeta amyloid protofibrils by atomic force microscopy. *Chem Biol* 4, 119–125.

Hashimoto M., Hsu L. J., Xia Y., Takeda A., Sisk A., Sundsmo M. & Masliah E. (1999) Oxidative stress induces amyloid-like aggregate formation of NACP/alpha-synuclein in vitro. *Neuro Report* 10, 717–721.

Hashimoto M., Takeda A., Hsu L. J., Takenouchi T. & Masliah E. (1999b) Role of cytochrome c as a stimulator of alpha-synuclein aggregation in Lewy body disease. *J Biol Chem* 274, 28849–28852.

Hassler R. (1938) Zur pathologie der paralysis agitans und des postenzephalitischen parkinsonismus. *J Psychol Neurol* 48, 387–486.

Heise H., Hoyer W., Becker S., Andronesi O. C., Riedel D. & Baldus M. (2005) Molecular level secondary structure, polymorphism, and dynamics of full-length alpha-synuclein fibrils studied by solid-state NMR. *Proc Nat Acad Sci USA* 102, 15871–15876.

Hope J. , Morton L. J., Farquhar C. F., Multhaup G., Beyreuther K. & Kimberlin R. H. (1986) The major polypeptide of scrapie-associated fibrils (SAF) has the same size, charge distribution and N-terminal protein sequence as predicted for the normal brain protein (PrP). *EMBO J* 5, 2591–2597.

Horwich A. (2002) Protein aggregation in disease: a role for folding intermediates forming specific multimeric interactions. *J Clin Invest* 110, 1221–1232.

Hoyer W., Cherny D., Subramaniam V. & Jovin T. M. (2004) Impact of the acidic C-terminal region comprising amino acids 109-140 on α-synuclein aggregation in vitro. *Biochemistry* 43, 16233–16242.

Huang C., Ren G., Zhou H. & Wang C. C. (2005) A new method for purification of recombinant human alpha-synuclein in Escherichia coli. *Protein Expr Purif* 42, 173–177.

Jao C. C., Der-Sarkissian A., Chen J. & Langen R. (2004) Structure of membrane-bound alpha-synuclein studied by site-directed spin labeling. *Proc Nat Acad Sci USA* 101, 8331–8336.

Jao C. C., Hegde B. G., Chen J., Haworth I. S. & Langen R. (2008) Structure of membrane-bound alpha-synuclein from site-directed spin labeling and computational refinement. *Proc Natl Acad Sci U S A* 105, 19666–19671.

Jenco J. M., Rawlingson A., Daniels B. & Morris A. J. (1998) Regulation of phospholipase D2: selective inhibition of mammalian phospholipase D isoenzymes by alpha- and beta-synucleins. *Biochemistry* 37, 4901–4909.

Jensen P. H., Nielsen M. S., Jakes R., Dotti C. G. & Goedert M. (1998) Binding of alpha-synuclein to brain vesicles is abolished by familial Parkinson's disease mutation. *J Biol Chem* 273, 26292–26294.

Jo E., McLaurin J., Yip C. M., St George-Hyslop P. & Fraser P. E. (2000) alpha-Synuclein membrane interaction and lipid specificity. *J Biol Chem* 275, 34328–34334.

Jo E., Fuller N., Rand R. P., St George-Hyslop P. & Fraser P. E. (2002) Defective membrane interactions of familial Parkinson's disease mutant A30P alpha-synuclein. *J Mol Biol* 315, 799–807.

Joachim C. L. & Selkoe D. J. (1989) Amyloid protein in Alzheimer's disease. *J Gerontol* 44, B77–82.

Kahle P. J., Neumann M., Ozmen L., Muller V., Odoy S., Okamoto N., Jacobsen H., Iwatsubo T., Trojanowski J. Q., Takahashi H., Wakabayashi K., Bogdanovic N., Riederer P., Kretzschmar H. A. & Haass C. (2001) Selective insolubility of alpha-synuclein in human Lewy body diseases is recapitulated in a transgenic mouse model. *Am J Pathol* 159, 2215–2225.

Kapurniotu A., Schmauder A. & Tenidis K. (2002) Structure-based designed and study of non-amyloidogenic, double N-methylated IAPP amyloid core sequence as inhibitors of IAPP amyloid formation and cytotoxicity. *J Mol Biol* 315, 339–350.

Kawamata H., McLean P. J., Sharma N. & Hyman B. T. (2001) Interaction of alpha-synuclein and synphilin-1: effect of Parkinson's disease-associated mutations. *J Neurochem* 77, 929–934.

Kawamoto Y., Akiguchi I., Nakamura S., Honjyo Y., Shibasaki H. & Budka H. (2002) 14-3-3 proteins in Lewy bodies in Parkinson disease and diffuse Lewy body disease brains. *J Neuropathol Exp Neurol* 61, 245–253.

Kellermayer M. S., Smith S. B., Granzier H. L. & Bustamante C. (1997) Folding-unfolding transitions in single titin molecules characterized with laser tweezers. *Science* 276, 1112–1116.

Kelly J. W. (1998) Alternative conformation of amyloidogenic proteins and their multi-step assembly pathways. *Curr Opin Struct Biol* 8, 101–106.

Kim H. Y., Heise H., Fernandez C. O., Baldus M. & Zweckstetter M. (2007) Correlation of amyloid fibril beta-structure with the unfolded alpha-synuclein. *Chembiochem* 8, 1671–1674.

Kitada T., Asakawa S., Hattori N., Matsumine H., Yamamura Y., Minoshima S., Yokochi M., Mizuno Y. & Shimizu N. (1998) Mutations in the parkin gene cause autosomal recessive juvenile parkinsonism. *Nature* 392, 605–608.

Koo E. H., Lansbury P. T. Jr & Kelly J. W. (1999) Amyloid diseases: abnormal protein aggregation in neurodegeneration. *Proc Natl Acad Sci USA* 96, 9989–9990.

Krüger R., Kuhn W., Müller T., Woitalla D., Graeber M., Kösel S., Przuntek H., Epplen J. T., Schöls L. & Riess O. (1998) Ala30Pro mutation in the gene encoding alpha-synuclein in Parkinson's disease. *Nat Genet* 18, 106–108.

Laemmli U. K. (1970) Cleavage of structural proteins during the assembly of the head of bacteriophage T4. *Nature* 227, 680–685.

Lashuel H. A., Petre B. M., Wall J., Simon M., Nowak R. J., Walz T. & Lansbury P. T. Jr (2002) Alpha-synuclein, especially the Parkinson's disease associated mutants, forms pore like annular and tubular protofibrils. *J Mol Biol* 322, 1089–1102.

Lee D., Lee S.-Y., Lee E.-N., Chang C.-S. & Paik S. R. (2002) Alpha-synuclein exhibits competitive interaction between calmodulin and synthetic membranes. *J Neurochem* 82, 1007–1017.

Lee J. C., Langen R., Hummel P. A., Gray H. B. & Winkler J. R. (2004) Alpha-synuclein structures from fluorescence energy-transfer kinetics: implications for the role of the protein in Parkinson's disease. *Proc Nat Acad Sci USA* 101, 16466–16471.

Lee J. C., Gray H. B. & Winkler J. R (2005) Tertiary contact formation in alpha-synuclein probed by electron transfer. *J Am Chem Soc* 127, 16388–16389.

Lewy F. (1912) in Hancbuch der Neurologie 3, (eds Lewandowski M. & Adeldorff G., Springer Verlag, Berlin) 920–933.

Lewis P. A., Greggio E., Beilina A., Jain S., Baker A. & Cookson M. R. (2007) The R1441C mutation of LRRK2 disrupts GTP hydrolysis. *Biochem Biophys Res Commun 357*, 668-71.

Li W., West N., Colla E., Pletnikova O., Troncoso J. C., Marsh L., Dawson T. M., Jäkälä P., Hartmann T., Price D. L. & Lee MK. (2005) Aggregation promoting C-terminal truncation of alpha-synuclein is a normal cellular process and is enhanced by the familial Parkinson's disease-linked mutations. *Proc Natl Acad Sci USA* 102, 2162–2167.

Lindersson E., Lundvig D., Petersen C., Madsen P., Nyengaard J. R., Højrup P., Moos T., Otzen D., Gai W. P., Blumbergs P. C. & Jensen P. H. (2005) p25alpha stimulates alpha-synuclein aggregation and is co-localized with aggregated alpha-synuclein in alpha-synucleinopathies. *J Biol Chem* 280, 5703–5715.

Lippa C. F., Fujiwara H., Mann D. M., Giasson B., Baba M., Schmidt M. L., Nee L. E., O'Connell B., Pollen D. A., St George-Hyslop P., Ghetti B., Nochlin D., Bird T. D., Cairns N. J., Lee V. M., Iwatsubo T. & Trojanowski J. Q. (1998) Lewy bodies contain altered α-synuclein in the brains of many familial Alzheimer's disease patients with mutations in presenilin and amyloid precursor protein genes. *Am J Pathol* 153, 1365–1370.

Lippa C. F., Schmidt M. L., Lee V. M-Y. & Trojanowski I. Q. (1999) Dementia with Lewy bodies. *Neurology* 52, 893.

Lotharius J. & Brundin P. (2002) Pathogenesis of Parkinson's disease: dopamine, vesicles and α-synuclein. *Nat Rev Neurosci* 3, 932–942.

Luk K. C., Hyde E. G., Trojanowski J. Q. & Lee V. M.-Y. (2007) Sensitive fluorescence polarization technique for rapid screening of alpha-synuclein oligomerization/fibrillization inhibitors. *Biochemistry* 46, 12522–12529.

Lundvig D., Lindersson E. & Jensen P. H. (2005) Pathogenic effects of alpha-synuclein aggregation. *Brain Res Mol Brain Res* 134, 3–17.

Maiti N. C., Apetri M. M., Zagorski M. G., Carey P. R. & Anderson V. E. (2004) Raman spectroscopic characterization of secondary structure in natively unfolded protein: alpha-synuclein. *J Am Chem Soc* 126, 16388–16389.

Makin O. S. & Serpell L. C. (2005) Structures for amyloid fibrils. *FEBS J* 272, 5950–5961.

Martinez J., Moeller I., Erdjument-Bromage H., Tempst P. & Lauring B. (2003) Parkinson's disease-associated alpha-synuclein is a calmodulin substrate. *J Biol Chem* 278, 17379–17387.

Masuda M., Dohmae N., Nonaka T., Oikawa T., Hisanaga S., Goedert M. & Hasegawa M. (2006) Cysteine misincorporation in bacterially expressed human a-synuclein. *FEBS Lett* 580, 1775–1779.

Munishkina L. A., Phelan C., Uversky V. N. & Fink A. L. (2003) Conformational behaviour and aggregation of α-synuclein in organic solvents: modeling the effects of membranes. *Biochemistry* 42, 2720–2730.

Muntané G., Dalfó E., Martinez A. & Ferrer I. (2008) Phosphorylation of tau and alpha-synuclein in synaptic-enriched fractions of the frontal cortex in Alzheimer's disease, and in Parkinson's disease and related alpha-synucleinopathies. *Neuroscience* 152, 913–923.

Murphy R. M. (2007) Kinetics of amyloid formation and membrane interaction with amyloidogenic proteins. *Biochim Biophys Acta* 1768, 1923–1934.

Nagano Y., Yamashita H., Takahashi T., Kishida S., Nakamura T., Iseki E., Hattori N., Mizuno Y., Kikuchi A. & Matsumoto M. (2003) Siah-1 facilitates ubiquitination and degradation of synphilin-1. *J Biol Chem* 278, 51504–51514.

Neystat M., Rzhetskaya M., Kholodilov N. & Burke R. E. (2002) Analysis of synphilin-1 and synuclein interactions by yeast two-hybrid beta-galactosidase liquid assay. *Neurosci Lett* 325, 119–123.

Nichols M. R., Moss M. A., Reed D. K., Lin W. L., Mukhopadhyay R., Hoh J. H. & Rosenberry T. L. (2002) Growth of beta-amyloid(1-40) protofibrils by monomer elongation and lateral association. Characterization of distinct products by light scattering and atomic force microscopy. *Biochemistry* 41, 6115–6127.

Nichols W. C., Pankratz N., Hernandez D., Paisan-Ruiz C., Jain S., Halter C. A., Michaels V. E., Reed T., Rudolph A., Shults C. W., Singleton A. & Foroud T. (2005) Genetic screening for a single
common LRRK2 mutation in familial Parkinson's disease. *Lancet* 365, 410–412.

Norris E. H. & Giasson B. I. (2005) Role of oxidative damage in protein aggregation associated with Parkinson's disease and related disorders. *Antioxid Redox Signal* 7, 672–684.

Ostrerova N., Petrucelli L., Farrer M., Mehta N., Choi P., Hardy J. & Wolozin B. (1999) Alpha-synuclein shares physical and functional homology with 14-3-3 proteins. *J Neurosci* 19, 5782–5791.

Ostrerova-Golts N., Petrucelli L., Hardy J., Lee J. M., Farer M. & Wolozin B. (2000) The A53T alpha-synuclein mutation increases iron-dependent aggregation and toxicity. *J Neurosci* 20, 6048–6054.

Paik S. R., Shin H. J., Lee J. H., Chang C. S. & Kim J. (1999) Copper(II)-induced self-oligomerization of alpha-synuclein. *Biochem J* 340, 821–828.

Paisan-Ruiz C., Jain S., Evans E. W., Gilks W. P., Simon J., van der Brug M., Lopez de Munain A., Aparicio S., Gil A. M., Khan N., Johnson J., Martinez J. R., Nicholl D., Carrera I. M., Pena A. S., de Silva R., Lees A., Marti-Masso J. F., Perez-Tur J., Wood N. W. & Singleton A. B. (2004) Cloning of the gene containing mutations that cause PARK8-linked Parkinson's disease. *Neuron* 44, 595–600.

Paleologou K. E., Schmid A. W., Rospigliosi C. C., Kim H. Y., Lamberto G. R., Fredenburg R. A., Lansbury P. T. Jr, Fernandez C. O., Eliezer D., Zweckstetter M. & Lashuel H. A. (2008) Phosphorylation at Ser-129 but not the phosphomimics S129E/D inhibits the fibrillation of alpha-synuclein. *J Biol Chem* 283, 16895–168905.

Pappolla M. A. (1986) Lewy bodies of Parkinson’s disease. Immune electron microscopic demonstration of neurofilament antigens in constituent filaments. *Arch Pathol Lab Med* 110, 1160–1163.

Paravastu A. K., Leapman R. D., Yau W. M. & Tycko R. (2008) Molecular structural basis for polymorphism in Alzheimer's beta-amyloid fibrils. Proc Natl Acad Sci USA 105, 18349–18354.

Parkinson J. (1871) An essay on the shaking palsy. Sherwood, Neely & Jones, London.

Payton J. E., Perrin R. J., Woods W. S. & George J. M. (2004) Structural determinants of PLD2 inhibition by alpha-synuclein. *J Mol Biol* 337, 1001–1009.

Perez R. G., Waymire J. C., Lin E., Liu J. J., Guo F. & Zigmond M. J. (2002) A role for alpha-synuclein in the regulation of dopamine biosynthesis. *J Neurosci* 22, 3090–3099.

Perrin R. J., Woods W. S., Clayton D. F. & George J. M. (2000) Interaction of human alpha-synuclein and Parkinson's disease variants with phospholipids. Structural analysis using site-directed mutagenesis. *J Biol Chem* 275, 34393–34398.

Perrin R. J., Woods W. S., Clayton D. F. & George J.M. (2001) Exposure to long chain polyunsaturated fatty acids triggers rapid multimerization of synucleins. *J Biol Chem* 276, 41958–41962.

Petit A., Kawarai T., Paitel E., Sanjo N., Maj M., Scheid M., Chen F., Gu Y., Hasegawa H., Salehi-Rad S., Wang L., Rogaeva E., Fraser P., Robinson B., St George-Hyslop P. & Tandon A. (2005) Wild-type PINK1 prevents basal and induced neuronal apoptosis, a protective effect abrogated by Parkinson disease-related mutations. *J Biol Chem* 280, 34025–34032.

Petsko G. A. & Ringe D. (2004) Protein structure and function. Edited from Primers in Biology, New Science Press.

Polymeropoulos M. H., Lavedan C., Leroy E., Ide S. E., Dehejia A., Dutra A., Pike B., Root H., Rubenstein J., Boyer R., Stenroos E. S., Chandrasekharappa S., Athanassiadou A., Papapetropoulos T., Johnson W. G., Lazzarini A. M., Duvoisin R. C., Di Iorio G., Golbe L. I. & Nussbaum R. L. (1997) Mutation in the alpha-synuclein gene identified in families with Parkinson's disease. *Science* 276, 2045–2047.

Quist A., Doudevski I., Lin H., Azimova R., Ng D., Frangione B., Kagan B., Ghiso J. & Lal R. (2005) Amyloid ion channels: a common structural link for protein-misfolding disease. *Proc Natl Acad Sci USA* 102, 10427–10432.

van Raaij M. E., van Gestel J., Segers-Nolten I. M., de Leeuw S. W. & Subramaniam V. (2008) Concentration dependence of alpha-synuclein fibril length assessed by quantitative atomic force microscopy and statistical-mechanical theory. *Biophys J* Aug 1. [Epub ahead of print].

Radford S. E. & Dobson C. M. (1999) From computer simulations to human disease: emerging themes in protein folding. *Cell* 97, 291–298.

Rappley I., Gitler A. D., Selvy P. E., Lavoie M. J., Levy B. D., Brown H. A., Lindquist S. & Selkoe D. J. (2009) Evidence That alpha-Synuclein Does Not Inhibit Phospholipase D (dagger). *Biochemistry* Jan 15, [Epub ahead of print].

Ren G., Wang X., Hao S., Hu H. & Wang C. C. (2007) Translocation of alpha-synuclein expressed in Escherichia coli. *J Bacteriol* 189, 2777–2786.

Rhoades E., Ramlall T. F., Webb W. W. & Eliezer D. (2006) Quantification of alpha-synuclein binding to lipid vesicles using fluorescence correlation spectroscopy. *Biophys J* 90, 4692–4770.

Ribeiro C. S., Carneiro K., Ross C. A., Menezes J. R. & Engelender S. (2002) Synphilin-1 is developmentally localized to synaptic terminals, and its association with synaptic vesicles is modulated by alpha-synuclein. *J Biol Chem* 277, 23927–23933.

Sandal M., Valle F., Tessari I., Mammi S., Bergantino E., Musiani F., Brucale M., Bubacco L. & Samorì B (2008) Conformational equilibria in monomeric alpha-synuclein at the single-molecule level. *PLoS Biol* 6, e6.

Sato C., Kascsak R. J., Saborio G. P., Aucouturier P., Wisniewski T., Prelli F., Kascsak R., Mendez E., Harris D. A., Ironside J., Tagliavini F., Carp R. I. & Frangione B. (2000) Reversion of prion protein conformational changes by synthetic β-sheet breakers peptides. *Lancet* 355, 192–197.

Sensor Surface Handbook, Biacore.

Serpell L. C. (2000) Alzheimer's amyloid fibrils: structure and assembly. *Biochim Biophys Acta* 1502, 16–30.

Shafer D. E., Inman J. K & Lees A. (2000) Reaction of Tris(2-carboxyethyl)phosphine (TCEP) with maleimide and α-haloacyl groups: anomalous elution of TCEP by gel filtration. *Anal Biochem* 282, 161–164.

Sharon R., Bar-Joseph I., Frosch M. P., Walsh D. M., Hamilton J. A. & Selkoe D. J. (2003) The formation of highly soluble oligomers of alphasynuclein is regulated by fatty acids and enhanced in Parkinson's disease. *Neuron* 37, 583–595.

Shendelman S., Jonason A., Martinat C., Leete T. & Abeliovich A. (2004) DJ-1 is a redox-dependent molecular chaperone that inhibits alpha-synuclein aggregate formation. *PLoS Biol* 2, e362.

Shimura H., Hattori N., Kubo S., Mizuno Y., Asakawa S., Minoshima S., Shimizu N., Iwai K., Chiba T., Tanaka K. & Suzuki T. (2000) Familial Parkinson disease gene product, parkin, is a ubiquitin-protein ligase. *Nat Genet* 25, 302–305.

Sidhu A., Wersinger C. & Vernier P. (2004) alpha-Synuclein regulation of the dopaminergic transporter: a possible role in the pathogenesis of Parkinson's disease. *FEBS Lett* 565, 1–5.

Silvestri L., Caputo V., Bellacchio E., Atorino L., Dallapiccola B., Valente E. M. & Casari G. (2005) Mitochondrial import and enzymatic activity of PINK1 mutants associated to recessive parkinsonism. *Hum Mol Genet* 14, 3477–3492.

Singleton A., Gwinn-Hardy K., Sharabi Y., Li S. T., Holmes C., Dendi R., Hardy J., Singleton A., Crawley A. & Goldstein D. S. (2004) Association between cardiac denervation and parkinsonism caused by alpha-synuclein gene triplication. *Brain* 127, 768–772.

Smith W. W., Pei Z., Jiang H., Liang Y., Engelender S., Dawson V. L., Dawson T. M. & Ross C. A. (2006) LRRK2 interacts with Synphilin-1. Program No. 276.16/U86.Washington, DC: Society for Neuroscience, 2006. Available online.

Spillantini M. G., Schmidt M. L., Lee V. M.-J., Trojanowski J. Q., Jakes R. & Goedert M. (1997) Alpha-synuclein in Lewy bodies. *Nature* 388, 839–840.

Szargel R., Rott R. & Engelender S. (2008) Synphilin-1 isoforms in Parkinson's disease: regulation by phosphorylation and ubiquitylation. *Cell Mol Life Sci* 65, 80–88.

Taira T., Saito Y., Niki T., Iguchi-Ariga S. M., Takahashi K. & Ariga H. (2004) DJ-1 has a role in antioxidative stress to prevent cell death. *EMBO Rep* 5, 213–218.

Takahashi M., Kanuka H., Fujiwara H., Koyama A., Hasegawa M., Miura M. & Iwatsubo T. (2003) Phosphorylation of alpha-synuclein characteristic of synucleinopathy lesions is recapitulated in alpha-synuclein transgenic Drosophila. *Neurosci Lett* 336, 155–158.

Takahashi M., Ko L. W., Kulathingal J., Jiang P., Sevlever D. & Yen S. H. (2007) Oxidative stress-induced phosphorylation, degradation and aggregation of alpha-synuclein are linked to upregulated CK2 and cathepsin D. *Eur J Neurosci* 26, 863–874.

Takahashi T. & Mihara H. (2008) Peptide and protein mimetics inhibiting amyloid beta-peptide aggregation. *Acc Chem Res* 41, 1309–1318.

Takamori S., Holt M., Stenius K., Lemke E. A., Grønborg M., Riedel D., Urlaub H., Schenck S., Brügger B., Ringler P., Müller S. A., Rammner B., Gräter F., Hub J. S., De Groot B. L., Mieskes G., Moriyama Y., Klingauf J., Grubmüller H., Heuser J., Wieland F. & Jahn R. (2006) Molecular anatomy of an trafficking organelle. *Cell* 17, 831–846.

Tan S. Y. & Pepys M. B. (1994) Amyloidosis. *Histopathology* 25, 403–414.

The Handbook, Molecular Proves, Invitrogen.

Thomas B. & Flint Beal M. (2007) Parkinson's disease. *Hum Mol Genet* 16, R183–R194.

Thomas P. J., Qu B. H. & Pedersen P. L. (1995) Defective protein folding as a basis of human disease. *Trends Biochem Sci* 20, 456–459.

Tretiakoff C. (1919) Contribution à l'étude de l'anatomie pathologique du locus niger de Soemmering avec quelques deductions relatives à la pathogénie des troubles du tonus muscolaire et de la maladie de Parkinson. Thesis, Univ. Paris.

Tu P.-H., Galvin J. E., Baba M., Giasson B., Tomita T., Leight S., Nakajo S., Iwatsubo T., Trojanowski J. Q. & Lee V. M. (1998) Glial cytoplasmic inclusions in white matter oligodendrocytes in multiple system atrophy brains contains insoluble α-synuclein. *Ann Neurol* 44, 415–422.

Tycko R. (2004) Progress towars a molecular understanding of amyloif fibrils. *Curr Opin Struc Biol* 14, 96–103.

Ulmer T. S., Bax A., Cole N. B. & Nussbaum R. L. (2005) Structure and dynamics of micelle-bound human α-synuclein. *J Biol Chem* 280, 9595–9603.

Ulmer T. S. & Bax A. (2005) Comparison of structure and dynamics of micelle-bound human alpha-synuclein and Parkinson disease variants. *J Biol Chem* 280, 43179–43187.

Uversky V. N., Li J. & Fink A. L. (2001) Metal-triggered structural transformations, aggregation, and fibrillation of human α-synuclein. *J Biol Chem* 276, 44284–44296.

Uversky V. N., Li J. & Fink A. L. (2001b) Evidence for a partially folded intermediate in α-synuclein fibril formation. *J Biol Chem* 276, 10737–10744.

Uversky V. N. & Fink A. L. (2002) Amino acid determinants of alpha-synuclein aggregation: putting together pieces of the puzzle. *FEBS Lett* 522, 9–13.

Uversky V. N., Li J., Souillac P., Millett I. S., Doniach S., Jakes R., Goedert M. & Fink A. L. (2002) Biophysical properties of the synucleins and their propensities to fibrillate: inhibition of alpha-synuclein assembly by beta- and gamma-synucleins. *J Biol Chem* 277, 11970–11978.

Uversky V. N., Yamin G., Souillac P. O., Goers J., Glaser C. B. & Fink A. L. (2002b) Methionine oxidation inhibits fibrillation of human alphasynuclein in vitro. *FEBS Lett* 517, 239–244.

Uversky V. N. (2003) A protein chameleon: conformational plasticity of α-synuclein, a disordered protein involved in neurodegenerative disorders. *J Biomol Struct Dyn* 21, 211–234.

Uversky V. N. & Fink A. L. (2004) Conformational constraints for amyloid fibrillation: the importance of being unfolded. *Biochim Biophys Acta* 1698, 131–153.

Vilar M., Chou H. T., Luhrs T., Maji S. K., Riek-Loher D., Verel R., Manning G., Stahlberg H. & Riek R. (2008) The fold of alpha-synuclein fibrils. *Proc Nat Acad Sci USA* 105, 8637–8642.

Volles M. J. & Lansbury P. T. Jr (2002) Vesicle permeabilization by protofibrillar alpha-synuclein is sensitive to Parkinson's disease-linked mutations and occurs by a pore-like mechanism. *Biochemistry* 41, 4595–4602.

Wakabayashi K., Engelender S., Yoshimoto M., Tsuji S., Ross C. A. & Takahashi H. (2000) Synphilin-1 is present in Lewy bodies in Parkinson's disease. *Ann Neurol* 47, 521–523.

Waxman E. A. & Giasson B. I. (2008) Molecular mechanism of α-synuclein neurodegeneration. *Biochim Biophys Acta* Oct 9, [Epub ehead of print].

Wolynes P. G., Onuchic J .N. & Thirumalai D. (1995) Navigating the folding routes. *Science* 267, 1619–1620.

Wood S. J., Wypych J., Steavenson S., Louis J. C., Citron M. & Biere A. L. (1999) alpha-Synuclein fibrillogenesis is nucleation-dependent. Implications for the pathogenesis of Parkinson's disease. *J Biol Chem* 274, 19509–19512.

Wood-Kaczmar A., Gandhi S. & Wood N. W. (2006) Understanding the molecular causes of Parkinson's disease. *Trends Mol Med* 12, 521–528.

Yamin G., Uversky V. N. & Fink A. L. (2003) Nitration inhibits fibrillation of human alpha-synuclein in vitro by formation of soluble oligomers. *FEBS Lett* 542, 147–152.

Zakharov S. D., Hulleman J. D., Dutseva E. A., Antonenko Y. N., Rochet J. C. & Cramer W. A. (2007) Helical alpha-synuclein forms highly conductive ion channels. *Biochemistry* 46, 14369–14379.

Zarranz J .J., Alegre J., Gómez-Esteban J. C., Lezcano E., Ros R., Ampuero I., Vidal L., Hoenicka J., Rodriguez O., Atarés B., Llorens V., Gomez Tortosa E., del Ser T., Muñoz D. G.

& de Yebenes J. G. (2004) The new mutation, E46K, of alpha-synuclein causes Parkinson and Lewy body dementia. *Ann Neurol* 55, 164–173.

Zhang Y., Gao J., Chung K. K., Huang H., Dawson V. L. & Dawson T. M. (2000) Parkin functions as an E2-dependent ubiquitin- protein ligase and promotes the degradation of the synaptic vesicle-associated protein, CDCrel-1. *Proc Natl Acad Sci USA* 97, 13354–13359.

Zhou Y., Gu G., Goodlett D. R., Zhang T., Pan C., Montine T. J., Montine K. S., Aebersold R. H. & Zhang J. (2004) Analysis of alpha-synuclein-associated proteins by quantitative proteomics. *J Biol Chem* 279, 39155–39164.

Zhu M., Li J. & Fink A. L. (2003) The association of alpha-synuclein with membranes affects bilayer structure, stability, and fibril formation. *J Biol Chem* 278, 40186–40197.

Zhu M. & Fink A. L. (2003) Lipid binding inhibits alpha-synuclein fibril formation. *J Biol Chem* 278, 16873–16877.

Zimprich A., Biskup S., Leitner P., Lichtner P., Farrer M., Lincoln S., Kachergus J., Hulihan M., Uitti R. J., Calne D. B., Stoessl A. J., Pfeiffer R. F., Patenge N., Carbajal I. C., Vieregge P., Asmus F., Muller-Myhsok B., Dickson D. W., Meitinger T., Strom T. M., Wszolek Z. K. & Gasser T. (2004) Mutations in LRRK2 cause autosomal-dominant parkinsonism with pleomorphic pathology. *Neuron* 44, 601–607.